March 31, 2014

To: Ryoji Noyori, RIKEN President

Report on STAP Cell Research Paper Investigation

Research Paper Investigative Committee
Shunsuke Ishii, Chair
Atsushi Iwama
Haruhiko Koseki
Yoichi Shinkai
Tetsuya Taga
Jun Watanabe

1. Circumstances

On Thursday, February 13, 2014, a RIKEN researcher who had been notified of doubts concerning research papers published by RIKEN scientists contacted the RIKEN Auditing and Compliance Office through one of RIKEN's executive officers. The director of the Auditing and Compliance Office decided that this matter should be handled in compliance with the provisions for reports on research misconduct stipulated in Article 10, paragraph 3 of RIKEN's Regulations on the Prevention of Research Misconduct (September 13, 2012, Reg. 61, hereafter "Regulations"), and from that same day through February 17, the Office conducted a preliminary inquiry, in accordance with the provisions of Article 11 of the Regulations. This preliminary inquiry was carried out by the following five people: Shunsuke Ishii, Atsushi Iwama, Haruhiko Koseki, Yoichi Shinkai, and Tetsuya Taga. In response to the results of this preliminary inquiry, RIKEN decided to carry out a full investigation as stipulated in Article 12 of the Regulations, and an Investigative Committee was established on February 17, with Shunsuke Ishii serving as Chair.

2. Methods and contents of the investigation

2-1. Purpose of the investigation and items investigated

The investigation sought to clarify whether or not the following items constituted "research misconduct" as defined in Article 12, paragraph 2 of the Regulations.

(1) Obokata, et al, Nature 505:641-647 (2014) (Paper 1)
- (1-1) Unnatural appearance of colored cell parts shown by arrows in d2 and d3 images of Figure 1f.
- (1-2) In Figure 1i, lane 3 appears to have been inserted later.
- (1-3) A part of the Methods section on karyotyping appears to have been copied from another paper.
- (1-4) A part of the procedures described in the Methods section on karyotyping appears to be different from the actual procedures used in the experiment.
- (1-5) The images for Figures 2d and 2e appear to be incorrect, and closely

resemble images in Dr. Obokata's PhD dissertation.

Haruko Obokata (lead author, corresponding author), Yoshiki Sasai (co-author), Teruhiko Wakayama (co-author), and Hitoshi Niwa (co-author)

(2) Obokata, et al, Nature 505: 676-680 (2014) (Paper 2)
(2-1) There is a strong resemblance between the rightmost panel in Figure 1b and the lower panel in 2g, both showing fluorescence in mice placenta.

Haruko Obokata (lead author, corresponding author), Yoshiki Sasai (corresponding author), Teruhiko Wakayama (corresponding author), Hitoshi Niwa (co-author)

2-2. Individuals investigated

The individuals investigated held the following positions at the time that papers 1 and 2 were submitted and when they were published.

Haruko Obokata
At the time of submission: Research Unit Leader of the Laboratory for Cellular Reprogramming, RIKEN Center for Developmental Biology
At the time of publication: Same as above

Yoshiki Sasai
At the time of submission: Group Director of the Laboratory for Organogenesis and Neurogenesis, RIKEN Center for Developmental Biology
At the time of publication: CDB Deputy Director

Teruhiko Wakayama
At the time of submission: Team Leader of the Laboratory for Genomic Reprogramming, RIKEN Center for Developmental Biology
At the time of publication: Professor at the Faculty of Life and Environmental Sciences, University of Yamanashi, and Senior visiting Scientist at RIKEN

Hitoshi Niwa
At the time of submission: Project Leader of the Laboratory for Pluripotent Stem Cell Studies, RIKEN Center for Developmental Biology
At the time of publication: Same as above

2-3. Investigation methods

From February 20 through March 31, 2014, the Investigative Committee collected and examined the relevant materials and conducted interviews with the individuals concerned.

The materials included the original data of the experiments described in the papers, lab notes, files showing the process of creation of the papers, documents provided by the individuals investigated, emails exchanged among the individuals concerned, and equipment that was used in the experiments.

In addition, opinions regarding the reconstruction of the imaging data were solicited from Professor Akihiko Nakano, Laboratory of Developmental Cell Biology, Department of Biological Sciences, Graduate School of Science, University of Tokyo, who is also Team Leader of the Live Cell Molecular Imaging Research Team, Extreme Photonics Research Group, RIKEN Center for Advanced Photonics, and an authority on imaging.

The Investigative Committee based its inquiry on examinations of these materials

and interviews.

2-4. Results of the investigation and opinions

(1-1)	Paper 1: Unnatural appearance of colored cell parts shown by arrows in d2 and d3 images of Figure 1f. (*Investigation results already covered in interim report)*

Results of investigation

Dr. Obokata stated that she performed the live imaging, from which the still images published in the paper were made, that she submitted these as compressed images, that the original images in the submitted manuscript contained no distortion, that she did not notice the presence of distortion in the published images, and that she does not know why such distortions were generated.

The submitted original live imaging data were examined. Upon reproducing the images on several computers, it was confirmed that the images submitted with the manuscript contained no distortion, while the images in the published papers contained some distortion.

Dr. Akihiko Nakano explained the possible causes of the distortion as follows. Although it was not possible to reproduce from the submitted live imaging still images identical to those in the paper, very similar images were created. Distortions result when the resolution is decreased and the images are compressed using JPEG or some other method. Reproducing the same distortion is difficult, because it depends on the degree of the compression. Therefore, if the distortions were generated in the process of figure preparation at the *Nature* editorial office, it is difficult to accurately reproduce those distortions. It is possible, along with compression, for block noises to be generated that could cause the appearance of colors that are not in the original image. Given these reasons, it can be concluded that the published images constitute single frames captured from the live imaging.

Opinions

It is reasonable to conclude that the still images published in the papers were generated from the submitted live imaging. The images in the submitted manuscript contained no distortions, but distortions are evident in the published images. It is plausible these distortions were produced during figure processing at the *Nature* editorial office. Block noise, which can be generated during compression, is a widely known phenomenon. Therefore, it is judged that there was no falsification in the process of generating the images in question from the live imaging.

(1-2)	In Figure 1i, lane 3 appears to have been inserted later.

Results of investigation

Drs. Obokata and Sasai submitted an electronic file of the photos of the gels on which Figure 1i is based, lab notes, and a written explanation of the process and methods used to create the figure. The two were also interviewed separately.

After careful review of all of the information acquired, it was confirmed that Figure 1i is a processed image of 2 photos taken of 2 pulse-field electrophoresed gels. There were a total of 29 samples, with samples 1 through 14 electrophoresed on gel 1 and samples 15 through 29 on gel 2. It was confirmed from the photos of the two gels that lanes 1, 2, 4, and 5 of Figure 1i correspond to lanes 1, 2, 4, and 5 of gel 1, counting from

the left (standard DNA size marker is lane 0 on the left), and lane 3 corresponds to lane 1 of gel 2 (standard DNA size marker is lane 0 on the left). Lane 3 of gel 1 and lane 1 of gel 2 were both positive controls indicating the rearrangement of T-cell receptor genes, and were, respectively, electrophoresed PCR products of $CD45^+$ hematopoietic cell and $CD45^+/CD3^+$ T lymphocyte DNA.

Regarding the image processing, it was confirmed that in the gel 1 photo of lanes 1, 2, 3, 4, and 5, lane 1 of gel 2 was not simply inserted in the location of gel 1's lane 3. The separation distance of the standard DNA size marker lane in gel 1 is approximately 0.63 times that in the latter gel 2. In preparing Figure 1i, the image of gel 1 was vertically elongated approximately 1.6 times before inserting the image of gel 2's lane 1. This was confirmed by the vertical warping seen in the images of dust in gel 1. A light smear in the photo of gel 2's lane 1 appears to have been erased, suggesting that contrast adjustments were also made.

When Dr. Obokata was queried on this, she explained that lane 1 of gel 2 was the most suitable for clearly showing the rearrangement of T-cell receptor genes as a positive control. She stated that after visually confirming that the log-scale values of molecular weight and separation distances for the standard DNA size markers had satisfactory linearity in their respective gels, she vertically elongated the photo of gel 1 and decided on the location for the insertion of lane 3 based on the location data for the standard DNA size marker. Upon verification, it was found that there was no linearity between the log-scale values of molecular weight and separation distances of the standard DNA size markers for gel 1 and gel 2, and that it would have been impossible to position lane 3 on the basis of the standard DNA size marker location data, as had been explained. In addition, her explanation was not supported by the fact that even if the image of lane 3 was positioned in conjunction with the standard DNA size markers located near the T-cell receptor gene rearrangement band group of lane 3 in Figure 1i, the T-cell receptor gene rearrangement band group would be placed differently from the T-cell receptor gene rearrangement band shown in lane 3 of Figure 1i. Contrary to her explanation, if the image in lane 3 is positioned in reference to the position of the T-cell receptor gene rearrangement band group in lane 3 of Figure 1i, a discrepancy appears between the positions of the standard DNA size marker bands in gels 1 and 2. As a result, this suggests that when Figure 1i was processed, it was not the standard DNA size marker bands that were taken as the standard, but rather the lane was inserted to fit with the shape of the T-cell receptor gene rearrangement band group in the adjacent lane 4.

With regard to the electrophoresed samples, the information provided by Dr. Obokata, including sample tube labels and the lab notes, indicated that lanes 1, 2, 4, and 5 in Figure 1i are consistent with the paper, and that the "Lymphocytes" label for lane 3 refers to $CD45^+/CD3^+$ T lymphocytes.

Opinions

It is clear from the detailed analysis of the figure in question that it is a composite image created from two separate images of the electrophoresed gels. The composite was created by deliberately manipulating—in what can hardly be called a minor way—images of multiple lanes including the two corresponding to FACS-Sorted Oct4-GFP positive cell group samples which play an important role in this paper. An image of these lanes had been vertically elongated approximately 1.6 times, in which a positive control lane from the other gel was placed after contrast adjustment. Furthermore, in placing the positive control lane, no scientific considerations were made nor scientifically reasonable procedures were followed; instead, the lane for the T-cell receptor gene rearrangement band group was positioned on the basis of visual confirmation. This not

only created the illusion that the data of two different gels belonged to only one gel, but may also lead to the danger of misinterpretation of the data.

It would appear that Dr. Obokata did not, at that time, sufficiently understand the prohibitions against the action that she had taken, nor did she appear to know *Nature*'s criteria for presenting such data in a way that would not call its authenticity into question. Even though her direct intent may not have been to deliberately mislead other researchers or lead them to incorrect interpretations of the data, our conclusion is that she was aware of the danger. It is evident that her purpose in creating the composite image was to articulate the T-cell receptor gene rearrangement band and that she did so without applying scientific consideration or procedures. We therefore conclude that this was an act of research misconduct corresponding to falsification.

The falsified image was created by Dr. Obokata using her own experimental data. Drs. Sasai, Wakayama, and Niwa had no involvement in the experiments or in creating the image data. The three were shown the already altered image prior to the submission of the paper to *Nature* without being told that it was a false image. Given that this alteration could not be easily detected, it must be concluded that there was no research misconduct on the part of these three researchers.

(1-3) A part of the Methods section on karyotyping in Paper 1 was found to have been copied from
Guo J., et al.; Multicolor Karyotype Analyses of Mouse Embryonic Stem Cells. in In Vitro Cell Dev Biol Anim 41(8-9), 278-283 (2005), and this also was investigated.

(1-4) A part of the procedures described in the Methods section on karyotyping appears to be different from the actual procedures used in the experiment.

Results of investigation

Regarding (1-3)

Dr. Obokata explained that in the Genomic Reprogramming Research Team under Dr. Wakayama, karyotyping was carried out on a day-to-day basis, but that the protocol used was a very simple one, and deciding that a more detailed explanation was needed, she referred to a paper that explained the protocol in detail, but forgot to include a note. She confirmed that she wrote the Methods section, and while she seemed to vaguely remember copying some part of it, she did not have a copy of the paper from which it was copied, and did not remember the source. The similarity of the text, the fact that Dr. Obotaka was not familiar with the protocol, and that the description in the paper does not correspond exactly to the procedures followed in the actual experiment, lead to the conclusion that the text was somehow copied from the Guo paper.

Regarding (1-4)

Drs. Wakayama and Obokata, and the staff who carried out the experiment, all explained that the karyotyping was carried out by Dr. Wakayama's staff, and that he gave the data to Dr. Obokata. The preparation of the cell sample was carried out in line with the explanation in the Methods section, but Dr. Wakayama explained that his staff carried out the hybridization and imaging using Applied Spectral Imaging's SKY FISH system, which was different from what was written in the Methods section. The image

files, including creation date information, were submitted. Dr. Wakayama explained that this section under Methods had been written by Dr. Obokata, and that she did not know the details of the experiment with hybridization and imaging.

Opinions

Regarding (1-3)

The Paper 1 Methods section in question consisted of 17 lines copied from the paper by Guo J., et al., without citing the source. This is absolutely not allowed, and this is something that is strictly taught at research institutions and universities. Appropriate quotation and citing of all sources is a matter of course for all researchers. Dr. Obokata's explanation that she did not possess a copy of the Guo paper, did not remember where she had copied the text from, and that it was simply oversight, is highly questionable.

Still, given the content of the text and the volume that was copied, the failure to cite the source cannot automatically be judged to have been done deliberately. Dr. Obokata correctly cites her sources in 40 places in the main text of the paper and in one other place in the Methods section. The Methods section in question is the only place where she fails to do so. Karyotyping is commonly carried out in many laboratories, and the same procedures are generally used. If Dr. Obokata was unfamiliar with the procedures, her explanation that Dr. Wakayama's protocol was a very simple one, and that she therefore searched for a more detailed explanation, is understandable. Given that the text she found provided an explanation of generally carried out procedures, it is not so irrational that she has no memory of where she got the text from. Likewise, the fact that she did not possess a copy of the Guo paper does not contradict her explanation that she merely forgot to cite the source. Her lack of memory on this point makes it impossible to conclude that her failure to cite the source constitutes misconduct.

Regarding (1-4)

Dr. Obokata failed to check the accuracy of her description with those who actually carried out the procedures or with Dr. Wakayama or the other co-authors. The co-authors also failed to check this section carefully before the paper was published. It is evident that some of the procedures in the description are different from what was actually carried out, but this cannot be judged as research misconduct.

The inaccuracies of (1-3) and (1-4) can be judged as the result of oversight, but a scientist has an obvious obligation to accurately record experimental procedures, and proper citation of quoted text is fundamental. Plagarism is unacceptable.

This experiment was carried out by Dr. Wakayama's staff, and the inaccuracy of the text could have been easily corrected if Dr. Wakayama had carefully checked this portion of the paper, and in this respect he bears responsibility. Still, his failure to detect Dr. Obokata's error was simple oversight, not research misconduct. There is no judgement of misconduct for Drs. Sasai and Niwa as they were not involved in this experiment.

(1-5)	The images for Figures 2d and 2e appear to be incorrect, and closely resemble images in Dr. Obokata's PhD dissertation.

Results of investigation

On February 20, the committee was presented by Drs. Sasai and Obokata with a request for correction and with supporting documentation. They brought up two points: One was that some of the immunofluorescence images of in vitro differentiated cells and teratoma (the central image in the bottom row of Figure 2d and the three images in the

bottom row of Figure 2e), actually were derived from STAP cells created out of bone marrow hematopoietic cells but not spleen hematopoietic cells; and the second point was that they were thinking of replacing the incorrect images. The supporting documentation they provided consisted of these image files. Dr. Obokata explained that she mistook the images because both the spleen and bone marrow hematopoietic cell samples had the same “hemato” (hematopoietic) label.

Later, it was discovered that the images in Paper 1 very closely resembled images she had used in her doctoral dissertation for Waseda University. At the time the request was made for a correction, however, it was not explained that the images had come from Dr. Obokata’s doctoral thesis. Both Dr. Sasai and Dr. Obokata said that they had thought it was allowable to use images from a doctoral thesis for a paper to be submitted to an academic journal and that there was therefore no need to explain that this is what had been done.

Paper 1 presents STAP cells created by subjecting the spleen cells of a 1-week old mouse to an acid bath, while in Dr. Obokata’s doctoral thesis she describes acquiring “sphere” cells (sphere-shaped cell clusters) by forcing the bone marrow cells of a 3 to 4-week old mouse through a narrow pipette in a process of applying mechanical stress to the cells. The two experimental conditions are quite different. Dr. Obokata claims not to have sufficiently recognized the difference between the two experiments and to have made a simple mistake in using the wrong images. An analysis of the images in Paper 1 confirmed that they were copied from a similarly positioned figure in her doctoral thesis. It was also found that the images in Paper 1 were the same as those in the paper that was submitted to *Nature* in April 2012 and which had been rejected. It was confirmed that in this rejected paper, there were 3 immunofluorescence images of differentiated cells from the “sphere” cells acquired through the mechanical stress procedure outlined in Dr. Obokata’s doctoral thesis, 3 hematoxylin and eosin stained images of teratoma generated by the “sphere” cells, as well as 3 more immunofluorescence images of teratoma, all closely resembling images in her doctoral thesis. When she later resubmitted her paper to *Nature*, Dr. Obokata replaced some of these images with those of STAP cells acquired through the acid treatment, but she explained that even then she did not notice the other incorrect images. We attempted to trace the source of the image data by looking through her lab notes, but there were only two notebooks covering a span of three years, and these contained so little detail that it was impossible to scientifically trace the source of the image data.

Dr. Sasai was informed of the incorrect images by Dr. Obokata only a few days before the February 20 interviews with the investigative committee. He explained that he immediately instructed Dr. Obokata to prepare accurate image data so that the submitted paper could be corrected. The immunofluorescence images of teratoma that were submitted to replace the incorrect images were created on February 19. Both Dr. Sasai and Dr. Obokata expressed deep regret for not telling the investigative committee that material had been used from a doctoral thesis, explaining that they had assumed it was permissible to do so, and that they did not think an explanation was necessary because they had been able to produce the correct images for replacement.

<u>Opinions</u>

It was determined that Dr. Obokata had used images in Paper 1 that very closely resembled images in her doctoral thesis. Yet the experimental criteria for the two papers were different. The core message of Paper 1 was that a very easy method using an acid bath had been discovered. It is hard to believe that Dr. Obokata was unaware of the different experiment conditions when she prepared the images. Also, there are traces around the images in Paper 1 that suggest they were cut out of an identical

arrangement of images in the doctoral thesis. This makes it very difficult to accept Dr. Obokata's assertion that she cut and pasted the images from the thesis to Paper 1 without realizing that they represented completely different experimental procedures. Still, it was found that data was handled extremely carelessly, so it is possible that data of unknown origin that could not be verified or traced scientifically was used in the submitted paper. Regardless, this data was extremely important in showing the pluripotency of the STAP cells, and the actions taken by Dr. Obokata completely undermine the credibility of the data. There is no doubt that she was fully aware of this danger, and we therefore conclude that this was an act of research misconduct involving fabrication.

Dr. Obokata carried out experiments to produce teratomas when she was working in Dr. Wakayama's laboratory as a visiting researcher, and later as the head of her own laboratory. As a laboratory head and the supervisor of these kinds of experiments, Dr. Wakayama had a responsibility to check the validity and accuracy of the data and to ensure that all data were handled properly. Dr. Sasai, also, was substantially involved in overseeing the writing of the paper, and was therefore equally responsible for confirming the validity and accuracy of the data. They were negligent in allowing this kind of fabrication, but though this does not extend to confirmation of their direct involvement in the fabrication, they still bear heavy responsibility given their standing. Dr. Niwa, on the other hand, did not become involved until at a very late stage in the paper preparation, and is therefore not considered to have been involved in research misconduct.

It is to be noted that the original explanations about the mistaken images by Dr. Sasai and others were insufficient. This failure endangered the accuracy of the investigation and an honest response was called for.

(2-1)	Paper 2: Regarding the images of fluorescence in mice placenta, the rightmost panel in Figure 1b is very similar to the lower panel in Figure 2g.

Results of investigation

Dr. Wakayama explained that these were two photos of the same chimera mouse generated from STAP cells, taken from different angles by Dr. Wakayama himself. He explained that he handed them to Dr. Obokata as electronic files after labeling them and including them with other chimeric embryo images.

Dr. Obokata explained that she obtained the two images from Dr. Wakayama, and with Dr. Sasai used them in preparing the figures for the paper. During the preliminary production of the paper, Dr. Obokata inserted the image under Fig. 2g as a control for comparison between STAP cells and the FI stem cells. Then, in the process of writing by Dr. Sasai, the structure of the paper changed, the order of the figures changed, and the image became unnecessary, so a decision was made not to include it. However, Dr. Obokata explained that they forgot to remove the image when they were editing the figures for the paper. Dr. Sasai further explained that the paper was submitted without him realizing the image had not been deleted, and that he failed to notice this during the editing and proofreading processes. He also explained that he neglected to instruct Dr. Obokata to delete the figure.

The bottom image of Figure 2g shows placenta GFP expression, but both the text and caption refer to embryo GFP expression, which only explains the top image of Figure 2g. The investigative committee was presented with date-stamped files showing the original structure of the figures with the location of the images and copies of the corresponding lab notes.

Opinions

The fluorescence placenta in Figure 1b (right panel) and that in Fig. 2g (bottom panel) are images that originated from the same chimera. There are, however, other images in the paper that are not referred to, either in the text or the figure legends, and it is possible to surmise that the bottom panel of Fig. 2g was included to show the existience of GFP-positive cells. Still, considering the fact that not all versions of the paper's editing were preserved so that the investigative committee could reconstruct the exact process as had been explained, it is plausible, given the date-stamped file data described above, that there was a previous version with the figures in a different position. As has already been pointed out, there are other images in the paper that are not referred to, either in the text or figure legends. Further investigation suggests that while there may be other reasons for these omissions besides forgetfullness, there are no materials that directly indicate anything exceeding negligence . Although this could be considered "falsification" as defined in RIKEN's Regulations on the Prevention of Research Misconduct, there is no evidence suggesting anything exceeding negligence, and this, therefore, is not judged to constitute research misconduct.

3. Summary

We concluded that there was research misconduct by Dr. Obokata on two points. Research misconduct warps the essence of science and significantly undermines credibility, not only within the science community, but also with the general public. Research misconduct is prohibited precisely because of the need to ensure robust, healthy exchange of information among scientists in their search for truth, and to promote the advancement of science. In manipulating the image data of two different gels and using data from two different experiments, Dr. Obokata acted in a manner that can by no means be permitted. This cannot be explained solely by her immaturity as a researcher. Given the poor quality of her laboratory notes it has become clearly evident that it will be extremely difficult for anyone else to accurately trace or understand her experiments, and this, too, is considered a serious obstacle to healthy information exchange. Dr. Obokata's actions and sloppy data management lead us to the conclusion that she sorely lacks, not only a sense of research ethics, but also integrity and humility as a scientific researcher. We were also forced to conclude that the normal system by which senior researchers should have been carefully checking all raw data did not work in this case. None of the other persons investigated were found to have actively participated in any kind of research misconduct, but as has already been noted, Drs. Wakayama and Sasai allowed the papers to be submitted to Nature without verifying the accuracy of the data, and they bear heavy responsibility for the research misconduct that resulted from this failure on their part.

Among the possible reasons for the failure of the normal system of checking on research results, is the change in research environment and the involvement of several senior researchers. Dr. Obokata continued research she had started at another institution at CDB, first while working in the Wakayama laboratory as a visiting researcher, and then later as the head of her own laboratory. As she neared the point of attaining results, Drs. Sasai and Niwa, two senior researchers other than Dr. Wakayama, became involved in reinforcing the data and writing the papers.

RIKEN must examine why the normal checking mechanisms did not function as they should have, and reconsider such issues as how responsibility should be allocated among different groups working together on joint research and among paper co-authors. RIKEN should also reexamine the whole process of data management, including the

management of laboratory notebooks, as well as the process from research proposal to collating results and presenting them in papers. RIKEN must promptly institute specific measures to ensure that this kind of research misconduct will never happen again.

RIKEN Research Paper Investigative Committee

Chair

Ishii, Shunsuke	Distinguished Senior Scientist, RIKEN Molecular Genetics Laboratory

Members

Iwama, Atsushi	Professor, Chiba University Graduate School of Medicine, Cellular & Molecular Medicine
Koseki, Haruhiko	Center Deputy Director, RIKEN Center for Integrated Medical Sciences Group Director, Laboratory for Developmental Genetics
Shinkai, Yoichi	Chief Scientist, RIKEN Cellular Memory Laboratory
Taga, Tetsuya	Vice President, Tokyo Medical and Dental University Professor, Department of Stem Cell Regulation
Watanabe, Jun	Attorney at Law, Watanabe Law Office

ARTICLE

doi:10.1038/nature12968

Stimulus-triggered fate conversion of somatic cells into pluripotency

Haruko Obokata[1,2,3], Teruhiko Wakayama[3]†, Yoshiki Sasai[4], Koji Kojima[1], Martin P. Vacanti[1,5], Hitoshi Niwa[6], Masayuki Yamato[7] & Charles A. Vacanti[1]

Here we report a unique cellular reprogramming phenomenon, called stimulus-triggered acquisition of pluripotency (STAP), which requires neither nuclear transfer nor the introduction of transcription factors. In STAP, strong external stimuli such as a transient low-pH stressor reprogrammed mammalian somatic cells, resulting in the generation of pluripotent cells. Through real-time imaging of STAP cells derived from purified lymphocytes, as well as gene rearrangement analysis, we found that committed somatic cells give rise to STAP cells by reprogramming rather than selection. STAP cells showed a substantial decrease in DNA methylation in the regulatory regions of pluripotency marker genes. Blastocyst injection showed that STAP cells efficiently contribute to chimaeric embryos and to offspring via germline transmission. We also demonstrate the derivation of robustly expandable pluripotent cell lines from STAP cells. Thus, our findings indicate that epigenetic fate determination of mammalian cells can be markedly converted in a context-dependent manner by strong environmental cues.

In the canalization view of Waddington's epigenetic landscape, fates of somatic cells are progressively determined as cellular differentiation proceeds, like going downhill. It is generally believed that reversal of differentiated status requires artificial physical or genetic manipulation of nuclear function such as nuclear transfer[1,2] or the introduction of multiple transcription factors[3]. Here we investigated the question of whether somatic cells can undergo nuclear reprogramming simply in response to external triggers without direct nuclear manipulation. This type of situation is known to occur in plants—drastic environmental changes can convert mature somatic cells (for example, dissociated carrot cells) into immature blastema cells, from which a whole plant structure, including stalks and roots, develops in the presence of auxins[4]. A challenging question is whether animal somatic cells have a similar potential that emerges under special conditions. Over the past decade, the presence of pluripotent cells (or closely relevant cell types) in adult tissues has been a matter of debate, for which conflicting conclusions have been reported by various groups[5–11]. However, no study so far has proven that such pluripotent cells can arise from differentiated somatic cells.

Haematopoietic cells positive for CD45 (leukocyte common antigen) are typical lineage-committed somatic cells that never express pluripotency-related markers such as Oct4 unless they are reprogrammed[12,13]. We therefore addressed the question of whether splenic CD45$^+$ cells could acquire pluripotency by drastic changes in their external environment such as those caused by simple chemical perturbations.

Low pH triggers fate conversion in somatic cells

CD45$^+$ cells were sorted by fluorescence-activated cell sorting (FACS) from the lymphocyte fraction of postnatal spleens (1-week old) of C57BL/6 mice carrying an *Oct4-gfp* transgene[14], and were exposed to various types of strong, transient, physical and chemical stimuli (described below). We examined these cells for activation of the *Oct4* promoter after culture for several days in suspension using DMEM/F12 medium supplemented with leukaemia inhibitory factor (LIF) and B27 (hereafter called LIF+B27 medium). Among the various perturbations, we were particularly interested in low-pH perturbations for two reasons. First, as shown below, low-pH treatment turned out to be most effective for the induction of *Oct4*. Second, classical experimental embryology has shown that a transient low-pH treatment under 'sublethal' conditions can alter the differentiation status of tissues. Spontaneous neural conversion from salamander animal caps by soaking the tissues in citrate-based acidic medium below pH 6.0 has been demonstrated previously[15–17].

Without exposure to the stimuli, none of the cells sorted with CD45 expressed *Oct4*-GFP regardless of the culture period in LIF+B27 medium. In contrast, a 30-min treatment with low-pH medium (25-min incubation followed by 5-min centrifugation; Fig. 1a; the most effective range was pH 5.4–5.8; Extended Data Fig. 1a) caused the emergence of substantial numbers of spherical clusters that expressed *Oct4*-GFP in day-7 culture (Fig. 1b). Substantial numbers of GFP$^+$ cells appeared in all cases performed with neonatal splenic cells ($n = 30$ experiments). The emergence of *Oct4*-GFP$^+$ cells at the expense of CD45$^+$ cells was also observed by flow cytometry (Fig. 1c, top, and Extended Data Fig. 1b, c). We next fractionated CD45$^+$ cells into populations positive and negative for CD90 (T cells), CD19 (B cells) and CD34 (haematopoietic progenitors[18]), and subjected them to low-pH treatment. Cells of these fractions, including T and B cells, generated *Oct4*-GFP$^+$ cells at an efficacy comparable to unfractionated CD45$^+$ cells (25–50% of surviving cells on day 7), except for CD34$^+$ haematopoietic progenitors[19], which rarely produced *Oct4*-GFP$^+$ cells (<2%; Extended Data Fig. 1d).

Among maintenance media for pluripotent cells[20], the appearance of *Oct4*-GFP$^+$ cells was most efficient in LIF+B27 medium, and did not occur in mouse epiblast-derived stem-cell (EpiSC) medium[21,22] (Extended Data Fig. 1e). The presence or absence of LIF during days 0–2 did not substantially affect the frequency of *Oct4*-GFP$^+$ cell generation on day 7 (Extended Data Fig. 1f), whereas the addition of LIF during days 4–7 was not sufficient, indicating that LIF dependency started during days 2–4.

[1]Laboratory for Tissue Engineering and Regenerative Medicine, Brigham and Women's Hospital, Harvard Medical School, Boston, Massachusetts 02115, USA. [2]Laboratory for Cellular Reprogramming, RIKEN Center for Developmental biology, Kobe 650-0047, Japan. [3]Laboratory for Genomic Reprogramming, RIKEN Center for Developmental biology, Kobe 650-0047, Japan. [4]Laboratory for Organogenesis and Neurogenesis, RIKEN Center for Developmental biology, Kobe 650-0047, Japan. [5]Department of Pathology, Irwin Army Community Hospital, Fort Riley, Kansas 66442, USA. [6]Laboratory for Pluripotent Stem Cell Studies, RIKEN Center for Developmental biology, Kobe 650-0047, Japan. [7]Institute of Advanced Biomedical Engineering and Science, Tokyo Women's Medical University, Tokyo 162-8666, Japan. †Present address: Faculty of Life and Environmental Sciences, University of Yamanashi, Yamanashi 400-8510, Japan.

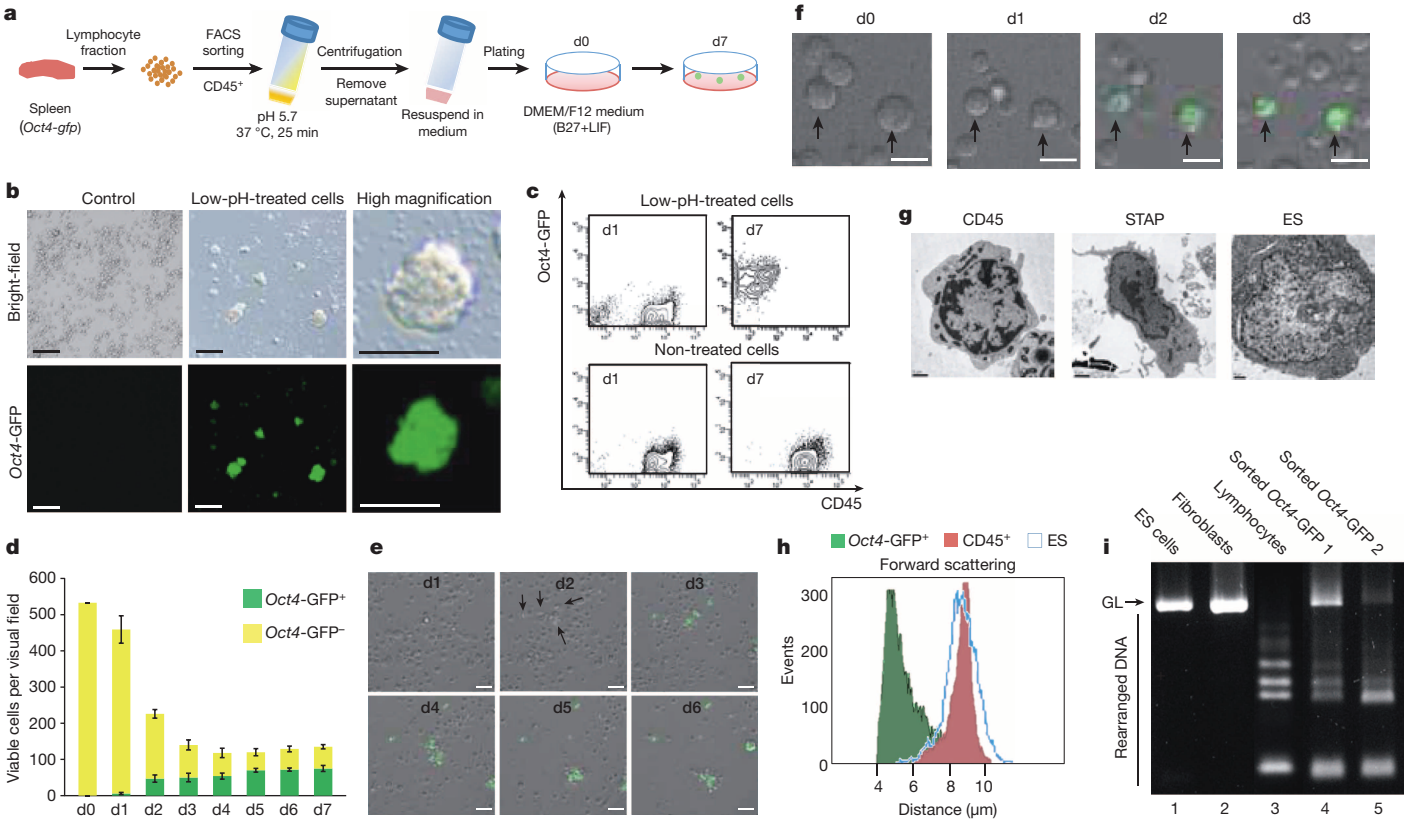

Figure 1 | Stimulus-triggered conversion of lymphocytes into *Oct4*-GFP$^+$ cells. **a**, Schematic of low-pH treatment. **b**, *Oct4*-GFP$^+$ cell clusters appeared in culture of low-pH-treated CD45$^+$ cells (middle; high magnification, right) on day 7 (d7) but not in culture of control CD45$^+$ cells (left). Top: bright-field view; bottom, GFP signals. Scale bar, 100 μm. **c**, FACS analysis. The *x* axis shows CD45 epifluorescence level; *y* axis shows *Oct4*-GFP level. Non-treated, cultured in the same medium but not treated with low pH. **d**, GFP$^+$ (green) and GFP$^-$ (yellow) cell populations (average cell numbers per visual field; ×10 objective lens). $n = 25$; error bars show average ± s.d. **e**, Snapshots of live imaging of culture of low-pH-treated CD45$^+$ cells (*Oct4-gfp*). Arrows indicate cells that started expressing *Oct4*-GFP. Scale bar, 50 μm. **f**, Cell size reduction in low-pH-treated CD45$^+$ cells on day 1 before turning on *Oct4*-GFP without cell division on day 2. In this live imaging, cells were plated at a half density for easier viewing of individual cells. Scale bar, 10 μm. **g**, Electron microscope analysis. Scale bar, 1 μm. **h**, Forward scattering analysis of *Oct4*-GFP$^-$CD45$^+$ cells (red) and *Oct4*-GFP$^+$CD45$^-$ cells (green) on day 7. Blue line, ES cells. **i**, Genomic PCR analysis of (D)J recombination at the *Tcrb* gene. GL is the size of the non-rearranged germline type, whereas the smaller ladders correspond to the alternative rearrangements of J exons. Negative controls, lanes 1, 2; positive controls, lane 3; FACS-sorted *Oct4*-GFP$^+$ cells (two independent preparations on day 7), lanes 4, 5.

Most of the surviving cells on day 1 were still CD45$^+$ and *Oct4*-GFP$^-$. On day 3, the total cell numbers were reduced to between one-third to one-half of the day 0 population (Fig. 1d; see Extended Data Fig. 1g, h for apoptosis analysis), and a substantial number of total surviving cells became *Oct4*-GFP$^+$ (Fig. 1d), albeit with relatively weak signal intensity. On day 7, a significant number of *Oct4*-GFP$^+$CD45$^-$ cells (one-half to two-thirds of total surviving cells) constituted a distinct population from the *Oct4*-GFP$^-$CD45$^-$ cells (Fig. 1c, top, day 7, and Fig. 1d). No obvious generation of *Oct4*-GFP$^+$CD45$^-$ populations was seen in non-treated CD45$^+$ cells cultured similarly but without low-pH treatment (Fig. 1c, bottom).

Low-pH-treated CD45$^+$ cells, but not untreated cells, gradually turned on GFP signals over the first few days (Fig. 1e, Supplementary Videos 1 and 2 and Extended Data Fig. 2a), whereas CD45 immunoreactivity became gradually reduced in the cells that demonstrated *Oct4*-GFP expression (Fig. 1f and Extended Data Fig. 2b). By day 5, the *Oct4*-GFP$^+$ cells attached together and formed clusters by accretion. These GFP$^+$ clusters (but not GFP$^-$ cells) were quite mobile and often showed cell processes on moving (Supplementary Video 1).

The *Oct4*-GFP$^+$ cells demonstrated a characteristic small cell size with little cytoplasm and also showed a distinct fine structure of the nucleus compared with that of parental CD45$^+$ lymphocytes (Fig. 1g). The *Oct4*-GFP$^+$ cells on day 7 were smaller than non-treated CD45$^+$ cells (Fig. 1g, h and Extended Data Fig. 2c) and embryonic stem (ES) cells (Fig. 1h), both of which are generally considered to be small in size. The diameter of low-pH-treated CD45$^+$ cells became reduced during the first 2 days, even before they started *Oct4*-GFP expression (Fig. 1f), whereas the onset of GFP expression was not accompanied by cell divisions. Consistent with this, no substantial 5-ethynyl-2′-deoxyuridine (EdU) uptake was observed in the *Oct4*-GFP$^+$ cells after the stressor (Extended Data Fig. 2d).

The lack of substantial proliferation argues against the possibility that CD45$^-$ cells, contaminating as a very minor population in the FACS-sorted CD45$^+$ cells, quickly grew and formed a substantial *Oct4*-GFP$^+$ population over the first few days after the low-pH treatment. In addition, genomic rearrangements of *Tcrb* (T-cell receptor gene) were observed in *Oct4*-GFP$^+$ cells derived from FACS-purified CD45$^+$ cells and CD90$^+$CD45$^+$ T cells (Fig. 1i, lanes 4, 5, and Extended Data Fig. 2e–g), indicating at least some contribution from lineage-committed T cells. Thus, *Oct4*-GFP$^+$ cells were generated *de novo* from low-pH-treated CD45$^+$ haematopoietic cells by reprogramming, rather than by simple selection of stress-enduring cells[23].

Low-pH-induced Oct4$^+$ cells have pluripotency

On day 7, the *Oct4*-GFP$^+$ spheres expressed pluripotency-related marker proteins[22] (Oct4, SSEA1, Nanog and E-cadherin; Fig. 2a) and marker genes (*Oct4*, *Nanog*, *Sox2*, *Ecat1* (also called *Khdc3*), *Esg1* (*Dppa5a*), *Dax1* (*Nrob1*) and *Rex1* (*Zfp42*); Fig. 2b and Extended Data Fig. 3a) in a manner comparable to those seen in ES cells[24]. Moderate levels of expression of these pluripotency marker genes were observed on day 3

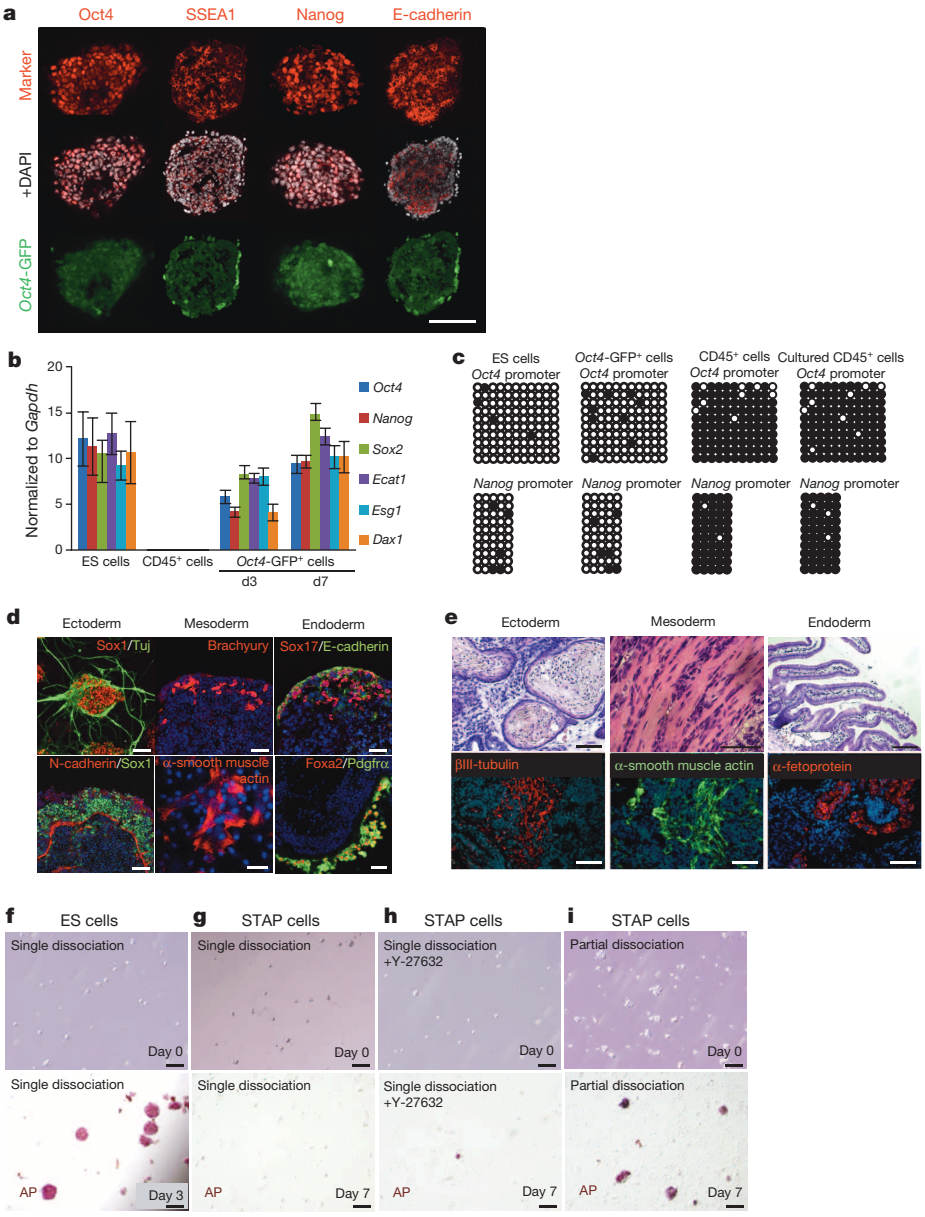

Figure 2 | Low-pH-induced *Oct4*-GFP$^+$ cells represent pluripotent cells. **a**, Immunostaining for pluripotent cell markers (red) in day 7 *Oct4*-GFP$^+$ (green) clusters. DAPI, white. Scale bar, 50 μm. **b**, qPCR analysis of pluripotency marker genes. From left to right, mouse ES cells; parental CD45$^+$ cells; low-pH-induced *Oct4*-GFP$^+$ cells on day 3; low-pH-induced *Oct4*-GFP$^+$ cells on day 7. $n = 3$; error bars show average ± s.d. **c**, DNA methylation study by bisulphite sequencing. Filled and open circles indicate methylated and non-methylated CpG, respectively. **d**, Immunostaining analysis of *in vitro* differentiation capacity of day 7 *Oct4*-GFP$^+$ cells. Ectoderm: the neural markers Sox1/Tuj1 (100%, $n = 8$) and N-cadherin (100%, $n = 5$). Mesoderm: smooth muscle actin (50%, $n = 6$) and brachyury (40%, $n = 5$). Endoderm: Sox17/E-cadherin (67%, $n = 6$) and Foxa2/Pdgfrα (67%, $n = 6$). Scale bar, 50 μm. **e**, Teratoma formation assay of day 7 clusters of *Oct4*-GFP$^+$ cells. Haematoxylin and eosin staining showed keratinized epidermis (ectoderm), skeletal muscle (mesoderm) and intestinal villi (endoderm), whereas immunostaining showed expression of Tuj1 (neurons), smooth muscle actin and α-fetoprotein. Scale bar, 100 μm. **f**–**i**, Dissociation culture of ES cells and STAP cells (additional 7 days from day 7; **f**, **g**) on gelatin-coated dishes. Top, bright-field; bottom, alkaline phosphatase (AP) staining. Partially dissociated STAP cells slowly generated small colonies (**i**), whereas dissociated STAP cells did not, even in the presence of the ROCK inhibitor (**g**, **h**), which allows dissociation culture of EpiSCs[29].

(Fig. 2b and Extended Data Fig. 3b). Notably, the *Oct4*-GFP$^+$ cells on day 3, but not on day 7, expressed early haematopoietic marker genes such as *Flk1* (also called *Kdr*) and *Tal1* (Extended Data Fig. 3c), indicating that *Oct4*-GFP$^+$ cells on day 3, as judged by their expression pattern at the population level, were still in a dynamic process of conversion.

On day 7, unlike CD45$^+$ cells and like ES cells, low-pH-induced *Oct4*-GFP$^+$ cells displayed extensive demethylation at the *Oct4* and *Nanog* promoter areas (Fig. 2c), indicating that these cells underwent a substantial reprogramming of epigenetic status in these key genes for pluripotency.

In vitro differentiation assays[25–27] demonstrated that low-pH-induced *Oct4*-GFP$^+$ cells gave rise to three-germ-layer derivatives (Fig. 2d) as well as visceral endoderm-like epithelium (Extended Data Fig. 3d). When grafted into mice, low-pH-induced *Oct4*-GFP$^+$ cell clusters formed teratomas (40%, $n = 20$) (Fig. 2e and Extended Data Fig. 4a–c) but no teratocarcinomas that persistently contained *Oct4*-GFP$^+$ cells ($n = 50$). Because some cellular variation was observed in the signal levels of *Oct4*-GFP within the clusters, we sorted GFP-strong cells (a major population) and GFP-dim cells (a minor population) by FACS on day 7 and separately injected them into mice. In this case, only GFP-strong cells formed teratomas (Extended Data Fig. 4d). In quantitative polymerase chain reaction (qPCR) analysis, the GFP-strong population expressed pluripotency marker genes but not early lineage-specific marker genes, whereas the GFP-dim cells showed substantial expression of some early lineage-specific marker genes (*Flk1*, *Gata2*, *Gata4*, *Pax6* and *Sox17*; Extended Data Fig. 4e) but not *Nanog* and *Rex1*. These observations indicate that three-germ-layer derivatives were generated from the GFP-strong cells expressing pluripotency marker genes, rather than from GFP-dim cells that seem to contain partially reprogrammed cells.

Collectively, these findings show that the differentiation state of a committed somatic cell lineage can be converted into a state of pluripotency by strong stimuli given externally. Hereafter, we refer to the fate conversion from somatic cells into pluripotent cells by strong external stimuli such as low pH as 'stimulus-triggered acquisition of pluripotency' (STAP) and the resultant cells as STAP cells. Under their establishment conditions, these STAP cells were rarely proliferative (Extended Data Figs 2d and 5a, b). Comparative genomic hybridization array analysis of STAP cells indicated no major global changes in chromosome number (Extended Data Fig. 5c).

STAP cells compared to ES cells

STAP cells, unlike mouse ES cells, showed a limited capacity for self-renewal in the LIF-containing medium and did not efficiently form

colonies in dissociation culture (Fig. 2f, g), even in the presence of the ROCK inhibitor Y-27632, which suppresses dissociation-induced apoptosis[28,29] (Fig. 2h). Also, even under high-density culture conditions after partial dissociation (Fig. 2i), STAP cell numbers started to decline substantially after two passages. Furthermore, expression of the ES cell marker protein Esrrβ was low in STAP cells (Extended Data Fig. 5d, e). In general, female ES cells do not show X-chromosomal inactivation[30] and contain no H3K27me3-dense foci (indicative of inactivated X chromosomes), unlike female CD45$^+$ cells and EpiSCs. In contrast, H3K27me3-dense foci were found in ~40% of female STAP cells strongly positive for *Oct4*-GFP (Extended Data Fig. 5f, g).

STAP cells were also dissimilar to mouse EpiSCs, another category of pluripotent stem cell[21,22,29,31], and were positive for Klf4 and negative for the epithelial tight junction markers claudin 7 and ZO-1 (Extended Data Fig. 5d, e).

STAP cells from other tissue sources

We next performed similar conversion experiments with somatic cells collected from brain, skin, muscle, fat, bone marrow, lung and liver tissues of 1-week-old *Oct4-gfp* mice. Although conversion efficacy varied, the low-pH-triggered generation of *Oct4*-GFP$^+$ cells was observed in day 7 culture of all tissues examined (Fig. 3a and Extended Data Fig. 6a–c), including mesenchymal cells of adipose tissues (Fig. 3a–c) and neonatal cardiac cells that were negatively sorted for CD45 by FACS (Fig. 3d–g; see Extended Data Fig. 6d for suppression of cardiac genes such as *Nkx2-5* and cardiac actin).

Chimaera formation and germline transmission in mice

We next performed a blastocyst injection assay with STAP cells that were generated from CD45$^+$ cells of neonatal mice constitutively expressing GFP (this C57BL/6 line with *cag-gfp* transgenes is referred to hereafter as B6GFP). We injected STAP cell clusters en bloc that were manually cut into small pieces using a microknife (Fig. 4a). A high-to-moderate contribution of GFP-expressing cells was seen in the chimaeric embryos (Fig. 4b and Extended Data Fig. 7a). These chimaeric mice were born at a substantial rate and all developed normally (Fig. 4c and Extended Data Fig. 7b).

CD45$^+$ cell-derived STAP cells contributed to all tissues examined (Fig. 4d). Furthermore, offspring derived from STAP cells were born to the chimaeric mice (Fig. 4e and Extended Data Fig. 7c), demonstrating their germline transmission, which is a strict criterion for pluripotency as well as genetic and epigenetic normality[32,33]. Furthermore, in a tetraploid (4N) complementation assay, which is considered to be the most rigorous test for developmental potency[34,35] (Fig. 4a, bottom), CD45$^+$ cell-derived STAP cells (from F_1 mice of B6GFP × 129/Sv or DBA/2) generated all-GFP$^+$ embryos on embryonic day (E)10.5 (Fig. 4f, Extended Data Fig. 7d and Supplementary Video 3), demonstrating that STAP cells alone are sufficient to construct an entire embryonic structure. Thus, STAP cells have the developmental capacity to differentiate into all somatic-cell lineages as well as germ-cell lineages *in vivo*.

Expandable pluripotent cell lines from STAP cells

STAP cells have a limited self-renewal capacity under the conditions used for establishment (Fig. 2g and Extended Data Figs 2e and 5a). However, in the context of the embryonic environment, a small fragment of a STAP cell cluster could grow even into a whole embryo (Fig. 4f). With this in mind, we next examined whether STAP cells have the potential to generate expandable pluripotent cell lines *in vitro* under certain conditions.

STAP cells could not be efficiently maintained for additional passages in conventional LIF+FBS-containing medium or 2i medium[20] (most STAP cells died in 2i medium within 7 days; Extended Data Fig. 8a). Notably, an adrenocorticotropic hormone (ACTH)+LIF-containing medium (hereafter called ACTH medium) known to facilitate clonal expansion of ES cells[36] supported outgrowth of STAP cell colonies. When cultured in this medium on a MEF feeder or gelatin, a portion of STAP cell clusters started to grow (Fig. 5a, bottom; such outgrowth was typically found in 10–20% of wells in single cluster culture using 96-well plates and in >75% when 12 clusters were plated

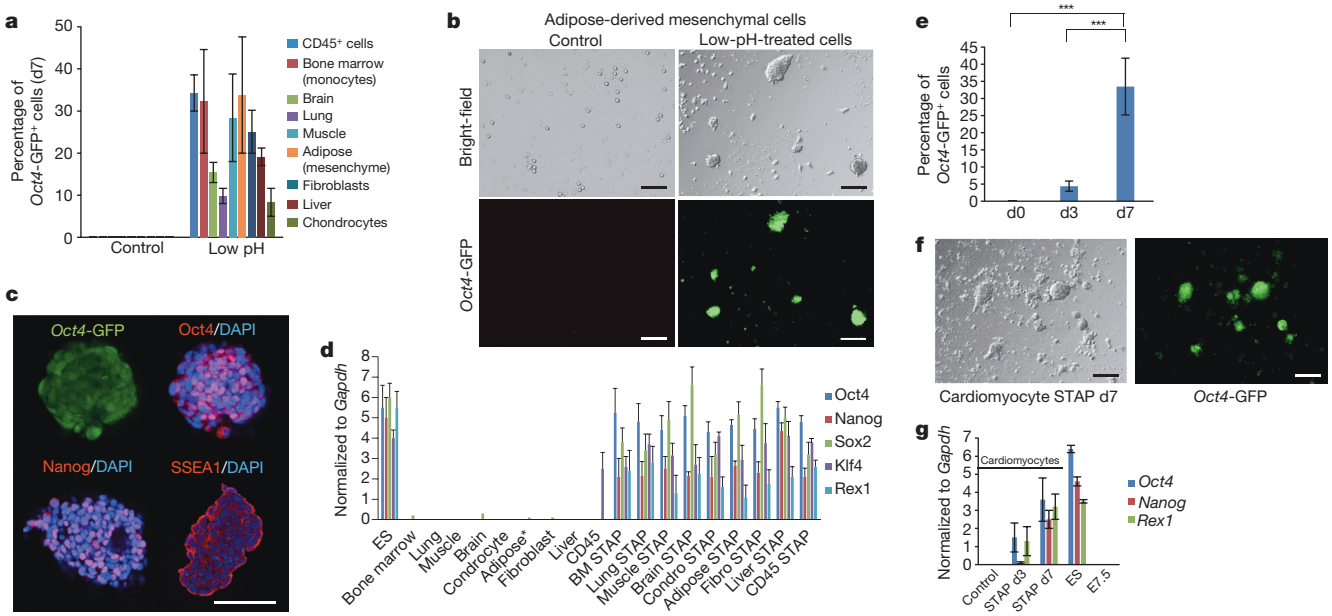

Figure 3 | STAP cell conversion from a variety of cells by low-pH treatment. **a**, Percentage of *Oct4*-GFP$^+$ cells in day 7 culture of low-pH-treated cells from different origins (1×10^5 cells per ml × 3 ml). The number of surviving cells on day 7 compared to the plating cell number was 20–30%, except for lung, muscle and adipose cells, for which surviving cells were ~10% (n=3, average ± s.d.). **b**, *Oct4*-GFP$^+$ cell clusters were induced by low-pH treatment from adipose-tissue-derived mesenchymal cells on day 7. Scale bar, 100 μm. **c**, Expression of pluripotent cell markers in day 7 clusters of low-pH-treated adipose-tissue-derived mesenchymal cells. Scale bar, 50 μm. **d**, Expression of pluripotency marker genes in STAP cells derived from various tissues. Gene expressions were normalized by *Gapdh* (n = 3, average ± s.d.). Asterisk indicates adipose tissue-derived mesenchymal cells. **e**, Quantification of *Oct4*-GFP$^+$ cells in culture of low-pH-treated neonatal cardiac muscle cells. ***$P < 0.001$; Tukey's test (n = 3). **f**, Generation of *Oct4*-GFP$^+$ cell clusters (d7) from CD45$^-$ cardiac muscle cells. **g**, qPCR analysis of pluripotency marker genes in STAP cells from CD45$^-$ cardiac muscle cells.

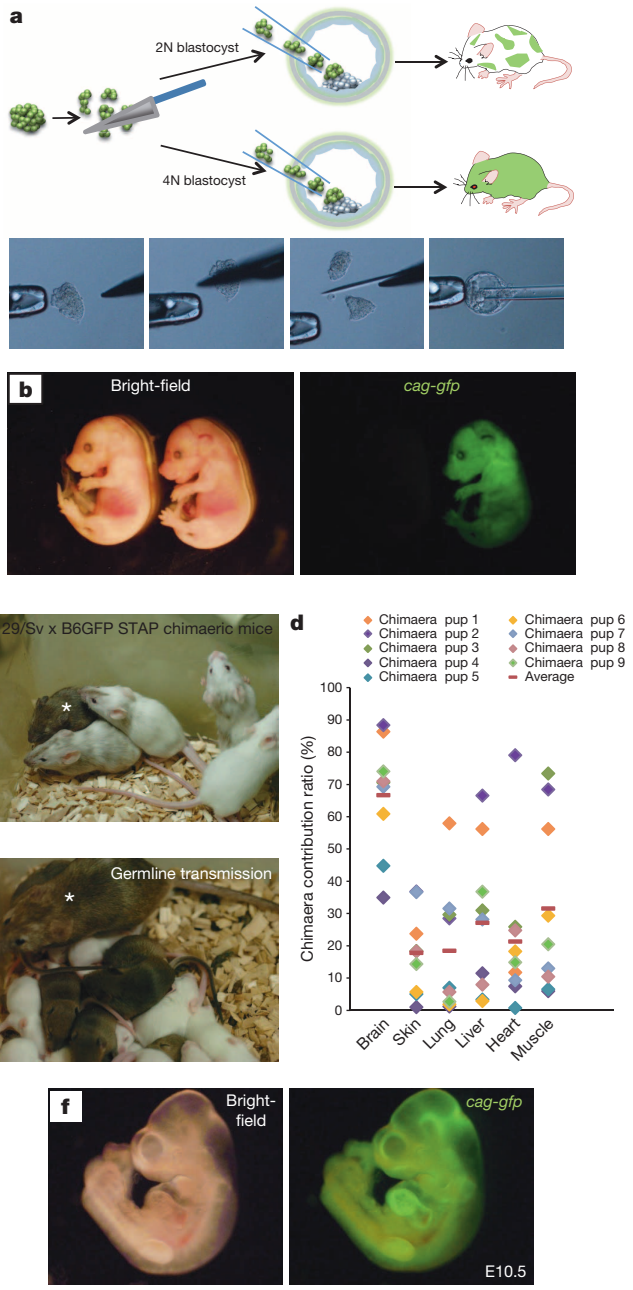

Figure 4 | Chimaeric mouse generation from STAP cells. **a**, Schematic of chimaeric mouse generation. **b**, E13.5 chimaera fetuses from 2N blastocytes injected with STAP cells (derived from B6GFP CD45$^+$ cells carrying *cag-gfp*). **c**, Adult chimaeric mice generated by STAP-cell (B6GFP × 129/Sv; agouti) injection into blastocysts (ICR strain; albino). Asterisk indicates a highly contributed chimaeric mouse. **d**, Chimaera contribution analysis. Tissues from nine pups were analysed by FACS. **e**, Offspring of chimaeric mice derived from STAP cells. Asterisk indicates the same chimaeric mouse shown in **c**. **f**, E10.5 embryo generated in the tetraploid complementation assay with STAP cells (B6GFP × 129/Sv).

per well). These growing colonies looked similar to those of mouse ES cells and expressed a high level of *Oct4*-GFP.

After culturing in ACTH medium for 7 days, this growing population of cells, unlike parental STAP cells, could be passaged as single cells (Fig. 5a, bottom, and Fig. 5b), grow in 2i medium (Extended Data Fig. 8a) and expand exponentially, up to at least 120 days of culture (Fig. 5c; no substantial chromosomal abnormality was seen; Extended Data Fig. 8b, c). Hereafter, we refer to the proliferative cells derived from STAP cells as STAP stem cells.

STAP stem cells expressed protein and RNA markers for pluripotent cells (Fig. 5d, e), showed low DNA methylation levels at the *Oct4* and *Nanog* loci (Extended Data Fig. 8d), and had a nuclear fine structure similar to that of ES cells (Extended Data Fig. 8e; few electron-dense areas corresponding to heterochromatin). In differentiation culture[25–27], STAP stem cells generated ectodermal, mesodermal and endodermal derivatives *in vitro* (Fig. 5f–h and Extended Data Fig. 8f, g), including beating cardiac muscles (Supplementary Video 4), and formed teratomas *in vivo* (Fig.5i and Extended Data Fig. 8h; no teratocarcinomas, $n = 40$). After blastocyst injection, STAP stem cells efficiently contributed to chimaeric mice (Fig. 5j), in which germline transmission was seen (Extended Data Fig. 8i). Even in tetraploid complementation assays, injected STAP stem cells could generate mice capable of growing to adults and producing offspring (Fig. 5k, l; in all eight independent lines, Extended Data Fig. 8j).

In addition to their expandability, we noticed at least two other differences between STAP stem cells and parental STAP cells. First, the expression of the ES cell marker protein Esrrβ, which was undetectable in STAP cells (Extended Data Fig. 5d, e), was clearly seen in STAP stem cells (Fig. 5e). Second, the presence of H3K27me3 foci, which was found in a substantial proportion of female STAP cells, was no longer observed in STAP stem cells (Extended Data Figs 5f and 8k). Thus, STAP cells have the potential to give rise to expandable cell lines that exhibit features similar to those of ES cells.

Discussion

This study has revealed that somatic cells latently possess a surprising plasticity. This dynamic plasticity—the ability to become pluripotent cells—emerges when cells are transiently exposed to strong stimuli that they would not normally experience in their living environments.

Low-pH treatment was also used in the 'autoneuralization' experiment[15–17] by Holtfreter in 1947, in which exposure to acidic medium caused tissue-autonomous neural conversion of salamander animal caps *in vitro* in the absence of Spemann's organizer signals. Although the mechanism has remained elusive, Holtfreter hypothesized that the strong stimulus releases the animal cap cells from some intrinsic inhibitory mechanisms that suppress fate conversion or, in his words, they pass through 'sublethal cytolysis' (meaning stimulus-evoked lysis of the cell's inhibitory state)[15,37]. Although Holtfreter's study and ours differ in the direction of fate conversion—orthograde differentiation and nuclear reprogramming, respectively—these phenomena may share some common aspects, particularly with regard to sublethal stimulus-evoked release from a static (conversion-resisting) state in the cell.

A remaining question is whether cellular reprogramming is initiated specifically by the low-pH treatment or also by some other types of sublethal stress such as physical damage, plasma membrane perforation, osmotic pressure shock, growth-factor deprivation, heat shock or high Ca^{2+} exposure. At least some of these stressors, particularly physical damage by rigorous trituration and membrane perforation by streptolysin O, induced the generation of *Oct4*-GFP$^+$ cells from CD45$^+$ cells (Extended Data Fig. 9a; see Methods). These findings raise the possibility that certain common regulatory modules, lying downstream of these distantly related sublethal stresses, act as a key for releasing somatic cells from the tightly locked epigenetic state of differentiation, leading to a global change in epigenetic regulation. In other words, unknown cellular functions, activated by sublethal stimuli, may set somatic cells free from their current commitment to recover the naive cell state.

Our present finding of an unexpectedly large capacity for radical reprogramming in committed somatic cells raises various important questions. For instance, why, and for what purpose, do somatic cells latently possess this self-driven ability for nuclear reprogramming, which emerges only after sublethal stimulation, and how, then, is this reprogramming mechanism normally suppressed? Furthermore, why isn't teratoma (or pluripotent cell mass) formation normally seen in *in vivo* tissues that may receive strong environmental stress? In our preliminary study, experimental reflux oesophagitis locally induced moderate

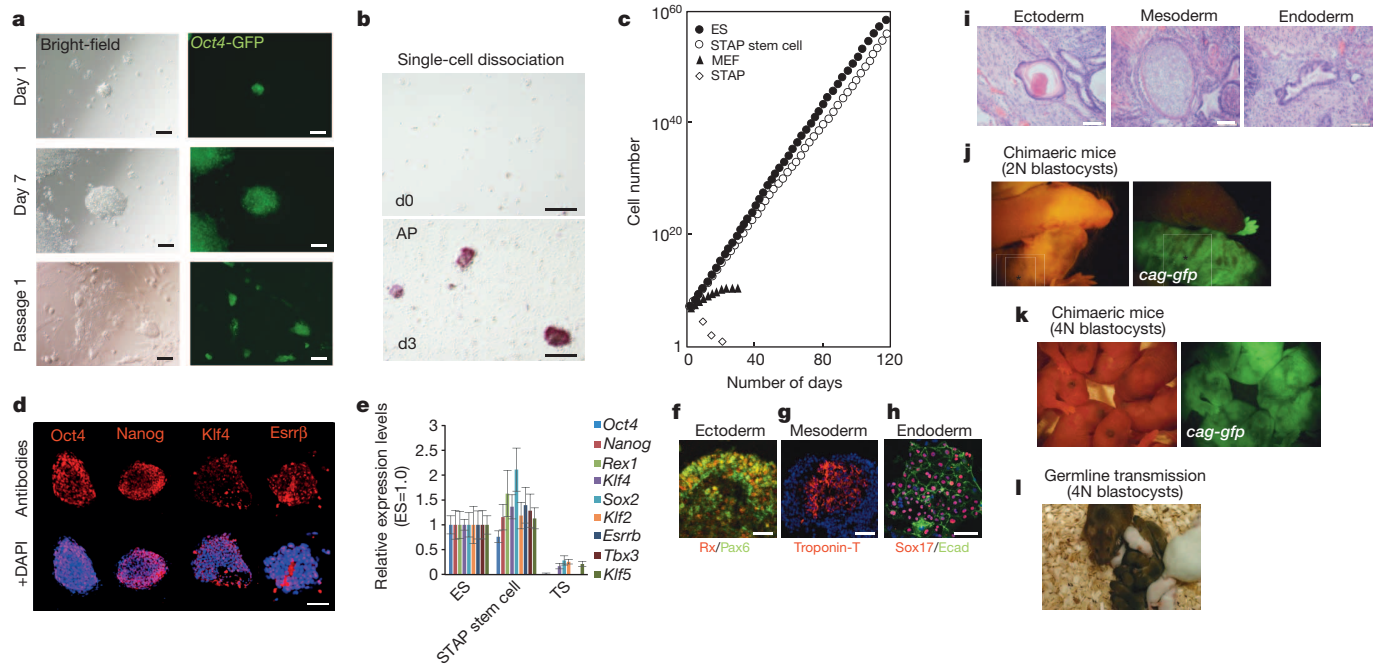

Figure 5 | ES-cell-like stem cells can be derived from STAP cells. **a**, Growth of STAP stem cells carrying *Oct4-gfp*. Scale bar, 50 μm. **b**, Dissociation culture of STAP stem cells to form colonies. Scale bar, 100 μm. **c**, Robust growth of STAP stem cells in maintenance culture. Similar results were obtained with eight independent lines. In contrast, parental STAP cells decreased in number quickly. **d**, Immunostaining of STAP stem cells for pluripotency markers (red). Scale bar, 50 μm. **e**, qPCR analysis of pluripotency marker gene expression. **f**–**h**, *In vitro* differentiation assays into three-germ-layer derivatives. **f**, Ectoderm: $Rx^+/Pax6^+$ (retinal epithelium; 83%, $n = 6$). **g**, Mesoderm: troponin-T^+ (cardiac muscle; 50%, $n = 6$). **h**, Endoderm: $Sox17^+$/E-cadherin$^+$ (endodermal progenitors; 67%, $n = 6$). Scale bar, 50 μm. **i**, Teratoma formation assays. Formation of keratinized epidermis (ectoderm; left), cartilage (mesoderm; middle) and bronchial-like epithelium (endoderm; right) is shown. Scale bar, 100 μm. **j**, Blastocyst injection assays. These pictures of live animals were taken serially (asterisk indicates the same chimaeric pup). **k**, **l**, Tetraploid complementation assay. 'All-GFP^+' pups were born (**k**) and germline transmission was observed (**l**).

expression of *Oct4*-GFP but not endogenous Nanog in the mouse oesophageal mucosa (Extended Data Fig. 9b). Therefore, an intriguing hypothesis for future research is that the progression from initial *Oct4* activation to further reprogramming is suppressed by certain inhibitory mechanisms *in vivo*.

The question of why and how this self-driven reprogramming is directed towards the pluripotent state is fundamentally important, given that STAP reprogramming takes a remarkably short period, only a few days for substantial expression of pluripotency marker genes, unlike transgene- or chemical-induced iPS cell conversion[38]. Thus, our results cast new light on the biological meaning of diverse cellular states in multicellular organisms.

METHODS SUMMARY

Tissue collection and low-pH exposure. To isolate haematopoietic cells, spleens were excised from 1-week-old *Oct4-gfp* C57BL/6 mice, minced by scissors and mechanically dissociated with pasture pipettes. Dissociated cells were collected, re-suspended in DMEM medium and added to the same volume of lympholyte (Cedarlane), then centrifuged at 1,000*g* for 20 min. CD45-positive cells were sorted by FACS Aria (BD Biosciences), and treated with low-pH HBSS solution (pH 5.7 for 25 min at 37 °C), centrifuged for 5 min to remove supernatant, and plated to non-adhesive culture plates in DMEM/F12 medium supplemented with 1,000 U LIF (Sigma) and B27 (Invitrogen). Although *Oct4*-GFP^+ cells (expressing pluripotency-related protein and gene markers and capable of differentiating into three germ-layer derivatives) were also generated from lymphocytes of young adult mice (for example, 6-week-old) under the same culture conditions, their proportion in culture was reduced by several to ten folds as compared to neonatal lymphocytes when lymphocytes were isolated from 1-month-old mice or older. Live imaging was performed using specially assembled confocal microscope systems with a CO_2 incubator[39], and CD45 immunoreactivity in live cells was examined as described[40].

***In vivo* and *in vitro* differentiation assay.** STAP cells were seeded onto a sheet $3 \times 3 \times 1$ mm, composed of a non-woven mesh of polyglycolic acid fibres and implanted subcutaneously into the dorsal flanks of 4-week-old NOD/SCID mice. To examine *in vitro* differentiation, STAP cells and STAP stem cells were collected at 7 days and subjected to SDIA or SFEBq culture[25,26] for neural differentiation and to embryoid body culture for mesodermal and endodermal[27] differentiation.

Online Content Any additional Methods, Extended Data display items and Source Data are available in the online version of the paper; references unique to these sections appear only in the online paper.

Received 10 March; accepted 20 December 2013.

1. Gurdon, J. B. The developmental capacity of nuclei taken from intestinal epithelium cells of feeding tadpoles. *J. Embryol. Exp. Morphol.* **10,** 622–640 (1962).
2. Wakayama, T., Perry, A. C., Zuccotti, M., Johnson, K. R. & Yanagimachi, R. Full-term development of mice from enucleated oocytes injected with cumulus cell nuclei. *Nature* **394,** 369–374 (1998).
3. Takahashi, K. & Yamanaka, S. Induction of pluripotent stem cells from mouse embryonic and adult fibroblast cultures by defined factors. *Cell* **126,** 663–676 (2006).
4. Thorpe, T. A. History of plant tissue culture. *Mol. Biotechnol.* **37,** 169–180 (2007).
5. Jiang, Y. *et al.* Pluripotency of mesenchymal stem cells derived from adult marrow. *Nature* **418,** 41–49 (2002).
6. D'Ippolito, G. *et al.* Marrow-isolated adult multilineage inducible (MIAMI) cells, a unique population of postnatal young and old human cells with extensive expansion and differentiation potential. *J. Cell Sci.* **117,** 2971–2981 (2004).
7. Kucia, M. *et al.* A population of very small embryonic-like (VSEL) $CXCR4^+SSEA\text{-}1^+Oct\text{-}4^+$ stem cells identified in adult bone marrow. *Leukemia* **20,** 857–869 (2006).
8. Kuroda, Y. *et al.* Unique multipotent cells in adult human mesenchymal cell populations. *Proc. Natl Acad. Sci. USA* **107,** 8639–8643 (2010).
9. Obokata, H. *et al.* The potential of stem cells in adult tissues representative of the three germ layers. *Tissue Eng. Part A* **17,** 607–615 (2011).
10. Lengner, C. J., Welstead, G. G. & Jaenisch, R. The pluripotency regulator Oct4: a role in somatic stem cells? *Cell Cycle* **7,** 725–728 (2008).
11. Berg, J. S. & Goodell, M. A. An argument against a role for Oct4 in somatic stem cells. *Cell Stem Cell* **1,** 359–360 (2007).
12. Hong, H. *et al.* Suppression of induced pluripotent stem cell generation by the p53-p21 pathway. *Nature* **460,** 1132–1135 (2009).
13. Hanna, J. *et al.* Direct reprogramming of terminally differentiated mature B lymphocytes to pluripotency. *Cell* **133,** 250–264 (2008).
14. Ohbo, K. *et al.* Identification and characterization of stem cells in prepubertal spermatogenesis in mice small star, filled. *Dev. Biol.* **258,** 209–225 (2003).
15. Holtfreter, J. Neural induction in explants which have passed through a sublethal cytolysis. *J. Exp. Zool.* **106,** 197–222 (1947).

16. Gerhart, J. Johannes Holtfreter's contributions to ongoing studies of the organizer. *Dev. Dyn.* **205,** 245–256 (1996).
17. Byrnes, W. M. Ernest Everett Just, Johannes Holtfreter, and the origin of certain concepts in embryo morphogenesis. *Mol. Reprod. Dev.* **76,** 912–921 (2009).
18. Gratama, J. W., Sutherland, D. R. & Keeney, M. Flow cytometric enumeration and immunophenotyping of hematopoietic stem and progenitor cells. *Semin. Hematol.* **38,** 139–147 (2001).
19. Inoue, K. *et al.* Inefficient reprogramming of the hematopoietic stem cell genome following nuclear transfer. *J. Cell Sci.* **119,** 1985–1991 (2006).
20. Ying, Q. L. *et al.* The ground state of embryonic stem cell self-renewal. *Nature* **453,** 519–523 (2008).
21. Tesar, P. J. *et al.* New cell lines from mouse epiblast share defining features with human embryonic stem cells. *Nature* **448,** 196–199 (2007).
22. Brons, I. G. *et al.* Derivation of pluripotent epiblast stem cells from mammalian embryos. *Nature* **448,** 191–195 (2007).
23. Kuroda, Y. *et al.* Isolation, culture and evaluation of multilineage-differentiating stress-enduring (Muse) cells. *Nature Protocols* **8,** 1391–1415 (2013).
24. Niwa, H. How is pluripotency determined and maintained? *Development* **134,** 635–646 (2007).
25. Watanabe, K. *et al.* Directed differentiation of telencephalic precursors from embryonic stem cells. *Nature Neurosci.* **8,** 288–296 (2005).
26. Kawasaki, H. *et al.* Induction of midbrain dopaminergic neurons from ES cells by stromal cell-derived inducing activity. *Neuron* **28,** 31–40 (2000).
27. Gouon-Evans, V. *et al.* BMP-4 is required for hepatic specification of mouse embryonic stem cell-derived definitive endoderm. *Nature Biotechnol.* **24,** 1402–1411 (2006).
28. Ohgushi, M. & Sasai, Y. Lonely death dance of human pluripotent stem cells: ROCKing between metastable cell states. *Trends Cell Biol.* **21,** 274–282 (2011).
29. Ohgushi, M. *et al.* Molecular pathway and cell state responsible for dissociation-induced apoptosis in human embryonic stem cells. *Cell Stem Cell* **7,** 225–239 (2010).
30. Murakami, K., Araki, K., Ohtsuka, S., Wakayama, T. & Niwa, H. Choice of random rather than imprinted X inactivation in female embryonic stem cell-derived extra-embryonic cells. *Development* **138,** 197–202 (2011).
31. Pera, M. F. & Tam, P. P. Extrinsic regulation of pluripotent stem cells. *Nature* **465,** 713–720 (2010).
32. Surani, M. A. & Barton, S. C. Development of gynogenetic eggs in the mouse: implications for parthenogenetic embryos. *Science* **222,** 1034–1036 (1983).
33. Wakayama, S. *et al.* Successful serial recloning in the mouse over multiple generations. *Cell Stem Cell* **12,** 293–297 (2013).
34. Nagy, A., Rossant, J., Nagy, R., Abramow-Newerly, W. & Roder, J. C. Derivation of completely cell culture-derived mice from early-passage embryonic stem cells. *Proc. Natl Acad. Sci. USA* **90,** 8424–8428 (1993).
35. Eakin, G. S., Hadjantonakis, A. K., Papaioannou, V. E. & Behringer, R. R. Developmental potential and behavior of tetraploid cells in the mouse embryo. *Dev. Biol.* **288,** 150–159 (2005).
36. Ogawa, K., Matsui, H., Ohtsuka, S. & Niwa, H. A novel mechanism for regulating clonal propagation of mouse ES cells. *Genes Cells* **9,** 471–477 (2004).
37. Hurtado, C. & De Robertis, E. M. Neural induction in the absence of organizer in salamander is mediated by MAPK. *Dev. Biol.* **307,** 282–289 (2007).
38. Hou, P. *et al.* Pluripotent stem cells induced from mouse somatic cells by small-molecule compounds. *Science* **341,** 651–654 (2013).
39. Eiraku, M. *et al.* Self-organizing optic-cup morphogenesis in three-dimensional culture. *Nature* **472,** 51–56 (2011).
40. Eilken, M. H., Nishikawa, S. & Schroeder, T. Continuous single-cell imaging of blood generation from haemogenic endothelium. *Nature* **457,** 896–900 (2009).

Supplementary Information is available in the online version of the paper.

Acknowledgements We thank S. Nishikawa for discussion and J. D. Ross, N. Takata, M. Eiraku, M. Ohgushi, S. Itoh, S. Yonemura, S. Ohtsuka and K. Kakiguchi for help with experiments and analyses. We thank A. Penvose and K. Westerman for comments on the manuscript. H.O. is grateful to T. Okano, S. Tsuneda and K. Kuroda for support and encouragement. Financial support for this research was provided by Intramural RIKEN Research Budget (H.O., T.W. and Y.S.), a Scientific Research in Priority Areas (20062015) to T.W., the Network Project for Realization of Regenerative Medicine to Y.S., and Department of Anesthesiology, Perioperative and Pain Medicine at Brigham and Women's Hospital to C.A.V.

Author Contributions H.O. and Y.S. wrote the manuscript. H.O., T.W. and Y.S. performed experiments, and K.K. assisted with H.O.'s transplantation experiments. H.O., T.W., Y.S., H.N. and C.A.V. designed the project. M.P.V. and M.Y. helped with the design and evaluation of the project.

Author Information Reprints and permissions information is available at www.nature.com/reprints. The authors declare no competing financial interests. Readers are welcome to comment on the online version of the paper. Correspondence and requests for materials should be addressed to H.O. (obokata@cdb.riken.jp) or C.A.V. (cvacanti@partners.org).

METHODS

Animal studies. Research involving animals complied with protocols approved by the Harvard Medical School/Brigham and Women's Hospital Committee on Animal Care, and the Institutional Committee of Laboratory Animal Experimentation of the RIKEN Center for Developmental Biology.

Tissue collection and low-pH treatment. To isolate CD45$^+$ haematopoietic cells, spleens were excised from 1-week-old *Oct4-gfp* mice (unless specified otherwise), minced by scissors and mechanically dissociated with pasture pipettes. Dissociated spleen cells were suspended with PBS and strained through a cell strainer (BD Biosciences). After centrifuge at 1,000 r.p.m. for 5 min, collected cells were re-suspended in DMEM medium and added to the same volume of lympholyte (Cedarlane), then centrifuged at 1,000*g* for 20 min. The lymphocyte layer was taken out and stained with CD45 antibody (ab25603, Abcam). CD45-positive cells were sorted by FACS Aria (BD Biosciences). After cell sorting, 1×10^6 CD45-positive cells were treated with 500 µl of low-pH HBSS solution (titrated to pH5.7 by HCl) for 25 min at 37 °C, and then centrifuged at 1,000 r.p.m. at room temperature for 5 min. After the supernatant (low-pH solution) was removed, precipitated cells were re-suspended and plated onto non-adhesive culture plates (typically, 1×10^5 cells ml^{-1}) in DMEM/F12 medium supplemented with 1,000 U LIF (Sigma) and 2% B27 (Invitrogen). Cell cluster formation was more sensitive to the plating cell density than the percentage of *Oct4*-GFP$^+$ cells. The number of surviving cells was sensitive to the age of donor mice and was low under the treatment conditions above when adult spleens were used. The addition of LIF during days 2–7 was essential for generating *Oct4*-GFP$^+$ STAP cell clusters on day 7, as shown in Extended Data Fig. 1f. Even in the absence of LIF, *Oct4*-GFP$^+$ cells (most of them were dim in signal) appeared transiently during days 2–5 in culture of low-pH-treated CD45$^+$ cells, but subsequently disappeared, indicating that there is a LIF-independent early phase, whereas the subsequent phase is LIF-dependent.

Chimaeric mouse generation and analyses. For production of diploid and tetraploid chimaeras with STAP cells, diploid embryos were obtained from ICR strain females. Tetraploid embryos were produced by electrofusion of 2-cell embryos. Because trypsin treatment of donor samples turned out to cause low chimaerism, STAP spherical colonies were cut into small pieces using a microknife under the microscope, and small clusters of STAP cells were then injected into day-4.5 blastocysts by a large pipette. The next day, the chimaeric blastocysts were transferred into day-2.5 pseudopregnant females. For experiments using STAP cells from CD45$^+$ cells without the *Oct4-gfp* reporter, STAP cell clusters were identified by their characteristic cluster morphology (they are made of very small cells with no strong compaction in the aggregate). When the STAP conversion conditions (low pH) were applied to CD45$^+$ lymphocytes, most day-7 clusters that were large and contained more than a few dozen small cells were positive for Oct4 (although the expression level varied). Therefore, we used only well-formed characteristic clusters (large ones) for this type of study and cut them by microknife to prepare donor cell clusters in a proper size for glass needle injection. For an estimate of the contribution of these injected cells, we used STAP cells that were generated from CD45$^+$ cells of mice constitutively expressing GFP (C57BL/6 line with *cag-gfp* transgenes; F_1 of C57BL/6 and 129/Sv or DBA/2 was used from the viewpoint of heterosis).

Because the number of CD45$^+$ cells from a neonatal spleen was small, we mixed spleen cells from male and female mice for STAP cell conversion. To make germline transmission more efficient, we intercrossed chimaeras in some experiments.

For the production of diploid and tetraploid chimaeras with STAP stem cells, diploid embryos were obtained from ICR strain females. Tetraploid embryos were produced by electrofusion of 2-cell embryos. STAP stem cells were dissociated into single cells and injected into day-4.5 blastocysts. In the chimaera studies with both STAP cells and STAP stem cells, we did not find tumorigenetic tendencies in their chimaeras or their offspring (up to 18 months).

***In vivo* differentiation assay.** 1×10^7 STAP cells were seeded onto a sheet composed of a non-woven mesh of polyglycolic acid fibres ($3 \times 3 \times 1$ mm; 200 µm in pore diameter), cultured for 24 h in DMEM + 10% FBS, and implanted subcutaneously into the dorsal flanks of 4-week-old mice. In this experiment, to better support tumour formation from slow growing STAP cells by keeping cells in a locally dense manner, we implanted STAP cells with artificial scaffold made of polyglycolic acid fibres. Given the artificial nature of the material, we used NOD/SCID mice as hosts, to avoid possible enhancement of post-graft inflammation caused by this scaffold even in syngenic mice. STAP stem cells were dissociated into single cells and cell suspension containing 1×10^7 cells was injected into the testis. Six weeks later, the implants were analysed using histochemical techniques. The implants were fixed with 10% formaldehyde, embedded in paraffin, and routinely processed into 4-µm-thick sections. Sections were stained with haematoxylin and eosin. Endoderm tissues were identified with expression of anti-α-fetoprotein (mouse monoclonal antibody; MAB1368, R&D Systems). Ectodermal tissues were identified with expression of anti-βIII tubulin (mouse monoclonal antibody; G7121, Promega). Mesodermal tissues were identified with expression of anti-α-smooth muscle actin (rabbit polyclonal; DAKO). In negative controls, the primary antibody was replaced with IgG-negative controls of the same isotype to ensure specificity.

STAP by exposure to other external stimuli. To give a mechanical stress to mature cells, a pasture pipette was heated and then stretched to create thin capillaries with the lumens approximately 50 µm in diameter, and then broken into appropriate lengths. Mature somatic cells were then repeatedly triturated through these pipettes for 20 min, and then cultured for 7 days. To provide a heat shock, cells were heated at 42 °C for 20 min and cultured for 7 days. A nutrition-deprivation stress was provided to mature cells, by culturing the cells in basal culture medium for 3 weeks. High Ca^{2+} concentration stress was provided to mature cells by culturing cells in medium containing 2 mM $CaCl_2$ for 7 days. To give a strong stress by creating pores in cell membranes, cells were treated with 230 ng ml^{-1} streptolysine O (SLO) (S5265, Sigma) for 2 h, then cultured for 7 days. After each treatment, the ratio of *Oct4*-GFP-positive cells was analysed by FACS.

Bisulphite sequencing. GFP-positive cells in STAP clusters were collected by FACS Aria. Genomic DNA was extracted from STAP cells and analysed. Bisulphite treatment of DNA was performed using the CpGenome DNA modification kit (Chemicon, http://www.chemicon.com), following the manufacturer's instructions. The resulting modified DNA was amplified by nested PCR using two forward (F) primers and one reverse (R) primer: Oct4 (F1, 5′-GTTGTTTTGTTTTGGTTTTGGATA T-3′; F2, 5′-ATGGGTTGAAATATTGGGTTTATTTA-3′; R, 5′-CCACCCTCT AACCTTAACCTCTAAC-3′). And Nanog (F1, 5′-GAGGATGTTTTTTAAGT TTTTTTT-3′; F2, 5′-AATGTTTATGGTGGATTTTGTAGGT-3′; R, 5′-CCCA CACTCATATCAATATAATAAC-3′). PCR was done using TaKaKa Ex Taq Hot Start Version (RR030A). DNA sequencing was performed using a M13 primer at the Genome Resource and Analysis Unit, RIKEN CDB.

Immunohistochemistry. Cultured cells were fixed with 4% paraformaldehyde and permeabilized with 0.1% Triton X-100/PBS before blocking with 1% BSA solution. Cells were incubated with the following primary antibodies: anti-Oct4 (Santa Cruz Biotechnology; C-10), anti-Nanog (eBioscience; MLC-51), anti-SSEA-1 (Millipore; MC480), anti-E-cadherin (Abcam), anti-ZO-1 (Santa Cruz Biotechnology; c1607), anti-claudin7 (Abcam), anti-Klf4 (R&D Systems), anti-Esrrβ (R&D Systems), anti-H3K27me3 (Millipore), anti-BrdU (BD Bioscience) and anti-Ki67 (BD Pharmingen). After overnight incubation, cells were incubated with secondary antibodies: goat anti-mouse or -rabbit coupled to Alexa-488 or -594 (Invitrogen). Cell nuclei were visualized with DAPI (Sigma). Slides were mounted with a SlowFade Gold antifade reagent (Invitrogen).

Fluorescence-activated cell sorting and flow cytometry. Cells were prepared according to standard protocols and suspended in 0.1% BSA/PBS on ice before FACS. Propidium iodide (BD Biosciences) was used to exclude dead cells. In negative controls, the primary antibody was replaced with IgG-negative controls of the same isotype to ensure specificity. Cells were sorted on a BD FACSAria SORP and analysed on a BD LSRII with BD FACS Diva Software (BD Biosciences). For haematopoietic fraction sorting, antibodies against T-cell marker (anti-CD90; eBioscience), B-cell marker (anti-CD19; Abcam) and haematopoietic progenitor marker (anti-CD34; Abcam) were used.

RNA preparation and RT–PCR analysis. RNA was isolated with the RNeasy Micro kit (Qiagen). Reverse transcription was performed with the SuperScript III first strand synthesis kit (Invitrogen). Power SYBR Green Mix (Roche Diagnostics) was used for amplification, and samples were run on a Lightcycler-II Instrument (Roche Diagnostics). The primer sets for each gene are listed in Supplementary Table 1.

***In vitro* differentiation assays.** For mesodermal differentiation assay, STAP cells were collected at 7 days, and *Oct4*-GFP-positive cells were collected by cell sorter and subjected to culture in DMEM supplemented with 20% FBS. Medium was exchanged every 3 days. After 7–14 days, muscle cells were stained with an anti-α-smooth muscle actin antibody (DAKO).

For neural lineage differentiation assay, STAP cells were collected at 7 days and subjected to SDIA or SFEBq culture. For SDIA culture, collected STAP cell clusters were plated on PA6 cell feeder as described previously[26]. For SFEBq culture, STAP cell clusters (one per well; non-cell-adhesive 96-well plate, PrimeSurface V-bottom, Sumitomo Bakelite) were plated and cultured in suspension as described previously[36].

For endodermal differentiation, STAP cells were collected at 7 days and subjected to suspension culture with inducers in 96-well plates[27].

TCR-β chain gene rearrangement analysis. Genomic DNA was extracted from STAP cells and tail tips from chimaeric mice generated with STAP cells derived from CD45$^+$ cells. PCR was performed with 50 ng DNA using the following primers (Dβ2: 5′-GCACCTGTGGGGAAGAAACT-3′ and Jβ2.6: 5′-TGAGAGCTGTCT CCTACTATCGATT-3′) that amplify the regions of the (D)J recombination. The PCR products were subjected to gel electrophoresis in Tris-acetate-EDTA buffer with 1.6% agarose and visualized by staining with ethidium bromide. PCR bands

from STAP cells were subjected to sequencing analysis and identified as rearranged genomic fragments of the (D)J recombination.

EdU uptake assay and apoptosis analysis. At various phases in STAP cell culture (days 0–2, 2–7, 7–14), EdU was added to the culture medium (final concentration: 10 μM) and EdU uptake was analysed by FACS. This assay was performed according to the manufacturer's protocol with the Click-iT EdU Flow cytometry assay kit (Invitrogen).

Apoptosis analysis was performed with flow cytometry using Annexin-V (Biovision) and propidium iodide. Annexin-V analysis by FACS on day 14 showed that most *Oct4*-GFP$^+$ cells were positive for this apoptotic marker; indeed, the number of surviving cells declined thereafter.

Soft agar assay. Sorted STAP cells (*Oct4*-GFP-strong or -dim) and control mouse ES cells (1,000 cells per well of 96-well plate) were plated into soft ager medium (0.4% agarose) in LIF-B27 medium. After 7 days of culture, cells were dissociated and their anchorage-independent growth was quantified by fluorescent measurement with the cytoselect 96-well cell transformation assay kit (Cell Biolabs) according to the manufacturer's protocol.

Comparative genomic hybridization (CGH) array analysis. Genomic DNA was extracted from STAP (male) and CD45-positive cells (male) by the Gene JET Genomic DNA purification kit (Thermo Scientific). Using CGH array (Agilent), the normality of chromosomes derived from STAP was compared with that of CD45-positive cells whose chromosomal normality was confirmed by a separate experiment. CGH array and data analysis were performed at TAKARA Bio.

Electron microscopy. For electron microscopic analysis, dissociated cells were fixed in 2.5% glutaraldehyde and 2% formaldehyde in 0.1 M cacodylate buffer (pH 7.2) and then processed for thin sectioning and transmission electron microscopy.

Live cell imaging. All live-cell imaging was performed with LCV110-CSUW1 (Olympus). For live-cell imaging of 'in culture CD45 antibody staining', CD45$^+$ cells treated with low pH were plated in culture medium containing 20 ng ml^{-1} of fluorescent-labelled CD45 antibody (eBioscience)[40].

RNA-sequencing and ChIP sequencing analyses. For RNA sequencing of cell lines, total RNA was extracted from cells by the RNasy mini kit (Qiagen). RNA-seq libraries were prepared from 1 μg total RNAs following the protocol of the TruSeq RNA Sample Prep kit (Illumina) and subjected to the deep sequencing analysis with Illumina Hi-Seq1500. Cluster tree diagram of various cell types was obtained from hierarchical clustering of global expression profiles ($\log_2$ FPKM of all transcripts; FPKM, fragments per kilobase of transcript per million mapped reads). Complete linkage method applied to $1 - r$ (r = Pearson's correlation between profiles) was used for generating the tree and 1,000 cycles of bootstrap resampling were carried out to obtain statistical confidence score in per cent units (also called AU P values).

ChIP-seq libraries were prepared from 20 ng input DNAs, 1 ng H3K4me3 ChIP DNAs, or 5 ng H3K27me3 ChIP DNAs using the KAPA Library Preparation kit (KAPA Biosystems). TruSeq adaptors were prepared in-house by annealing a TruSeq universal oligonucleotide and each of index oligonucleotides (5′-AATGATACGGCGACCACCGAGATCTACACTCTTTCCCTACACGACGCTCTTCCGATCT-3′, and 5′-GATCGGAAGAGCACACGTCTGAACTCCAGTCACXXXXXXATCTCGTATGCCGTCTTCTGCTTG-3′; where X represents index sequences).

Chromatin immunoprecipitation was performed as follows. Cells were fixed in PBS(-) containing 1% formaldehyde for 10 min at room temperature. Glycine was added to a final concentration of 0.25 M to stop the fixation. After washing the cells twice in ice-cold PBS(-), cells were further washed in LB1 (50 mM HEPES-KOH pH 7.5, 140 mM NaCl, 1 mM EDTA, 10% glycerol, 0.5% NP-40, 0.25% Triton X-100) and LB2 (10 mM Tris-HCl pH 8.0, 200 mM NaCl, 1 mM EDTA, 0.5 mM EGTA). Cells were then re-suspended in lysis buffer (50 mM Tris-HCl pH 8.0, 10 mM EDTA, 1% SDS). Lysates were prepared by sonication using Covaris S220 in a mini tube at duty cycle = 5%, PIP = 70, cycles per burst = 200, and the treatment time of 20 min. Lysates from 2×10^6 cells were diluted in ChIP dilution buffer (16.7 mM Tris-HCl pH 8.0, 167 mM NaCl, 1.2 mM EDTA, 1.1% Triton X-100, 0.01% SDS). ChIP was performed using sheep anti-mouse IgG beads (Invitrogen) or protein A beads (Invitrogen) coupled with anti-histone H3K4me3 antibody (Wako, catalogue no. 307-34813) or anti-histone H3K27me3 antibody (CST, catalogue no. 9733), respectively. After 4–6 h of incubation in a rotator at 4 °C, beads were washed five times in low-salt wash buffer (20 mM Tris HCl pH 8.0, 150 mM NaCl, 2 mM EDTA, 1% Triton X-100, 0.1% SDS), and three times in high-salt wash buffer (20 mM Tris-HCl pH 8.0, 500 mM NaCl, 2 mM EDTA, 1% Triton X-100, 0.1% SDS). Target chromatin was eluted off the beads in elution buffer (10 mM Tris-HCl pH 8.0, 300 mM NaCl, 5 mM EDTA, 1% SDS) at room temperature for 20 min. Crosslink was reversed at 65 °C, and then samples were treated with RNaseA and proteinase K. The prepared DNA samples were purified by phenol-chloroform extraction followed by ethanol precipitation and dissolved in TE buffer.

STAP stem-cell conversion culture. For establishment of STAP stem-cell lines, STAP cell clusters were transferred to ACTH-containing medium[36] on MEF feeder cells (several clusters, up to a dozen clusters, per well of 96-well plates). Four to seven days later, the cells were subjected to the first passage using a conventional trypsin method, and suspended cells were plated in ES maintain medium containing 20% FBS. Subsequent passaging was performed at a split ratio of 1:10 every second day before they reached subconfluency. We tested the following three different genetic backgrounds of mice for STAP stem-cell establishment from STAP cell clusters, and observed reproducible data of establishment: C57BL/6 carrying *Oct4-gfp* (29 of 29), 129/Sv carrying *Rosa26-gfp* (2 of 2) and 129/Sv × C57BL/6 carrying *cag-gfp* (12 of 16). STAP stem cells with all these genetic backgrounds showed chimaera-forming activity.

For clonal analysis of STAP stem cells, single STAP stem cells were manually picked by a thin-glass pipette, and plated into 96-well plates at one cell per well. The clonal colonies were cultured in ES medium containing 20% FBS, and expanded for subsequent experiments.

Karyotype analysis. Karyotype analysis was performed by Multicolor FISH analysis (M-FISH). Subconfluent STAP stem cells were arrested in metaphase by colcemid (final concentration 0.270 μg ml^{-1}) to the culture medium for 2.5 h at 37 °C in 5% CO_2. Cells were washed with PBS, treated with trypsin and EDTA (EDTA), re-suspended into cell medium and centrifuged for 5 min at 1,200 r.p.m. To the cell pellet in 3 ml of PBS, 7 ml of a pre-warmed hypotonic 0.0375 M KC1 solution was added. Cells were incubated for 20 min at 37 °C. Cells were centrifuged for 5 min at 1,200 r.p.m. and the pellet was re-suspended in 3–5 ml of 0.0375 M KC1 solution. The cells were fixed with methanol/acetic acid (3:1; vol/vol) by gently pipetting. Fixation was performed four times before spreading the cells on glass slides. For the FISH procedure, mouse chromosome-specific painting probes were combinatorially labelled using seven different fluorochromes and hybridized as previously described[41]. For each cell line, 9–15 metaphase spreads were acquired by using a Leica DM RXA RF8 epifluorescence microscope (Leica Mikrosysteme GmbH) equipped with a Sensys CCD camera (Photometrics). Camera and microscope were controlled by the Leica Q-FISH software (Leica Microsystems). Metaphase spreads were processed on the basis of the Leica MCK software and presented as multicolour karyograms.

Q-band analysis was performed at Chromocentre (Japan). After quinacrin staining, 20 cells from each sample were randomly selected and the normality of chromosomes was analysed. Five different independent lines of STAP stem cells showed no chromosomal abnormalities in Q-band analysis after >10 passages.

41. Jentsch, I., Geigl, J., Klein, C. A. & Speicher, M. R. Seven-fluorochrome mouse M-FISH for high-resolution analysis of interchromosomal rearrangements. *Cytogenet. Genome Res.* **103,** 84–88 (2003).

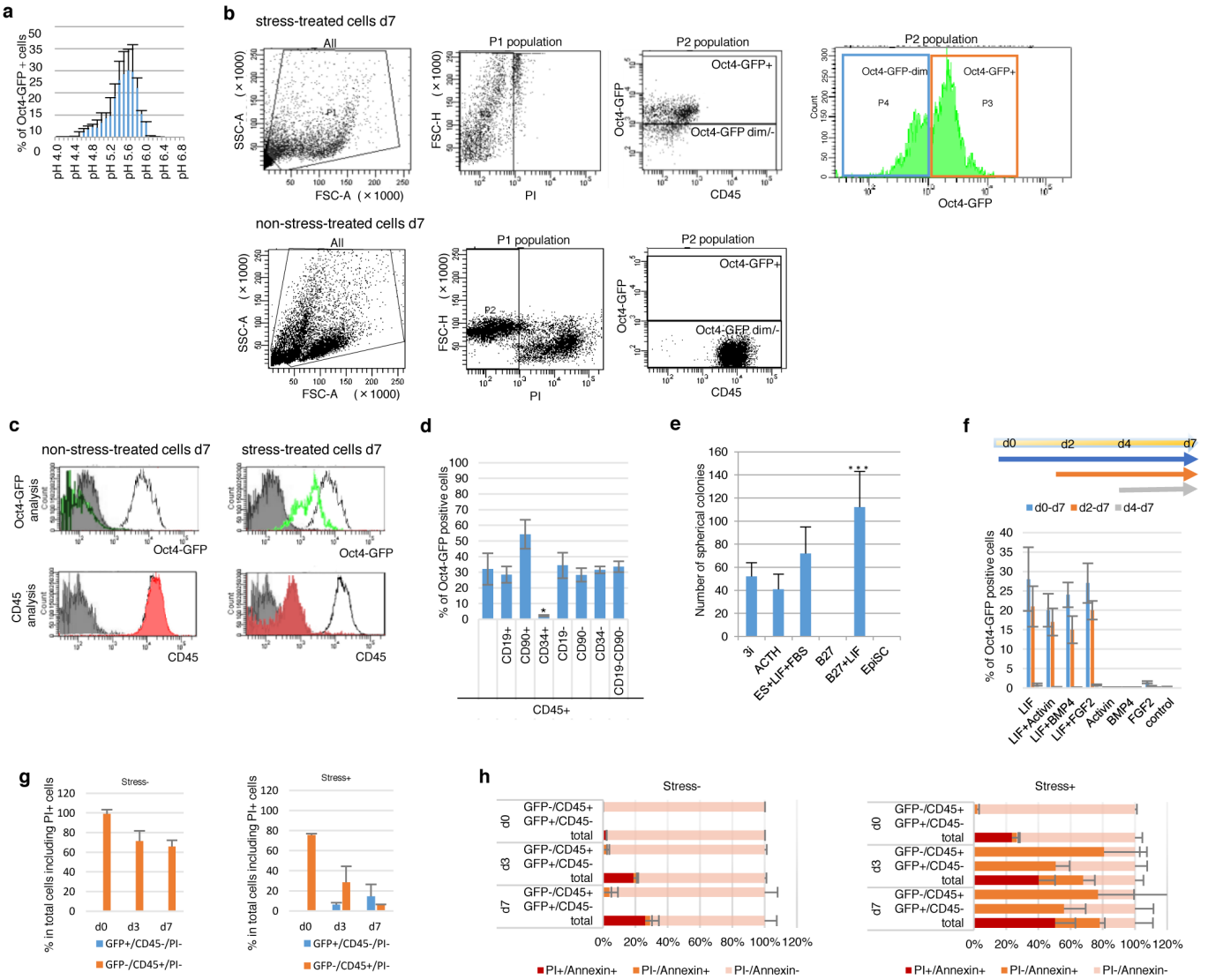

Extended Data Figure 1 | Conversion of haematopoietic cells into *Oct4*-GFP$^+$ cells by a low-pH exposure. **a**, Optimization of pH conditions for *Oct4*-GFP induction. Five days after CD45-positive cells were exposed to acidic solution treatment at different pH, *Oct4*-GFP expression was analysed by FACS ($n = 3$, average ± s.d.). **b**, Gating strategy for *Oct4*-GFP$^+$ cell sorting. Top: representative results 7 days after the stress treatment. Bottom: non-treated control. P3 populations were sorted and counted as *Oct4*-GFP$^+$ cells for all experiments. **c**, Controls for FACS analysis. In *Oct4*-GFP$^+$ cell analysis, the grey and white histograms indicate the negative control (non-stress-treated *Oct4-gfp* haematopoietic cells) and the positive control (*Oct4-gfp* ES cells), respectively. Also, the green histograms indicate non-treated cells (left) and stress-treated cells at day 7 (right). In CD45$^+$ cell analysis, the grey and white histograms indicate the negative (isotype) and positive controls, respectively. The red histograms indicate non-stress-treated cells (left) and stress-treated cells at day 7 (right). **d**, *Oct4*-GFP$^+$ cell generation from various subpopulations of CD45$^+$ cells. Seven days after the stress treatment, *Oct4*-GFP expression was analysed by FACS ($n = 3$, average ± s.d.). Among total CD45$^+$ fraction and its subfractions of CD19$^+$, CD90$^+$, CD34$^+$ and CD34$^-$ cells, the efficacy of CD34$^+$ cells was significantly lower than the others. $P < 0.05$ by the Newman–Keuls test and $P < 0.01$ by one-way ANOVA. **e**, Comparison of culture conditions for low-pH-induced conversion. Stress-treated cells were cultured in various media. The number of *Oct4*-GFP-expressing clusters was counted at day 14 ($n = 3$, average ± s.d.). ***$P < 0.001$ (B27+LIF versus all other groups); Tukey's test. In the case of 3i medium, although the clusters appeared at a moderate efficiency, they appeared late and grew slowly. ACTH, ACTH-containing ES medium; ES+LIF+FBS, 20% FBS+LIF-containing ES culture medium; B27, DMEM/F12 medium containing 2% B27; B27+LIF, DMEM/F12 medium containing 2% B27+LIF; EpiSC, EpiSC culture medium containing Fgf2+activin. **f**, Signalling factor dependency of STAP cell generation. Growth factors that are conventionally used for pluripotent cell culture such as LIF, activin, Bmp4 and Fgf2 were added to basal culture medium (B27-supplemented DMEM/F12) in different culture phases (days 0–7, 2–7 and 4–7), and *Oct4*-GFP expression was analysed by FACS at day 7 ($n = 3$, average ± s.d.). **g**, **h**, Time course of apoptosis after the low-pH exposure. Stress-treated cells and non-stress-treated control cells were stained with CD45, annexin-V and propidium iodide at day 0 (immediately after stress treatment), day 3 and day 7. **g**, Blue bars, GFP$^+$CD45$^-$; orange bars, GFP$^-$CD45$^+$. Percentages in total cells included propidium-iodide-positive cells. **h**, Annexin-V-positive cells in these cell populations were analysed by FACS.

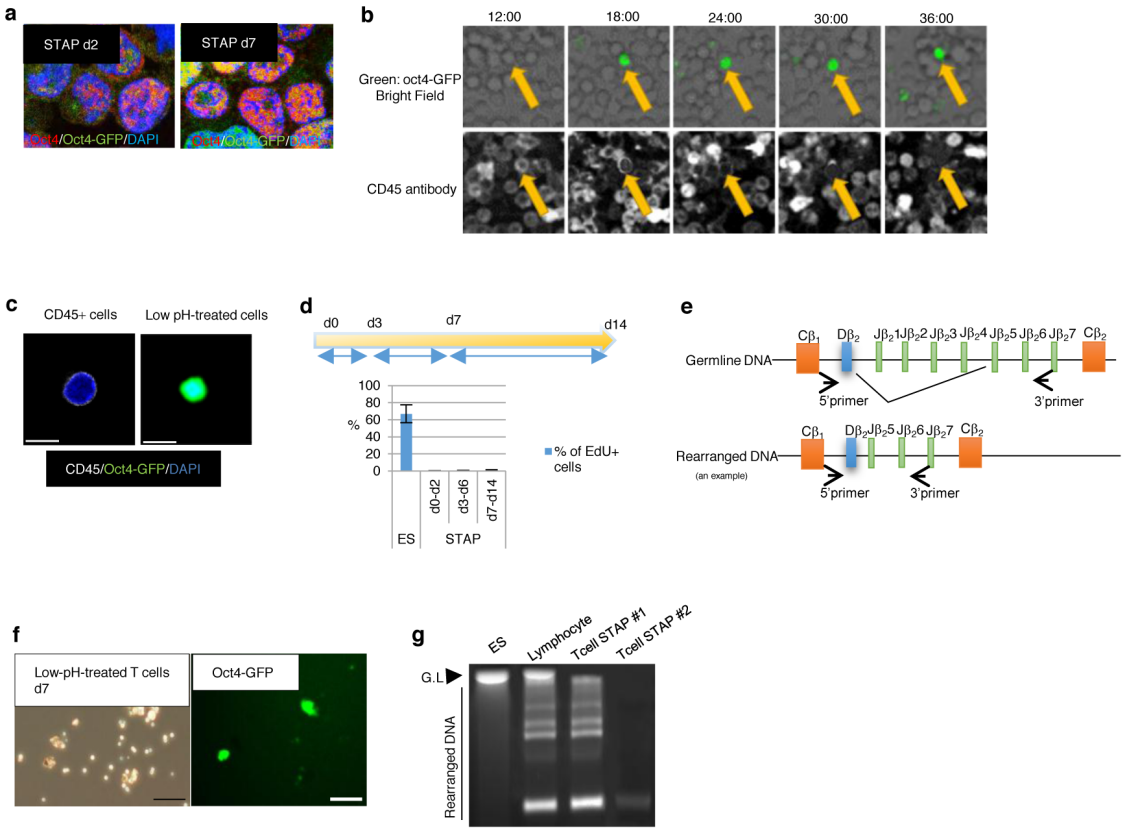

Extended Data Figure 2 | Phenotypic change during STAP cell conversion. **a**, Oct4 protein expression in STAP cells was detected by immunostaining at day 2 (left) and day 7 (right). **b**, Live cell imaging of STAP conversion (grey, CD45 antibody; green, *Oct4*-GFP). See Methods for experimental details to monitor live CD45 immunostaining. **c**, Immunostaining of a parental CD45^{+} cell (left) and an *Oct4*-GFP^{+} cell (right). Scale bar, 10 μm. **d**, EdU uptake assay ($n = 3$, average ± s.d.). **e**, Schematic of *Tcrb* gene rearrangement. **f**, T-cell-derived STAP cells. Scale bar, 100 μm. **g**, Genomic PCR analysis of (D)J recombination at the *Tcrb* gene of T-cell-derived STAP cells. G.L. is the size of the non-rearranged germline type, whereas the smaller ladders correspond to the alternative rearrangements of J exons (confirmed by sequencing). Negative controls (ES cells), positive controls (lymphocytes) and T-cell-derived STAP (two independent preparations on d7) are indicated.

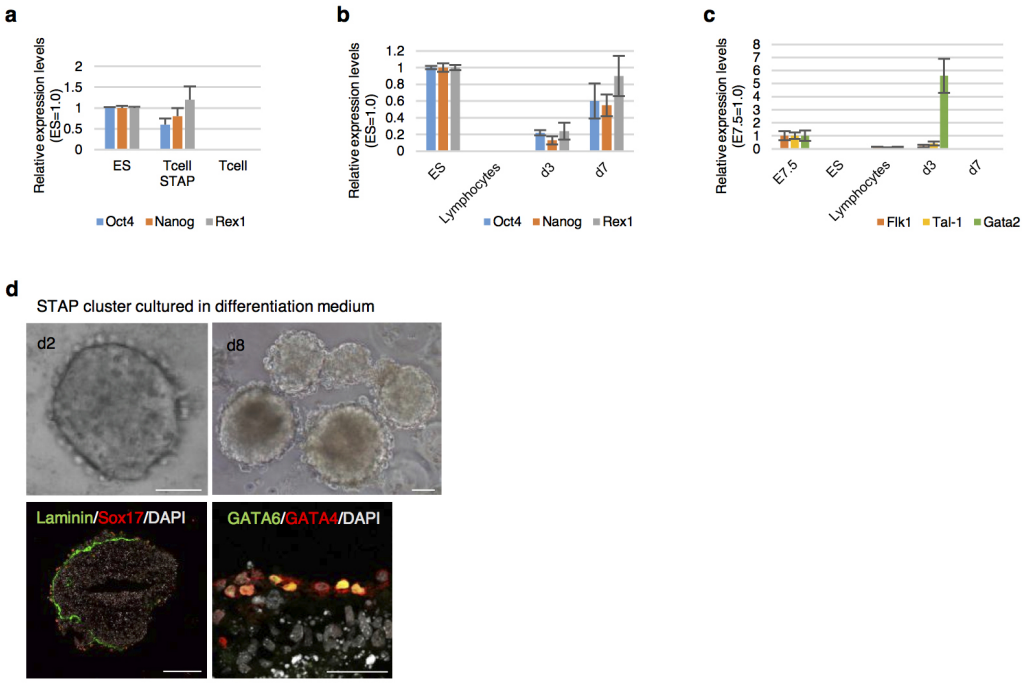

Extended Data Figure 3 | Gene expression analyses during STAP conversion and endoderm differentiation assay. **a**, Expression of pluripotency marker genes in STAP cells derived from T cells ($n = 3$, average ± s.d.). **b**, Expression of pluripotency marker genes in STAP cells. In this experiment, *Oct4*-GFP^{+} cells seen in live cell imaging (Extended Data Fig. 2b) were analysed to confirm their conversion into STAP cells ($n = 3$, average ± s.d.). **c**, Haematopoietic marker expression during STAP conversion from CD45^{+} cells ($n = 3$, average ± s.d.). **d**, Formation of visceral endoderm-like surface epithelium in differentiating STAP cluster on day 2 (left) and day 8 (right). Scale bars, 50 μm.

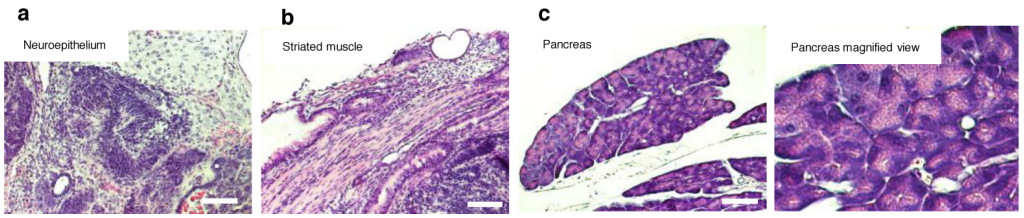

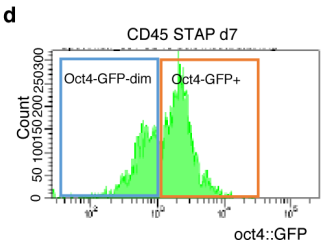

	Teratoma formation	Efficiency (%)	Weight (mg)
Oct4-GFP+ Fraction (dissociated)	Yes	3/20 (15%)	92±8
Oct4-GFP-dim Fraction (dissociated)	No	0/10 (0%)	Not applicable
STAP cluster (non-dissociated)	Yes	8/20 (40%)	122±16

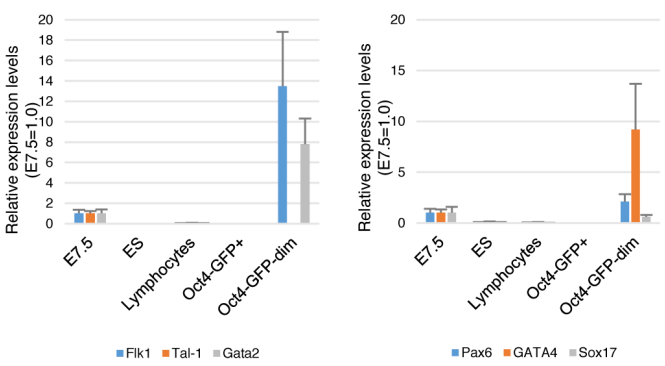

Extended Data Figure 4 | Teratoma formation assay and characterization of *Oct4*-GFP-dim cells. **a**–**c**, Teratomas formed from STAP cell clusters included neuroepithelium (**a**), striated muscle (**b**) and pancreas (**c**; right, high-magnification view showing a typical acinar morphology and ductal structures). Scale bars, 100 μm. **d**, Teratoma-forming ability of *Oct4*-GFP$^+$ and *Oct4*-GFP-dim cells (isolated by FACS, top). *Oct4*-GFP$^+$ cells, but not *Oct4*-GFP-dim cells, efficiently formed teratomas (table at the bottom). However, because STAP cells were dissociation-intolerant, the teratoma-forming efficiency of dissociated *Oct4*-GFP$^+$ cells was lower than that of non-dissociated STAP cell clusters. **e**, Gene expression of *Oct4*-GFP$^+$ and *Oct4*-GFP-dim cells ($n = 3$, the average ± s.d.). Haematopoietic marker gene expression (left) and early lineage marker gene expression (right) are shown.

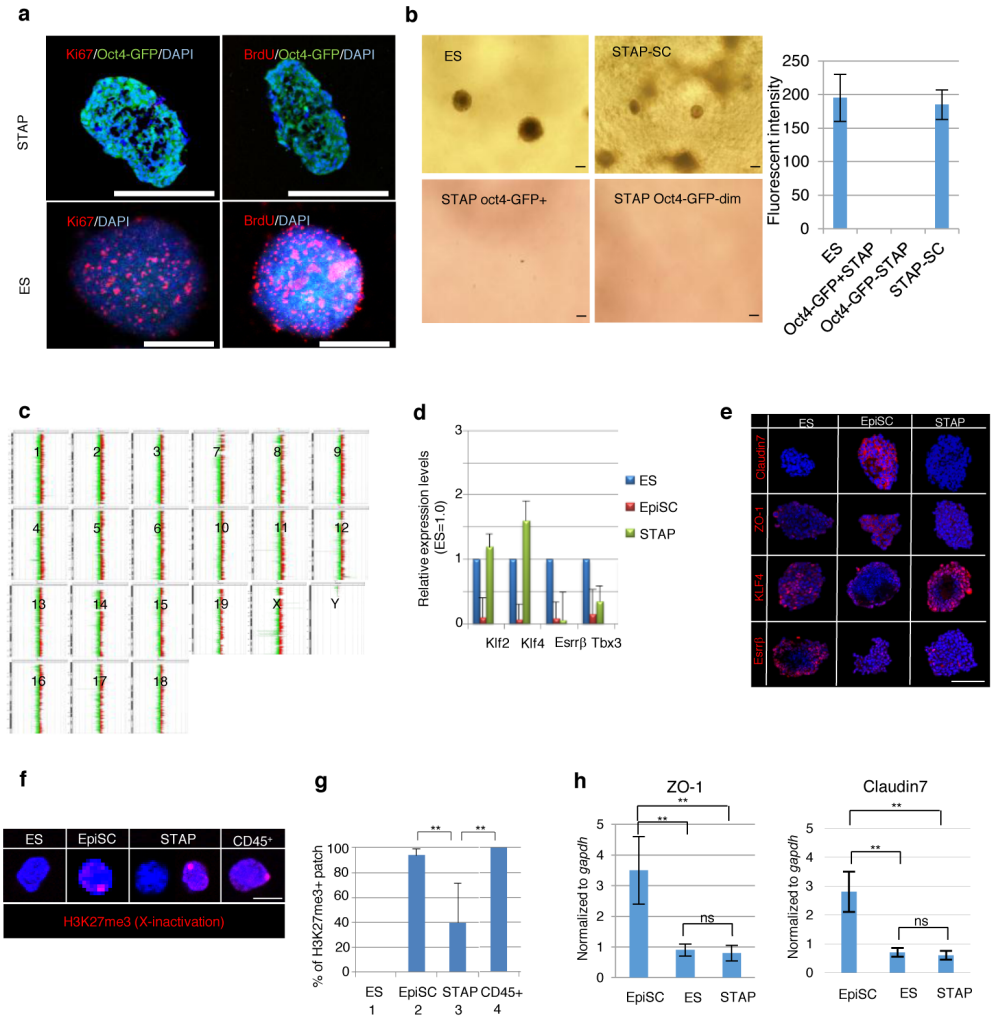

Extended Data Figure 5 | *In vitro* characterization of STAP cells. **a**, Immunostaining for Ki67 and BrdU. STAP cell clusters (top) and ES cell colonies (bottom) are shown. For BrdU uptake, BrdU was added into each culture medium (10 μM) for 12 h until fixation. Scale bar, 100 μm. **b**, Transformation assay by soft agar culture. Neither *Oct4*-GFP^{+} nor *Oct4*-GFP-dim cells showed colony formation in soft agar, whereas ES cells and STAP stem cells showed anchorage-independent growth in the same LIF-B27 medium. Scale bar, 100 μm. Proliferated cells were lysed and the amount of DNA in each well was estimated by chemical luminescence (graph). $n = 3$, average ± s.d. **c**, No substantial change in chromosome number was seen with STAP cells in the CGH array. Genomic DNA derived from CD45^{+} cells (male) was used as reference DNA. The spikes (for example, those seen in the X chromosome) were nonspecific and also found in the data of these parental CD45^{+} cells when the manufacturer's control DNA was used as a reference. **d**, qPCR analysis for pluripotency markers that highly express in ES cells, but not in EpiSCs. Average ± s.d. **e**, Immunostaining of markers for mouse EpiSC and ES cells. Scale bar, 100 μm. **f**, **g**, H3K27me3^{+} foci in female cells, which are indicative of X-chromosomal inactivation. These foci were not observed in male cells. Scale bar, 10 μm. In the case of female STAP cells, ~40% of cells retained H3K27me3^{+} foci (**g**). $^{**}P < 0.001$; Tukey's test. $n = 3$, average ± s.d. Although nuclear staining looked to be higher in STAP cells with H3K27me3^{+} foci (**f**), this appeared to be caused by some optical artefacts scattering from the strong focal signal. **h**, qPCR analysis for the tight junction markers *Zo-1* and claudin 7, which were highly expressed in EpiSCs, but not in ES cells or STAP cells. $^{**}P < 0.01$; ns, not significant; Tukey's test; $n = 3$, average ± s.d.

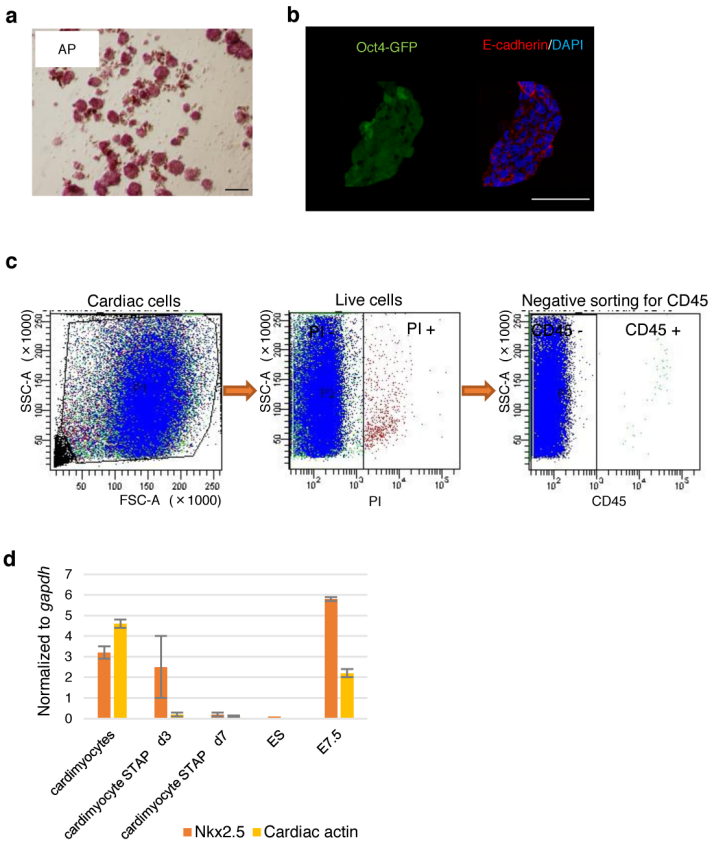

Extended Data Figure 6 | Conversion of somatic tissue cells into STAP cells. **a**, Alkaline phosphatase expression of STAP cells derived from adipose-derived mesenchymal cells. Scale bar, 100 μm. **b**, E-cadherin expression of STAP cells derived from adipose-derived mesenchymal cells. Scale bar, 50 μm. **c**, FACS sorting of dissociated neonatal cardiac muscle cells by removing $CD45^+$ cells. **d**, Cardiomyocyte marker gene expression during STAP conversion from cardiomyocytes ($n = 3$, average ± s.d.).

a

2N chimaeric mice generated with *Oct4-gfp/B6* STAP cells

2N chimaeric mice generated with *129F1* STAP cells

b

Mouse strain	Culture period of STAP	No. of fertilized embryos injected	No. offspring	No. of chimaeric mice obtained	
				Total	High contribution **
B6GFP*** × DBA/2	7 days	58	48*	16	4
129/Sv × B6GFP	7 days	98	64	20	6
BL6 (oct4-gfp)	7 days	73	35	24	2
BL6 (oct4-gfp)	10 days	35	20	4	0

c

Pair ID.	STAP contribution in chimaeras body		No. total pups (No. deliver)	No. of offspring with GFP or black eyes (%)
	Male	Female		
No. 1	High	Medium	9 (1)	5 (56)
No. 2	High	Wide type	25 (2)	8 (32)
No. 3	Medium	Low	32 (3)	0
No. 4	Medium	Medium	25 (3)	15 (60)
No. 5	Medium	Medium	14 (2)	7 (50)

d

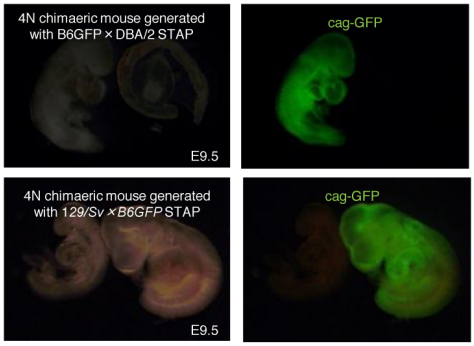

Extended Data Figure 7 | Generation chimaeras with STAP cells. **a**, 2N chimaeras generated with STAP cells derived from *Oct4-gfp* C57BL/6 mice (left) and 129/Sv × C57BL/6 F_1 mice (right). **b**, Generation of chimaeric mice from STAP cells by cluster injection. STAP cells used in the experiments above were generated from $CD45^+$ lymphocytes of multiple neonatal spleens (male and female tissues were mixed). *All fetuses were collected at 13.5 d.p.c. to 15.5 d.p.c. and the contribution rate of STAP cells into each organ was examined by FACS. **The contribution of STAP cells into each chimaera was scored as high (>50% of the coat colour of GFP expression). ***B6GFP: C57BL/6 mouse carrying *cag-gfp*. **c**, Production of offspring from STAP cells via germline transmission. Chimaeras generated with 129/Sv × B6GFP STAP cells (obtained from the experiments shown in **b**) were used for germline transmission study. **d**, 4N embryos at E9.5 generated with STAP cells derived from F_1 GFP mice (B6GFP and DBA/2 or 129/Sv). B6GFP, C57BL/6 mouse carrying *cag-gfp*.

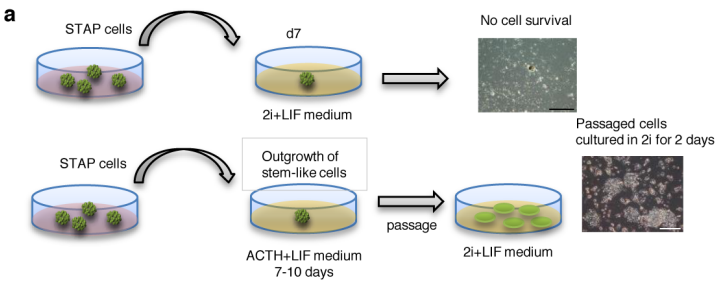

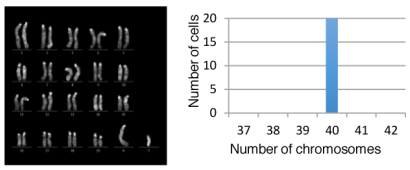

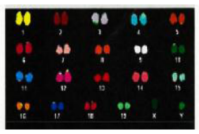

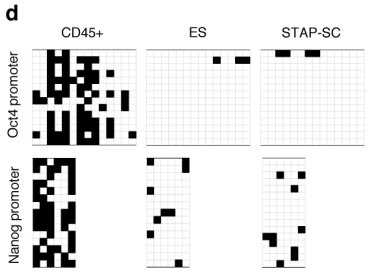

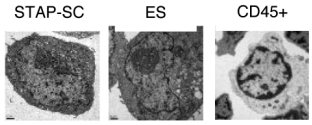

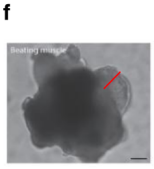

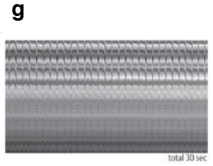

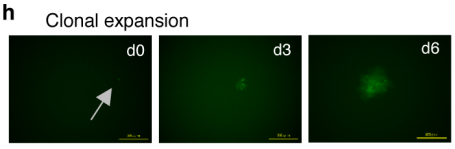

Clonability (clones/ single cells)	Frequency (teratoma formation/colony injected)	weight of teratoma (mg)
40/300	11/14	503±297

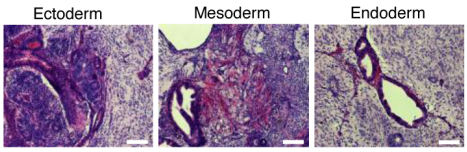

i

Cell line name*	No. of chimera embryos	No. of offspring	No. of chimeras				Germ-line transmission
			Total	Very high	High	low	
STAP-SC #1	16	7	6	2	3	1	Yes
STAP-SC #2	17	13	9	2	2	5	Yes
STAP-SC #3	32	16	12	6	4	2	Yes
STAP-SC #4	20	5	4	1	1	2	Yes
STAP-SC #5	21	5	4	3	0	1	Yes
STAP-SC #6	21	13	7	3	3	1	Yes
STAP-SC #7	32	14	11	5	5	1	Yes
STAP-SC #8	32	12	8	3	2	3	Yes
Subtotal	191	84	62 (73.8)				
Control ES #1	16	9	9	6	2	1	Yes
Control ES #2	18	12	8	3	2	3	Yes
Control ES #3	18	11	4	0	1	3	Yes
Subtotal	52	32	21 (65.6)				

j

Cell line name*	No. of chimera embryos	No. born	No. survived	No. adulthood	Germ-line transmission
STAP-SC #1	31	7	7	4	Yes
STAP-SC #2	29	3	2	2	Yes
STAP-SC #3	46	8	8	4	Yes
STAP-SC #4	46	9	8	2	Yes
STAP-SC #5	21	10	9	5	Yes
STAP-SC #6	12	4	4	4	Yes
STAP-SC #7	21	6	3	3	Yes
STAP-SC #8	22	5	2	2	Yes
Subtotal	228	52 (22.8)	43 (82.7)	26 (60.5)	
Control ES #1	8	5	5	4	Yes
Control ES #2	21	5	5	4	Yes
Control ES #3	21	3	1	0	-
Subtotal	50	13 (26.0)	11 (84.6)	8 (72.7)	

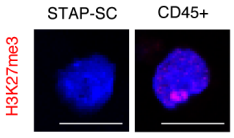

Extended Data Figure 8 | Molecular and cellular characterization of STAP stem cells. **a**, Compatibility of 2i conditions with STAP stem-cell derivation from STAP cells and STAP stem-cell maintenance. STAP stem cells could not be established directly from STAP cells in 2i + LIF medium (top). However, once established in ACTH medium, STAP stem cells were able to survive and expand in 2i + LIF medium. Scale bar, 100 μm. **b**, Q-band analysis ($n = 4$; all cell lines showed the normal karyotype). **c**, Multicolour FISH analysis ($n = 8$; all cell lines showed the normal karyotype) of STAP stem cells. **d**, Methylation status of the *Oct4* and *Nanog* promoters. **e**, Electron microscope analysis of STAP stem cells. Scale bar, 1 μm. **f**, **g**, Beating cardiac muscle (mesoderm; 38%, $n = 8$). Red line indicates an analysed region for kymograph (**g**). **h**, Clonability of STAP stem cells. Clonal expansion from single STAP stem cells was performed. Pluripotency of clonal cell lines was confirmed by teratoma formation assay, showing the formation of neuroectoderm (left), muscle tissue (middle) and bronchial-like epithelium (right). Scale bar, 100 μm. **i**, Production of chimaeric mice from STAP stem-cell lines using diploid embryos. *These STAP stem-cell lines were generated from independent STAP cell clusters. **j**, Production of mouse chimaeras from STAP stem-cell lines by the tetraploid complementation method. *These STAP stem-cell lines were generated from independent STAP cell clusters. **k**, No H3K27me3-dense foci are seen in female STAP stem cells ($n = 50$; the $CD45^+$ cell is a positive control). Scale bar, 10 μm.

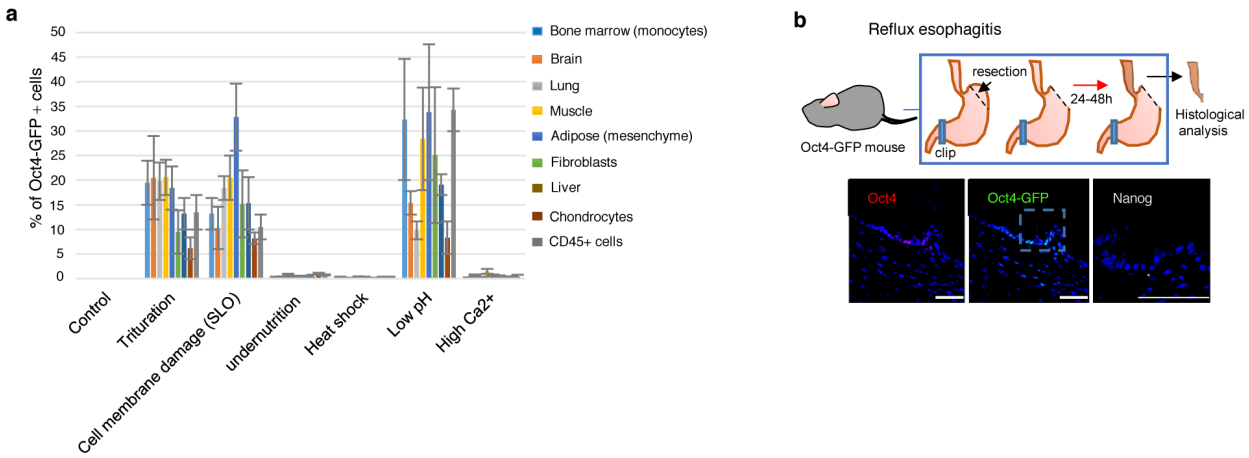

Extended Data Figure 9 | Effects of various stressors on STAP conversion. **a**, Percentages of *Oct4*-GFP-expressing cells 7 days after stress treatment. Somatic cells were isolated from various tissues and exposed to different stressors. *Oct4*-GFP expression was analysed by FACS. **b**, Oct4 and *Oct4*-GFP expression induced in the reflux oesophagitis mouse model as an *in vivo* acid exposure model (top, experimental procedure). Oct4, but not Nanog, expression was observed in the oesophageal epithelium exposed to gastric acid (75% of 12 operated mice).

RETRACTION

doi:10.1038/nature13598

Retraction: Stimulus-triggered fate conversion of somatic cells into pluripotency

Haruko Obokata, Teruhiko Wakayama, Yoshiki Sasai, Koji Kojima, Martin P. Vacanti, Hitoshi Niwa, Masayuki Yamato & Charles A. Vacanti

Nature **505,** 641–647 (2014); doi:10.1038/nature12968

Several critical errors have been found in our Article and Letter (http://dx.doi.org/10.1038/nature12969), which led to an in-depth investigation by the RIKEN Institute. The RIKEN investigation committee has categorized some of the errors as misconduct (see Supplementary Data 1 and Supplementary Data 2). Additional errors identified by the authors that are not discussed in RIKEN's report are listed below.

(1) Figure 1a and b in the Letter both show embryos generated from STAP cells, not a comparison of ES- and STAP-derived chimaeric embryos, as indicated in the legend.

(2) Extended Data Fig. 7d in the Article and Extended Data Fig. 1a in the Letter are different images of the same embryo and not, as indicated in the legends, a diploid chimaera embryo and tetraploid chimaera embryo.

(3) There is an erroneous description in Fig. 1a in the Letter. The right panel of Fig. 1a is not a 'long exposure' image at the camera level but a digitally enhanced one.

(4) In Fig. 4b of the Letter, STAP cell and ES cell are wrongly labelled in a reverse manner.

(5) In the Article, one group of STAP stem cells (STAP-SCs) was reported as being derived from STAP cells induced from spleens of F_1 hybrids from the cross of mouse lines carrying identical *cag-gfp* insertions in chromosome 18 in the background of 129/Sv and B6, respectively, and that they were maintained in the Wakayama laboratory. However, further analysis of the eight STAP-SC lines indicates that, while sharing the same 129×B6 F_1 genetic background, they have a different GFP insertion site. Furthermore, while the mice used for STAP cell induction are homozygous for the GFP transgene, the STAP-SCs are heterozygous. The GFP transgene insertion site matches that of the mice and ES cells kept in the Wakayama laboratory. Thus, there are inexplicable discrepancies in genetic background and transgene insertion sites between the donor mice and the reported STAP-SCs.

We apologize for the mistakes included in the Article and Letter. These multiple errors impair the credibility of the study as a whole and we are unable to say without doubt whether the STAP-SC phenomenon is real. Ongoing studies are investigating this phenomenon afresh, but given the extensive nature of the errors currently found, we consider it appropriate to retract both papers.

Supplementary Information is available in the online version of this Retraction.

RETRACTED

LETTER

doi:10.1038/nature12969

Bidirectional developmental potential in reprogrammed cells with acquired pluripotency

Haruko Obokata[1,2,3], Yoshiki Sasai[4], Hitoshi Niwa[5], Mitsutaka Kadota[6], Munazah Andrabi[6], Nozomu Takata[4], Mikiko Tokoro[2], Yukari Terashita[1,2], Shigenobu Yonemura[7], Charles A. Vacanti[3] & Teruhiko Wakayama[2,8]

We recently discovered an unexpected phenomenon of somatic cell reprogramming into pluripotent cells by exposure to sublethal stimuli, which we call stimulus-triggered acquisition of pluripotency (STAP)[1]. This reprogramming does not require nuclear transfer[2,3] or genetic manipulation[4]. Here we report that reprogrammed STAP cells, unlike embryonic stem (ES) cells, can contribute to both embryonic and placental tissues, as seen in a blastocyst injection assay. Mouse STAP cells lose the ability to contribute to the placenta as well as trophoblast marker expression on converting into ES-like stem cells by treatment with adrenocorticotropic hormone (ACTH) and leukaemia inhibitory factor (LIF). In contrast, when cultured with Fgf4, STAP cells give rise to proliferative stem cells with enhanced trophoblastic characteristics. Notably, unlike conventional trophoblast stem cells, the Fgf4-induced stem cells from STAP cells contribute to both embryonic and placental tissues *in vivo* and transform into ES-like cells when cultured with LIF-containing medium. Taken together, the developmental potential of STAP cells, shown by chimaera formation and *in vitro* cell conversion, indicates that they represent a unique state of pluripotency.

We recently discovered an intriguing phenomenon of cellular fate conversion: somatic cells regain pluripotency after experiencing sublethal stimuli such as a low-pH exposure[1]. When splenic CD45$^+$ lymphocytes are exposed to pH 5.7 for 30 min and subsequently cultured in the presence of LIF, a substantial portion of surviving cells start to express the pluripotent cell marker Oct4 (also called Pou5f1) at day 2. By day 7, pluripotent cell clusters form with a bona fide pluripotency marker profile and acquire the competence for three-germ-layer differentiation as shown by teratoma formation. These STAP cells can also efficiently contribute to chimaeric mice and undergo germline transmission using a blastocyst injection assay[1]. Although these characteristics resemble those of ES cells, STAP cells seem to differ from ES cells in their limited capacity for self-renewal (typically, for only a few

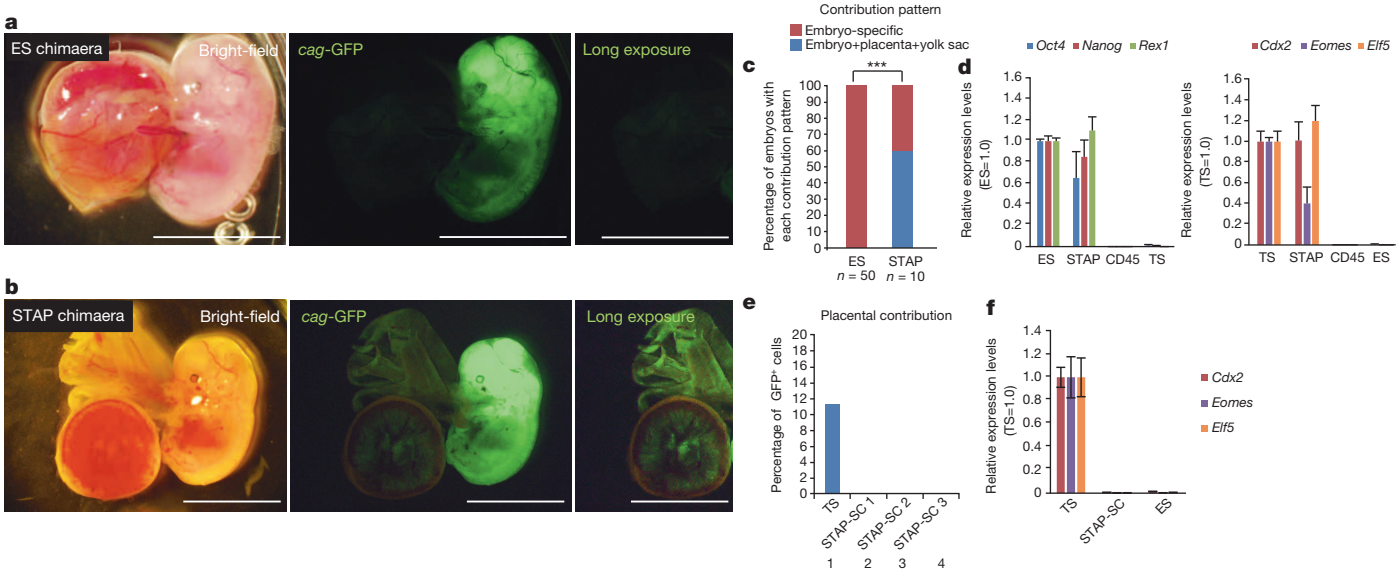

Figure 1 | STAP cells contribute to both embryonic and placental tissues *in vivo*. **a**, **b**, E12.5 embryos from blastocysts injected with ES cells (**a**) and STAP cells (**b**). Both cells are genetically labelled with GFP driven by a constitutive promoter. Progeny of STAP cells also contributed to placental tissues and fetal membranes (**b**), whereas ES-cell-derived cells were not found in these tissues (**a**). Scale bar, 5.0 mm. **c**, Percentages of fetuses in which injected cells contributed only to the embryonic portion (red) or also to placental and yolk sac tissues (blue). ***$P < 0.001$ with Fisher's exact test. **d**, qPCR analysis of FACS-sorted *Oct4*-GFP-strong STAP cells for pluripotent marker genes (left) and trophoblast marker genes (right). Values are shown as ratio to the expression level in ES cells. Error bars represent s.d. **e**, Contribution to placental tissues. Unlike parental STAP cells and trophoblast stem (TS) cells, STAP stem cells (STAP-SCs) did not retain the ability for placental contributions. Three independent lines were tested and all showed substantial contributions to the embryonic portions. **f**, qPCR analysis of trophoblast marker gene expression in STAP stem cells. Error bars represent s.d.

[1]Laboratory for Cellular Reprogramming, RIKEN Center for Developmental Biology, Kobe 650-0047, Japan. [2]Laboratory for Genomic Reprogramming, RIKEN Center for Developmental Biology, Kobe 650-0047, Japan. [3]Laboratory for Tissue Engineering and Regenerative Medicine, Brigham and Women's Hospital, Harvard Medical School, Boston, Massachusetts 02115, USA. [4]Laboratory for Organogenesis and Neurogenesis, RIKEN Center for Developmental Biology, Kobe 650-0047, Japan. [5]Laboratory for Pluripotent Stem Cell Studies, RIKEN Center for Developmental Biology, Kobe 650-0047, Japan. [6]Genome Resource and Analysis Unit, RIKEN Center for Developmental Biology, Kobe 650-0047, Japan. [7]Electron Microscopy Laboratory, RIKEN Center for Developmental Biology, Kobe 650-0047, Japan. [8]Faculty of Life and Environmental Sciences, University of Yamanashi, Yamanashi 400-8510, Japan.

passages) and in their vulnerability to dissociation[1]. However, when cultured in the presence of ACTH and LIF for 7 days, STAP cells, at a moderate frequency, further convert into pluripotent 'stem' cells that robustly proliferate (STAP stem cells).

Here we have investigated the unique nature of STAP cells, focusing on their differentiation potential into the two major categories (embryonic and placental lineages) of cells in the blastocyst[5–8]. We became particularly interested in this question after a blastocyst injection assay revealed an unexpected finding. In general, progeny of injected ES cells are found in the embryonic portion of the chimaera, but rarely in the placental portion[5,7] (Fig. 1a; shown with *Rosa26*-GFP). Surprisingly, injected STAP cells contributed not only to the embryo but also to the placenta and fetal membranes (Fig. 1b and Extended Data Fig. 1a–c) in 60% of the chimaeric embryos (Fig. 1c).

In quantitative polymerase chain reaction (qPCR) analysis, STAP cells (sorted for strong *Oct4*-GFP signals) expressed not only pluripotency marker genes but also trophoblast marker genes such as *Cdx2* (Fig. 1d and Supplementary Table 1 for primers), unlike ES cells. Therefore, the blastocyst injection result is not easily explained by the idea that STAP cells are composed of a simple mixture of pluripotent cells ($Oct4^+Cdx2^-$) and trophoblast-stem-like cells ($Oct4^-Cdx2^+$).

In contrast to STAP cells, STAP stem cells did not show the ability to contribute to placental tissues (Fig. 1e, lanes 2–4), indicating that the derivation of STAP stem cells from STAP cells involves the loss of competence to differentiate into placental lineages. Consistent with this idea, STAP stem cells show little expression of trophoblast marker genes (Fig. 1f).

We next examined whether an alteration in culture conditions could induce *in vitro* conversion of STAP cells into cells similar to trophoblast stem cells[8,9], which can be derived from blastocysts during prolonged adhesion culture in the presence of Fgf4. When we cultured STAP cell clusters under similar conditions (Fig. 2a; one cluster per well in a 96-well plate), flat cell colonies grew out by days 7–10 (Fig. 2b, left; typically in ~30% of wells). The Fgf4-induced cells strongly expressed the trophoblast marker proteins[9–12] integrin α7 (Itga7) and eomesodermin (Eomes) (Fig. 2c, d) and marker genes (for example, *Cdx2*; Fig. 2e).

These Fgf4-induced cells with trophoblast marker expression could be expanded efficiently in the presence of Fgf4 by passaging for more than 30 passages with trypsin digestion every third day. Hereafter, these proliferative cells induced from STAP cells by Fgf4 treatment are referred to as Fgf4-induced stem cells. This type of derivation into trophoblast-stem-like cells is not common with ES cells (unless genetically manipulated)[13] or STAP stem cells.

In the blastocyst injection assay, unlike STAP stem cells, the placental contribution of Fgf4-induced stem cells (*cag*-GFP-labelled) was observed with 53% of embryos (Fig. 2f, g; $n = 60$). In the chimaeric

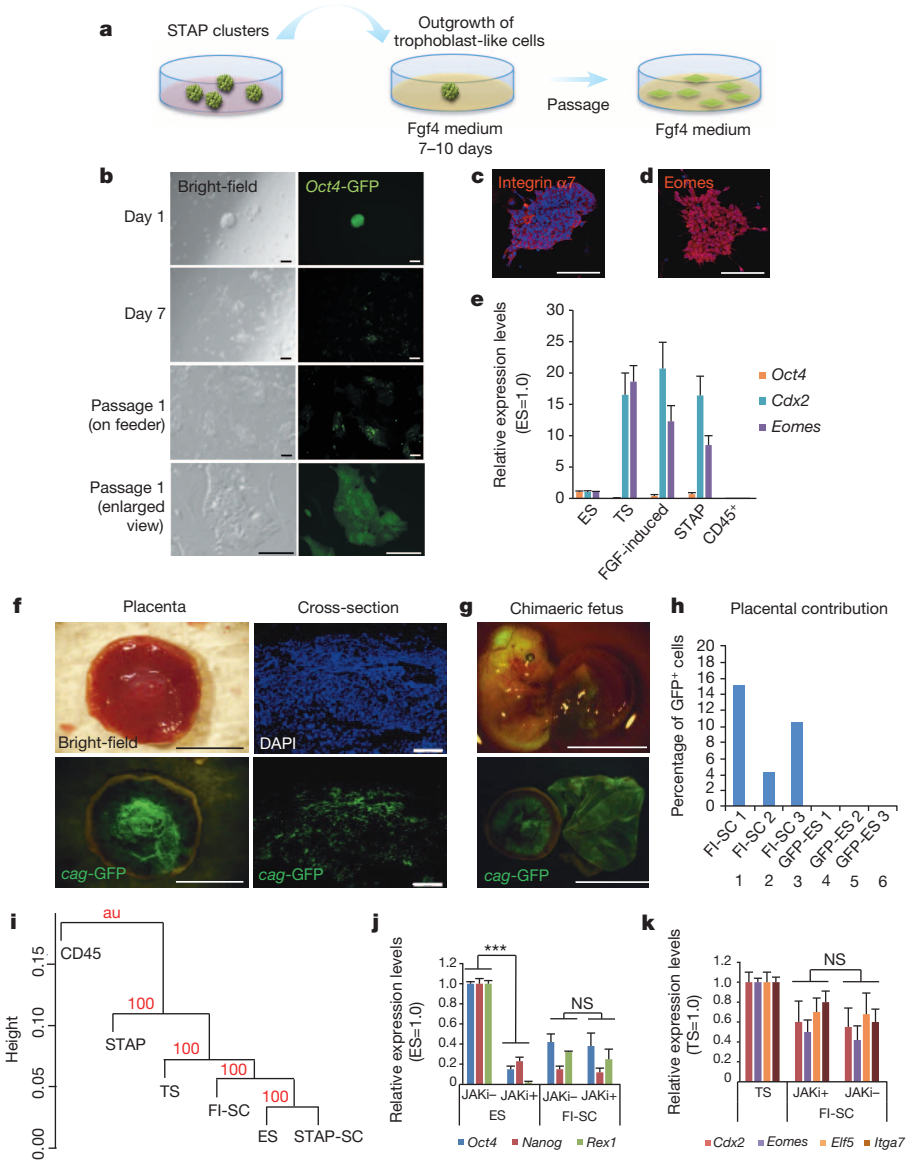

Figure 2 | Fgf4 treatment induces some trophoblast-lineage character in STAP cells. **a**, Schematic of Fgf4 treatment to induce Fgf4-induced stem cells from STAP cells. **b**, Fgf4 treatment promoted the generation of flat cell clusters that expressed *Oct4*-GFP at moderate levels (right). Top and middle: days 1 and 7 of culture with Fgf4, respectively. Bottom: culture after the first passage. Scale bar, 50 μm. **c**, **d**, Immunostaining of Fgf4-induced cells with the trophoblast stem cell markers integrin α7 (**c**) and eomesodermin (**d**). Scale bar, 50 μm. **e**, qPCR analysis of marker expression. **f**, **g**, Placental contribution of Fgf4-induced stem cells (FI-SCs) (genetically labelled with constitutive GFP expression). Scale bars: 5.0 mm (**f** (left panel) and **g**); 50 μm (**f**, right panel). In addition to placental contribution, Fgf4-induced stem cells contributed to the embryonic portion at a moderate level (**g**). **h**, Quantification of placental contribution by FACS analysis. Unlike Fgf4-induced cells, ES cells did not contribute to placental tissues at a detectable level. **i**, Cluster tree diagram from hierarchical clustering of global expression profiles. Red, approximately unbiased *P* values. **j**, qPCR analysis of Fgf4-induced cells (cultured under feeder-free conditions) with or without JAK inhibitor (JAKi) treatment for pluripotent marker genes. **k**, qPCR analysis of FI-SCs with or without JAK inhibitor (JAKi) treatment for trophoblast marker genes. Values are shown as ratio to the expression level in ES cells (**j**) or trophoblast stem cells (**k**). $***P < 0.001$; NS, not significant; *t*-test for each gene between groups with and without JAK inhibitor treatment. $n = 3$. Statistical significance was all the same with three pluripotency markers. None of the trophoblast marker genes showed statistical significance. Error bars represent s.d.

placentae, Fgf4-induced stem cells typically contributed to ~10% of total placental cells (Fig. 2h and Extended Data Fig. 2a, b).

Despite their similarities, we noted that Fgf4-induced stem cells also possessed some critical differences compared with blastocyst-derived trophoblast stem cells. First, Fgf4-induced stem cells exhibited moderate GFP signals and expressed a moderate level of *Oct4* (Fig. 2b; moderate and low levels of immunostaining signals were also seen for Oct4 and Nanog proteins, respectively; Extended Data Fig. 2c), unlike conventional trophoblast stem cells[9] that have little *Oct4* expression (Fig. 2e). Second, unlike trophoblast stem cells, blastocyst-injected Fgf4-induced stem cells also contributed to embryonic tissues (in all cases that involved chimaeric placentae; $n = 32$), although the extent of contribution was generally modest (Fig. 2g). Third, immunostaining revealed that the level of Cdx2 protein accumulation in the nuclei of Fgf4-induced stem cells was marginal as compared to the cytoplasmic level, although the transcript expression level was substantial (Fig. 2e). This may suggest complex and dynamic post-transcriptional regulations for this key transcription factor in Fgf4-induced stem cells (a similar situation was seen for STAP cells, in which clear nuclear localization was not observed for either Cdx2 or Eomes, despite substantial expression of their transcripts). Fourth, in the absence of Fgf4, Fgf4-induced stem cells gradually died in 7–10 days and did not differentiate into large and multi-nuclear cells, unlike trophoblast stem cells (Extended Data Fig. 2d).

To investigate the relationship among STAP cells, STAP stem cells, Fgf4-induced stem cells, ES cells and trophoblast stem cells, we performed genome-wide RNA-sequencing analysis (Fig. 2i for dendrogram; Extended Data Figs 3 and 4 for expression analyses of representative genes[14,15]; Supplementary Tables 2 and 3 for analysis conditions). Whereas STAP cells formed a cluster with STAP stem cells, Fgf4-induced stem cells, ES cells and trophoblast stem cells and not with the parental $CD45^+$ cells, STAP cells were an outlier to the rest of the cell types in the cluster. In contrast, STAP stem cells were closely clustered with ES cells. Fgf4-induced stem cells formed a cluster with a sub-cluster of ES cells and STAP stem cells, whereas trophoblast stem cells comprised an outlier to this cluster, indicating a close relationship of Fgf4-induced stem cells with these pluripotent cells.

However, as Fgf4-induced stem cells lay between STAP stem cells and trophoblast stem cells in the dendrogram, the possibility of contamination of STAP stem cells in the Fgf4-induced stem-cell population cannot be ruled out. Previous studies have indicated that inner cell mass (ICM)-type pluripotent cells can be removed from culture by treating the culture with a JAK inhibitor[16] (Extended Data Fig. 5a, b). In contrast, the JAK inhibitor treatment had no substantial effect on *Oct4*-GFP expression in Fgf4-induced stem-cell culture (Extended Data Fig. 5c, d; see Extended Data Fig. 5e, f for control). Expression of neither pluripotency markers (Fig. 2j) nor trophoblast markers (Fig. 2k) was substantially affected, indicating that pluripotency marker expression is unlikely to reflect contaminating STAP stem cells (ICM-type). Consistent with this idea, Fgf4-induced stem cells that were strongly positive for the trophoblast marker Itga7 (a surface marker for trophoblasts but not ES cells) also expressed high levels of *Oct4*-GFP (Extended Data Fig. 5g).

Notably, when cultured in LIF+FBS-containing medium for 4 days, Fgf4-induced stem cells underwent substantial changes in morphology and started to form ES-cell-like compact colonies with strong GFP signals (Fig. 3a). These cells showed expression of pluripotency makers, but not trophoblast markers (Fig. 3b and Extended Data Fig. 6a), and formed teratomas in mice (Extended Data Fig. 6b). These ES-like cells were generated from Fgf4-induced stem cells sorted for strong expression of the trophoblast marker Itga7, but rarely from Itga7-dim cells (Fig. 3c, d).

To confirm further that Fgf4-induced stem cells with a trophoblast-like nature were converted into ES-like cells, rather than just selecting ES-like cells pre-existing in the Fgf4-induced stem cell culture, we examined the effect of the MEK inhibitor PD0325901 on the ES-like cell generation from Fgf4-induced stem cells. Like trophoblast stem cells, Fgf4-induced stem-cell survival is dependent on FGF–MEK signals, and

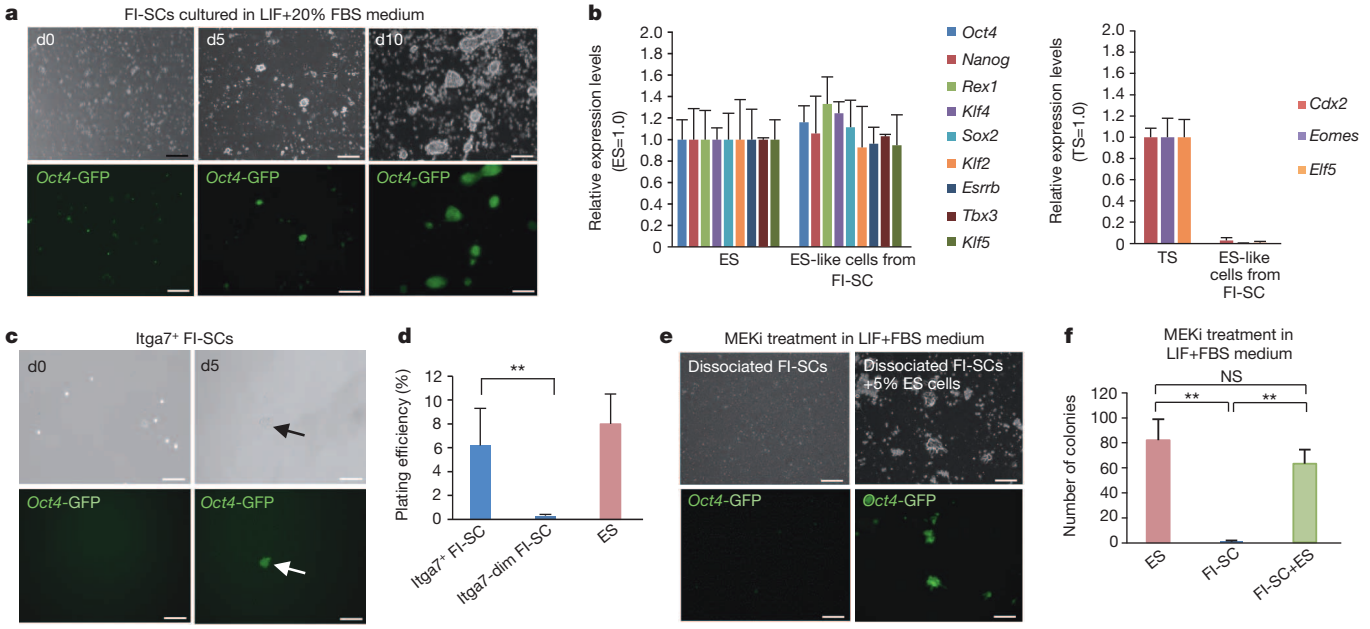

Figure 3 | Fgf4 treatment induces some trophoblast-lineage character in STAP cells. **a**, Culture of *Oct4*-GFP Fgf4-induced cells in LIF + 20% FBS medium. **b**, qPCR analysis of ES-like cells derived from Fgf4-induced cells for pluripotent marker genes (left) and trophoblast marker genes (right). Values are shown as ratio to the expression level in ES cells (left) or trophoblast stem (TS) cells (right). **c**, **d**, Culture of *Oct4*-GFP Fgf4-induced cells sorted by FACS for strong integrin α7 (Itga7) expression in LIF + 20% FBS medium. **d**, Formation frequency (shown by percentage) of *Oct4*-GFP^+ colonies from cells plated on gelatin-coated dishes at a clonal density. $^{**}P < 0.01$; *t*-test; $n = 3$. **e**, **f**, Culture of *Oct4*-GFP Fgf4-induced cells (dissociated) in LIF + 20% FBS medium with MEK inhibitor. $^{**}P < 0.01$; NS, not significant; Tukey's test; $n = 3$. **e**, No substantial formation of *Oct4*-GFP^+ colonies was seen from Fgf4-induced cells in the presence of MEK inhibitor (left), whereas colonies frequently formed when cells were co-plated with *Oct4*-GFP ES cells (right; plated cells were 1/20 of Fgf4-induced cells). **f**, Quantification of colony formation per plated cells (1×10^3 Fgf4-induced cells and/or 1×10^3 ES cells). Unlike Fgf4-induced cells, ES cells formed colonies (regardless of co-plating with FI-SCs) in the presence of MEK inhibitor. Bars and error bars represent mean values and s.d., respectively (**b**, **d**, **f**). Scale bars: 100 μm (**a**, **c**, **e**).

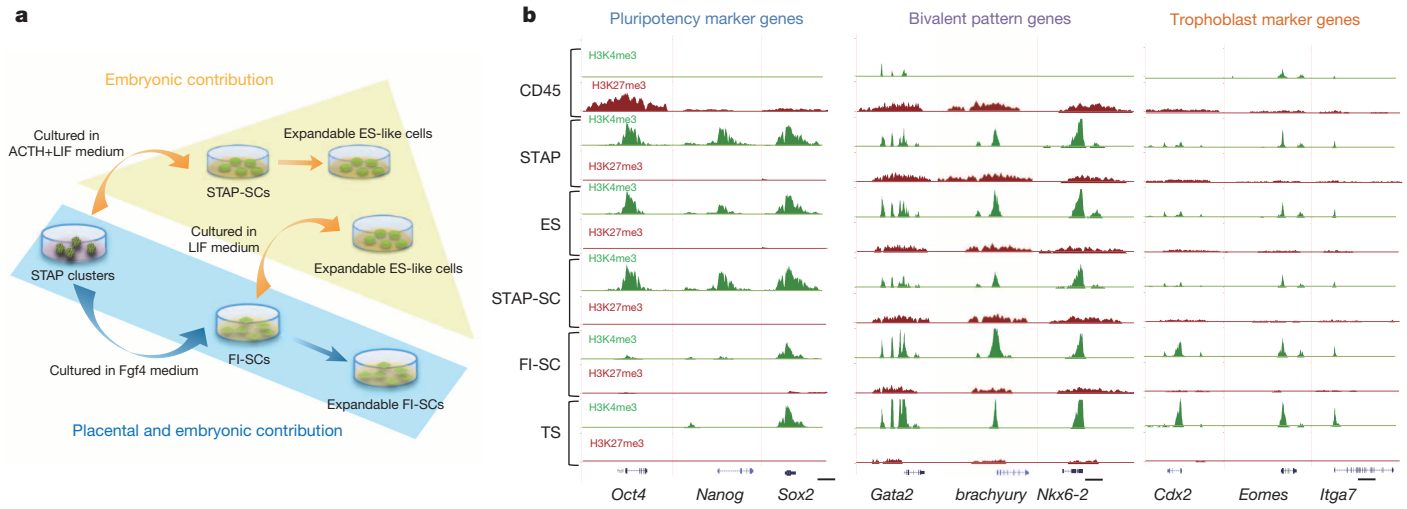

Figure 4 | Differentiation potential and epigenetic state of STAP and STAP-derived stem cells. **a**, Schematic diagram of stem-cell conversion cultures from STAP cells under different conditions. **b**, ChIP-sequencing results of histone H3K4 (green) and H3K27 (red) trimethylation at the loci of pluripotent marker genes (left), bivalent pattern genes (middle) and trophoblast marker genes (right). Scale bars indicate 10 kb for pluripotency marker genes and trophoblast marker genes, and 20 kb for bivalent pattern genes.

the inhibition of MEK activity caused massive cell death (Extended Data Fig. 6c). However, PD0325901 is also known to be a main effector in 2i medium[17] and to promote ES cell maintenance. Addition of PD0325901 to LIF+FBS-containing medium strongly inhibited the formation of ES-like colonies from Fgf4-induced stem cells (Fig. 3e, left, and Fig. 3f). This inhibition was unlikely to be due to secondary toxic effects from massive cell death of Fgf4-induced stem cells, as colonies formed in the presence of PD0325901 when ES cells were co-plated in the same culture with Fgf4-induced stem cells (Fig. 3e, right, and Fig. 3f).

Collectively, these findings demonstrate that STAP-derived Fgf4-induced stem cells not only express both pluripotency markers and trophoblast genes but also have the potential to convert into ES-like cells when cultured in LIF+FBS-containing medium (Fig. 4a).

Here we demonstrate that STAP cells, which have a limited self-renewal ability, can be induced to generate two distinct types of robustly self-renewing stem cells—STAP stem cells and Fgf4-induced stem cells—under different culture conditions. Chromatin immunoprecipitation (ChIP) sequencing analysis showed distinct accumulation patterns of modified histone H3 in the two types of STAP-cell-derived stem cells (Fig. 4b). STAP stem cells (as well as STAP cells) had accumulation patterns of H3K4 and H3K27 trimethylation that resembled those of ES cells at the loci of pluripotency marker genes (*Oct4*, *Nanog*, *Sox2*), bivalent pattern genes[18] (*Gata2*, *brachyury*, *Nkx6-2*) and trophoblast marker genes (*Cdx2*, *Eomes*, *Itga7*). In contrast, the accumulation patterns in Fgf4-induced stem cells at these loci matched more closely those of trophoblast stem cells, except that low levels of accumulation of H3K4 trimethylation in *Oct4* and *Nanog* and of H3K27 trimethylation in the trophoblast marker genes were observed in Fgf4-induced stem cells but not trophoblast stem cells.

Recent studies have also begun to reveal dynamic regulations in multiple cellular states related to pluripotency. These include reports of co-expression of Oct4 and Cdx2 in rat ES cells maintained in the presence of a GSK-3β inhibitor[19,20] and of Oct4 expression in rat extra-embryonic precursors[21]. Another recent study has indicated that conventional ES cell culture also contains a very minor population of Oct4$^-$ cells with features resembling those of very early-stage embryos[22], including bidirectional potential. However, these cells are dissimilar to STAP cells as they are Oct4$^-$, unlike STAP cells and Fgf4-induced stem cells. Our preliminary genome-wide RNA-sequencing analysis indicated that both morulae and blastocysts are outliers to the cluster of STAP and ES cells (Extended Data Fig. 6d–f and Supplementary Tables 4 and 5).

A key conclusion drawn from this study is that the reprogramming in STAP conversion goes beyond the pluripotent state of ES cells and involves the acquisition of a wider developmental potential related to both ICM- and trophoectoderm-like states. Because of the inability to clone STAP cells from single cells, we must await future technical advancement to examine whether their dual-directional differentiation potential at the population level may reflect one totipotent state at the single-cell level or two different states of STAP cells coexisting (or fluctuating between them) in culture. As for STAP-cell-derived Fgf4-induced stem cells, which can also contribute to both embryonic and placental tissues, our *in vitro* conversion study combined with inhibitor treatments clearly indicate that the bidirectional potential of Fgf4-induced stem cells is unlikely to reflect the co-presence of separate subpopulations of ES-like and trophoblast-stem-like cells in the culture. Collectively, our study indicates that STAP-based conversion can reprogram somatic cells to acquire not only pluripotency but also the ability of trophoblast differentiation.

METHODS SUMMARY

Cell culture. STAP cells were generated from mouse splenic CD45$^+$ cells by a transient exposure to low-pH solution, followed by culture in B27+LIF medium[1]. For establishment of the Fgf4-induced stem-cell line, STAP cell clusters were transferred to Fgf4 (25 ng μl)-containing trophoblast stem-cell medium[9] on MEF feeder cells in 96-well plates. The cells were subjected to the first passage during days 7–10 using a conventional trypsin method. For inducing conversion from Fgf4-induced stem cells into ES-like cells, Fgf4-induced stem cells were trypsinized, and suspended cells were plated in ES maintenance medium containing LIF and 20% FBS. For the establishment of STAP stem-cell lines, STAP spheres were transferred to ACTH-containing medium[15] on a MEF feeder or gelatin-coated dish. Four to seven days later, the cells were subjected to the first passage using a conventional trypsin method, and suspended cells were plated in ES maintain medium containing 5% FBS and 1% KSR.

Chimaeric mice generation and analyses. For injection of STAP stem cells, Fgf4-induced stem cells and ES cells, a conventional blastocyst injection method was used. For STAP cell injection, STAP cell clusters were injected en bloc, because trypsin treatment caused low chimaerism. STAP spherical colonies were cut into small pieces using a microknife under microscopy, then small clusters of STAP colony were injected into day-4.5 blastocysts by large pipette. The next day, the chimaeric blastocysts were transferred into day-2.5 pseudopregnant females.

Online Content Any additional Methods, Extended Data display items and Source Data are available in the online version of the paper; references unique to these sections appear only in the online paper.

Received 10 March; accepted 20 December 2013.

1. Obokata, H. *et al.* Stimulus-triggered fate conversion of somatic cells into pluripotency. *Nature* **505,** 641–647 (2014).

2. Gurdon, J. B. The developmental capacity of nuclei taken from intestinal epithelium cells of feeding tadpoles. *J. Embryol. Exp. Morphol.* **10,** 622–640 (1962).
3. Wakayama, T., Perry, A. C., Zuccotti, M., Johnson, K. R. & Yanagimachi, R. Full-term development of mice from enucleated oocytes injected with cumulus cell nuclei. *Nature* **394,** 369–374 (1998).
4. Takahashi, K. & Yamanaka, S. Induction of pluripotent stem cells from mouse embryonic and adult fibroblast cultures by defined factors. *Cell* **126,** 663–676 (2006).
5. Nagy, A., Rossant, J., Nagy, R., Abramow-Newerly, W. & Roder, J. C. Derivation of completely cell culture-derived mice from early-passage embryonic stem cells. *Proc. Natl Acad. Sci. USA* **90,** 8424–8428 (1993).
6. Niwa, H. How is pluripotency determined and maintained? *Development* **134,** 635–646 (2007).
7. Beddington, R. S. & Robertson, E. J. An assessment of the developmental potential of embryonic stem cells in the midgestation mouse embryo. *Development* **105,** 733–737 (1989).
8. Quinn, J., Kunath, T. & Rossant, J. Mouse trophoblast stem cells. *Methods Mol. Med.* **121,** 125–148 (2006).
9. Tanaka, S., Kunath, T., Hadjantonakis, A. K., Nagy, A. & Rossant, J. Promotion of trophoblast stem cell proliferation by FGF4. *Science* **282,** 2072–2075 (1998).
10. Tanaka, T. S. *et al.* Gene expression profiling of embryo-derived stem cells reveals candidate genes associated with pluripotency and lineage specificity. *Genome Res.* **12,** 1921–1928 (2002).
11. Klaffky, E. *et al.* Trophoblast-specific expression and function of the integrin alpha 7 subunit in the peri-implantation mouse embryo. *Dev. Biol.* **239,** 161–175 (2001).
12. Russ, A. P. *et al.* Eomesodermin is required for mouse trophoblast development and mesoderm formation. *Nature* **404,** 95–99 (2000).
13. Niwa, H. *et al.* Interaction between Oct3/4 and Cdx2 determines trophectoderm differentiation. *Cell* **123,** 917–929 (2005).
14. Mikkelsen, T. S. *et al.* Dissecting direct reprogramming through integrative genomic analysis. *Nature* **454,** 49–55 (2008).
15. van Oosten, A. L., Costa, Y., Smith, A. & Silva, J. C. JAK/STAT3 signalling is sufficient and dominant over antagonistic cues for the establishment of naive pluripotency. *Nature Commun.* **3,** 817 (2012).
16. Yang, J. *et al.* Stat3 activation is limiting for reprogramming to ground state pluripotency. *Cell Stem Cell* **7,** 319–328 (2010).
17. Ying, Q. L. *et al.* The ground state of embryonic stem cell self-renewal. *Nature* **453,** 519–523 (2008).
18. Bernstein, B. E. *et al.* A bivalent chromatin structure marks key developmental genes in embryonic stem cells. *Cell* **125,** 315–326 (2006).
19. Meek, S. *et al.* Tuning of β-catenin activity is required to stabilize self-renewal of rat embryonic stem cells. *Stem Cells* **31,** 2104–2115 (2013).
20. Chen, Y., Blair, K. & Smith, A. Robust self-renewal of rat embryonic stem cells requires fine-tuning of glycogen synthase kinase-3 inhibition. *Stem Cell Rep.* **1,** 209–217 (2013).
21. Debeb, B. G. *et al.* Isolation of Oct4-expressing extraembryonic endoderm precursor cell lines. *PLoS ONE* **4,** e7216 (2009).
22. Macfarlan, T. S. *et al.* Embryonic stem cell potency fluctuates with endogenous retrovirus activity. *Nature* **487,** 57–63 (2012).

Supplementary Information is available in the online version of the paper.

Acknowledgements We thank S. Nishikawa and N. Love for discussion and M. Ohgushi, S. Kuraku, M. Eiraku, S. Ohtsuka and K. Kakiguchi for help with experimental planning, material preparation and analyses. Financial support for this research was provided by Intramural RIKEN Research Budget (H.O., T.W. and Y.S.), a Scientific Research in Priority Areas (20062015) to T.W., the Network Project for Realization of Regenerative Medicine to Y.S., and Department of Anesthesiology, Perioperative and Pain Medicine at Brigham and Women's Hospital to C.A.V.

Author Contributions H.O. and Y.S. wrote the manuscript. H.O., Y.S., M.K., M.A., N.T., S.Y. and T.W. performed experiments, and M.T. and Y.T. assisted with H.O.'s experiments. H.O., Y.S., H.N., C.A.V. and T.W. designed the project.

Author Information RNA-seq and ChIP-seq files have been submitted to the NCBI BioSample databases under accessions SAMN02393426, SAMN02393427, SAMN02393428, SAMN02393429, SAMN02393430, SAMN02393431, SAMN02393432, SAMN02393433, SAMN02393434 and SAMN02393435. Reprints and permissions information is available at www.nature.com/reprints. The authors declare no competing financial interests. Readers are welcome to comment on the online version of the paper. Correspondence and requests for materials should be addressed to H.O. (obokata@cdb.riken.jp), T.W. (teru@cdb.riken.jp) or Y.S. (yoshikisasai@cdb.riken.jp).

METHODS

Animal studies. Research involving animals complied with protocols approved by the Harvard Medical School/Brigham and Women's Hospital Committee on Animal Care, and the Institutional Committee of Laboratory Animal Experimentation of the RIKEN Center for Developmental Biology.

Cell culture. STAP cells were generated from low-pH-treated $CD45^+$ cells, followed by culture in B27 + LIF medium for 7 days, as described[1]. For Fgf4-induced stem-cell line establishment, STAP cell clusters were transferred to Fgf4-containing trophoblast stem-cell medium[9] on MEF feeder cells in 96-well plates. In most cases (40 out of 50 experiments), colonies grew in 10–50% of wells in 96-well plates. In minor cases (10 out of 50 experiments), no colony growth was observed and/or only fibroblast-like cells appeared. The cells were subjected to the first passage during days 7–10 using a conventional trypsin method. Subsequent passages were performed at a split ratio of 1:4 every third day before they reached subconfluency.

STAP stem-cell lines were established as described[1]. STAP spheres were transferred to ACTH-containing medium[1] on MEF feeder cells (several spheres, up to a dozen spheres, per well of 96-well plates). Four to seven days later, the cells were subjected to the first passage using a conventional trypsin method, and suspended cells were plated in ES maintain medium containing 20% FBS. Subsequent passaging was performed at a split ratio of 1:10 every second day before they reached subconfluency.

Chimaera mouse generation and analyses. For production of diploid and tetraploid chimaeras with STAP cells, STAP stem cells and Fgf4-induced stem cells, diploid embryos were obtained from ICR strain females. Tetraploid embryos were produced by electrofusion of 2-cell embryos. Because trypsin treatment of donor samples turned out to cause low chimaerism, STAP spherical colonies were cut into small pieces using a microknife under microscopy, and small clusters of STAP cells were then injected into day-4.5 blastocysts by a large pipette. Next day, the chimaeric blastocysts were transferred into day-2.5 pseudopregnant females.

***In vivo* differentiation assay.** 1×10^5 cells of Fgf4-induced stem-cell-derived ES-like cells were injected subcutaneously into the dorsal flanks of 4-week-old NOD/SCID mice. Six weeks later, the implants were collected and histologically analysed. The implants were fixed with 10% formaldehyde, embedded in paraffin, and routinely processed into 4-μm-thick sections. Sections were stained with haematoxylin and eosin. So far, we have not investigated whether Fgf4-induced stem cells form tumours such as teratomas and yolk sac tumours *in vivo*.

Immunostaining. Cells were fixed with 4% PFA for 15 min and, after permeabilization, with 0.5% Triton X-100 and then incubated with primary antibodies: anti-H3K27me3 (Millipore; 1:300), anti-Oct3/4 (Santa Cruz Biotechnology; 1:300), anti-Nanog (eBioscience; 1:300), anti-KLF4 (R&D System; 1:300), anti-Esrrβ (R&D System; 1:300) and integrin α7 antibody (R&D system; 1:200). After overnight incubation, bound antibodies were visualized with a secondary antibody conjugated to Alexa546 (Molecular Probes). Nuclei were stained with DAPI (Molecular Probes).

RNA preparation and RT–PCR analysis. RNA was isolated with the RNeasy Mini kit (Qiagen). Reverse transcription was performed with the SuperScript III First Strand Synthesis kit (Invitrogen). Power SYBR Green Mix (Roche Diagnostics) was used for PCR amplification, and samples were run on a Lightcycler-II Instrument (Roche Diagnostics). The primer sets for each gene are listed in Supplementary Table 1.

Inhibitor assay. For JAK inhibitor assay, Fgf4-induced stem cells were cultured without feeders for 48 h in trophoblast stem-cell culture medium supplemented with 0.6 μM JAK inhibitor (CalBiochem, 420097). As a control, ES cells were also cultured for 48 h in ES medium supplemented with 0.6 μM JAK inhibitor. After the JAK inhibitor treatment, cells were collected and their gene expression was analysed by RT–PCR. For MEK inhibitor assay, dissociated Fgf4-induced stem cells were plated in either LIF containing ES medium supplemented with 1 μM MEK inhibitor (PD025901) or FGF4 containing trophoblast stem cell medium supplemented with 1 μM MEK inhibitor for 48 h. As controls, dissociated Fgf4-induced stem cells were co-plated with 5% or 50% of ES cells into the same culture conditions. After the MEK inhibitor treatment, colonies that formed in each culture condition were counted.

FACS sorting. Fgf4-induced stem cells were dissociated into single cells and were suspended in 0.5% BSA PBS. Suspended cells were Fc-blocked by treatment with 1 μg of mouse IgG per 10^5 cells for 15 min at room temperature. PE-conjugated integrin α7 antibody (R&D system, FAB3518P, dilution at 1:10) was added into cell suspension, and cells were incubated for 30 min on ice. Finally, cells were rinsed with PBS three times and propidium iodide was added for dead cell elimination. As a control, Fgf4-induced stem cells in a separate tube were treated with PE-labelled rat IgG_{2B} antibody. Integrin α7-positive and -dim cells were sorted by FACS aria II (BD).

RNA sequencing and ChIP sequencing analyses. RNA-sequencing of cell lines was performed with biological duplicate samples. Total RNA was extracted from T cells by the RNasy mini kit (Qiagen). RNA-seq libraries were prepared from 1 μg total RNAs following the protocol of the TruSeq RNA Sample Prep kit (Illumina) and subjected to the deep sequencing analysis with Illumina Hi-Seq1000. A cluster tree diagram of various cell types was obtained from hierarchical clustering of global expression profiles ($\log_2$ FPKM of all transcripts; FPKM, fragments per kilobase of transcript per million mapped reads). Complete linkage method applied to $1 - r$ (r = Pearson's correlation between profiles) was used for generating the tree and 1,000 cycles of bootstrap resampling were carried out to obtain statistical confidence score in % units (also called AU P values). For the analysis that included morula and blastocyst embryos (only small amounts of RNA can be obtained from them), we used pre-amplification with the SMARTer Ultra Low RNA kit for Illumina Sequencing (Clontech Laboratories). Differentially expressed genes were identified by the DESeq package[23].

ChIP-seq libraries were prepared from 20 ng input DNAs, 1 ng H3K4me3 ChIP DNAs, or 5 ng H3K27me3 ChIP DNAs using the KAPA Library Preparation kit (KAPA Biosystems). TruSeq adaptors were prepared in-house by annealing a TruSeq universal oligonucleotide and each of index oligonucleotides (5′-AATGATACGGCGACCACCGAGATCTACACTCTTTCCCTACACGACGCTCTTCCGATCT-3′, and 5′-GATCGGAAGAGCACACGTCTGAACTCCAGTCACXXXXXXATCTCGTATGCCGTCTTCTGCTTG-3′; where X represents index sequences).

Chromatin immunoprecipitation was performed as follows. Cells were fixed in PBS(-) containing 1% formaldehyde for 10 min at room temperature. Glycine was added to a final concentration of 0.25 M to stop the fixation. After washing the cells twice in ice-cold PBS(-), cells were further washed in LB1 (50 mM HEPES-KOH pH 7.5, 140 mM NaCl, 1 mM EDTA, 10% glycerol, 0.5% NP-40, 0.25% Triton X-100) and LB2 (10 mM Tris-HCl pH 8.0, 200 mM NaCl, 1 mM EDTA, 0.5 mM EGTA). Cells were then re-suspended in lysis buffer (50 mM Tris-HCl pH 8.0, 10 mM EDTA, 1% SDS). Lysates were prepared by sonication using COVARIS S220 in a mini tube at duty cycle = 5%, PIP = 70, cycles per burst = 200, and the treatment time of 20 min. Lysates from 2×10^6 cells were diluted in ChIP dilution buffer (16.7 mM Tris-HCl pH 8.0, 167 mM NaCl, 1.2 mM EDTA, 1.1% Triton X-100, 0.01% SDS). ChIP was performed using sheep anti-mouse IgG beads (Invitrogen) or protein A beads (Invitrogen) coupled with anti-histone H3K4me3 antibody (Wako, catalogue no. 307-34813) or anti-histone H3K27me3 antibody (CST, catalogue no. 9733), respectively. After 4–6 h of incubation in a rotator at 4 °C, beads were washed five times in low-salt wash buffer (20 mM Tris HCl pH 8.0, 150 mM NaCl, 2 mM EDTA, 1% Triton X-100, 0.1% SDS), and three times in high-salt wash buffer (20 mM Tris-HCl pH 8.0, 500 mM NaCl, 2 mM EDTA, 1% Triton X-100, 0.1% SDS). Target chromatin was eluted off the beads in elution buffer (10 mM Tris-HCl pH 8.0, 300 mM NaCl, 5 mM EDTA, 1% SDS) at room temperature for 20 min. Crosslink was reversed at 65 °C, and then samples were treated with RNaseA and proteinase K. The prepared DNA samples were purified by phenol-chloroform extraction followed by ethanol precipitation and dissolved in TE buffer.

23. Anders, S. & Huber, W. Differential expression analysis for sequence count data. *Genome Biol.* **11,** R106 (2010).

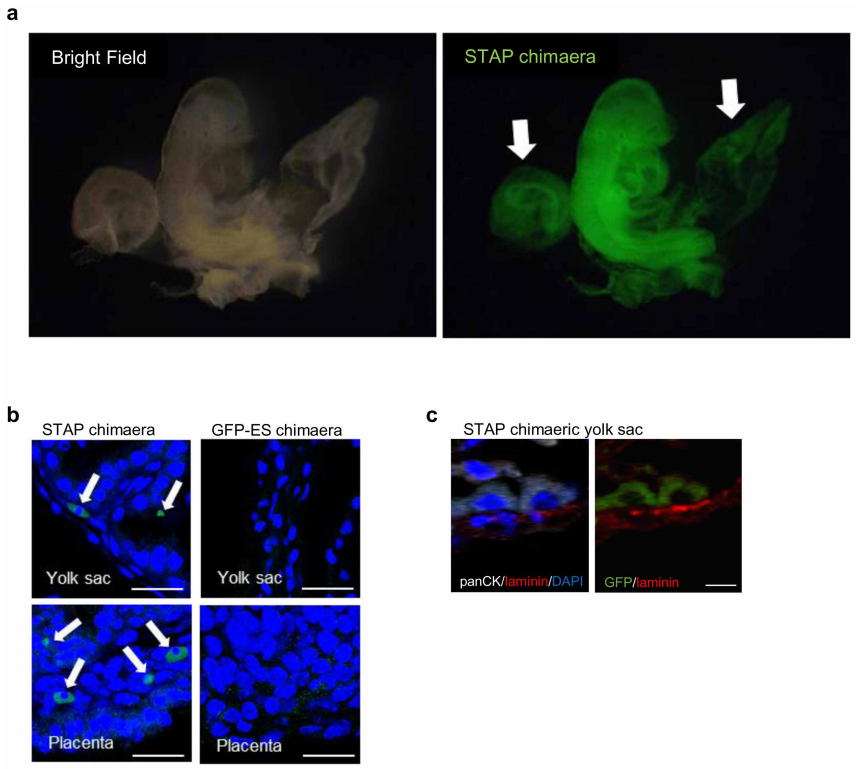

Extended Data Figure 1 | Placental contribution of STAP cells. a, Chimaeric mouse with STAP cells derived from $CD45^+$ cells of B6GFP × 129/Sv mice (B6GFP, C57BL/6 line with *cag-gfp* transgene). Arrows indicate a placenta and a yolk sac. **b**, Cross-sections of yolk sac (top) and placenta (bottom). GFP-positive cells (arrows) were seen only in yolk sac and placenta of the STAP cell chimaera. Scale bars, 50 μm. **c**, Co-immunostaining showed that these GFP-positive cells (right) were found in the extra-embryonic endoderm-derived epithelial cells (pan-cytokeratin$^+$ and overlying laminin$^+$ basement membrane; left) of the yolk sac. Scale bar, 10 μm.

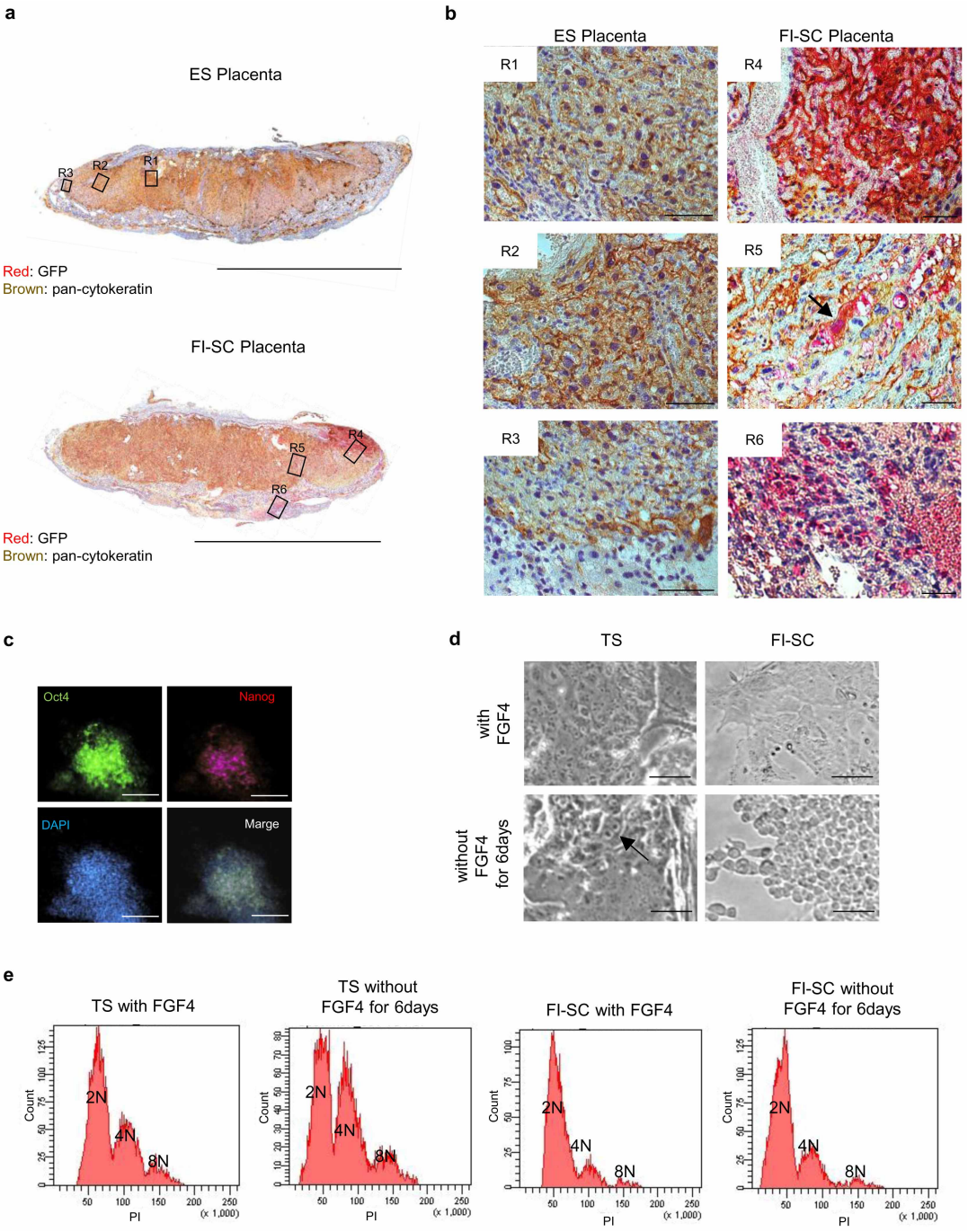

Extended Data Figure 2 | Trophoblast differentiation potential of Fgf4-induced stem cells. **a**, **b**, Immunostaining (cross-section) of placentae obtained in the blastocyst injection assay with GFP (constitutive)-labelled ES cells (upper) or Fgf4-induced stem cells (bottom). Brown shows pan-cytokeratin and red shows GFP (ES cell or Fgf4-induced stem cell contribution). Regions indicated in **a** are shown in **b**. Fgf4-induced stem cells contributed to all layers of placentae, whereas no contribution was observed with ES cells. **a**, Scale bars, 5 mm. **b**, Scale bars, 50 μm. **c**, Pluripotent marker expression of Fgf4-induced stem cells. Scale bars, 50 μm. **d**, **e**, Effects of Fgf4 withdrawal from Fgf4-induced stem cell culture. Unlike trophoblast stem cells (**d**, left), which generated multi-nucleated large cells (arrow) in the absence of Fgf4, Fgf4-induced stem cells (**d**, right) simply stopped proliferation and gradually died on Fgf4 withdrawal. Scale bars, 50 μm. This finding suggests that placental differentiation of Fgf4-induced stem cells *in vivo* may involve more than just Fgf4 signal suppression. **e**, The number of 4N and 8N cells increased within 6 days of Fgf4 withdrawal in trophoblast stem cells but not in Fgf4-induced stem cells.

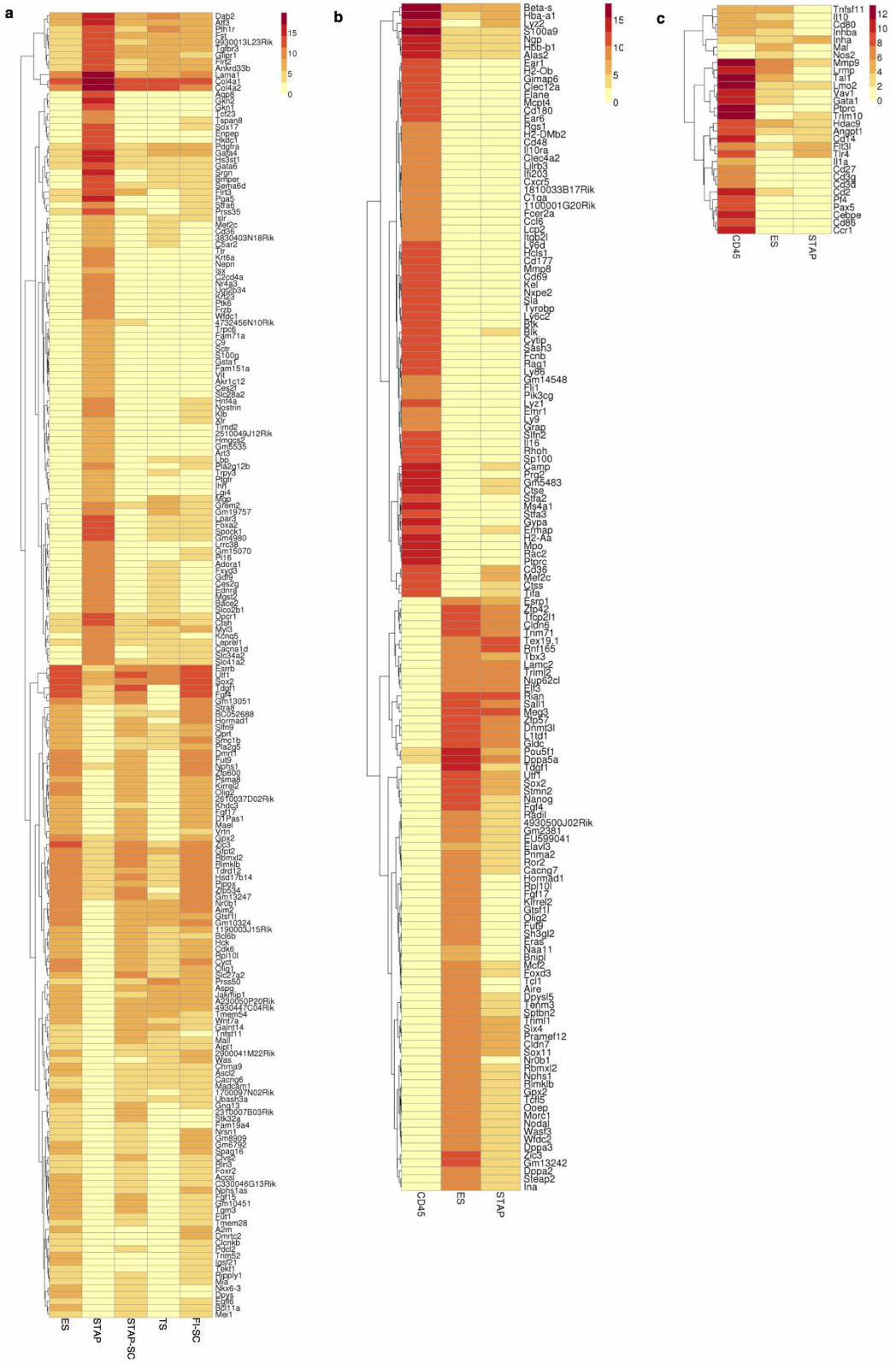

Extended Data Figure 3 | Transcriptome analyses of STAP cells shown by heat maps. **a**, Heat maps of expression profiles of top-ranked up- and downregulated genes in STAP cells (*Oct4*-GFP$^+$ clusters converted from CD45$^+$ cells) compared to ES cells. Their respective expression levels in STAP stem cells, trophoblast stem cells and Fgf4-induced stem cells are shown. Absolute expression values are scaled by $\log_2$. The genes expressed differentially between ES cells and STAP cells tended to show more similar expression profiles to ES cells in STAP stem cells and Fgf4-induced stem cells than in trophoblast stem cells. Expression of some early endodermal lineage genes such as *Gata4* and *Sox17* was moderately elevated in STAP cells as compared to ES cells, whereas its biological significance remains elusive (these genes are shown to be strongly expressed in *Oct4*-GFP-dim cells[1]). **b**, Heat maps of expression profiles of top-ranked up- and downregulated genes in ES cells compared to CD45$^+$ cells and their respective expression levels in STAP cells. The genes expressed differentially between CD45$^+$ and ES cells tended to show similar expression profiles in ES cells and STAP cells. **c**, Heat maps of expression profiles of representative genes implicated in haematopoietic lineage development in CD45$^+$, ES and STAP cells. No strong correlation was seen between CD45$^+$ cells and STAP cells in their expression profiles (a similar tendency of no correlation was seen for the data in **b**).

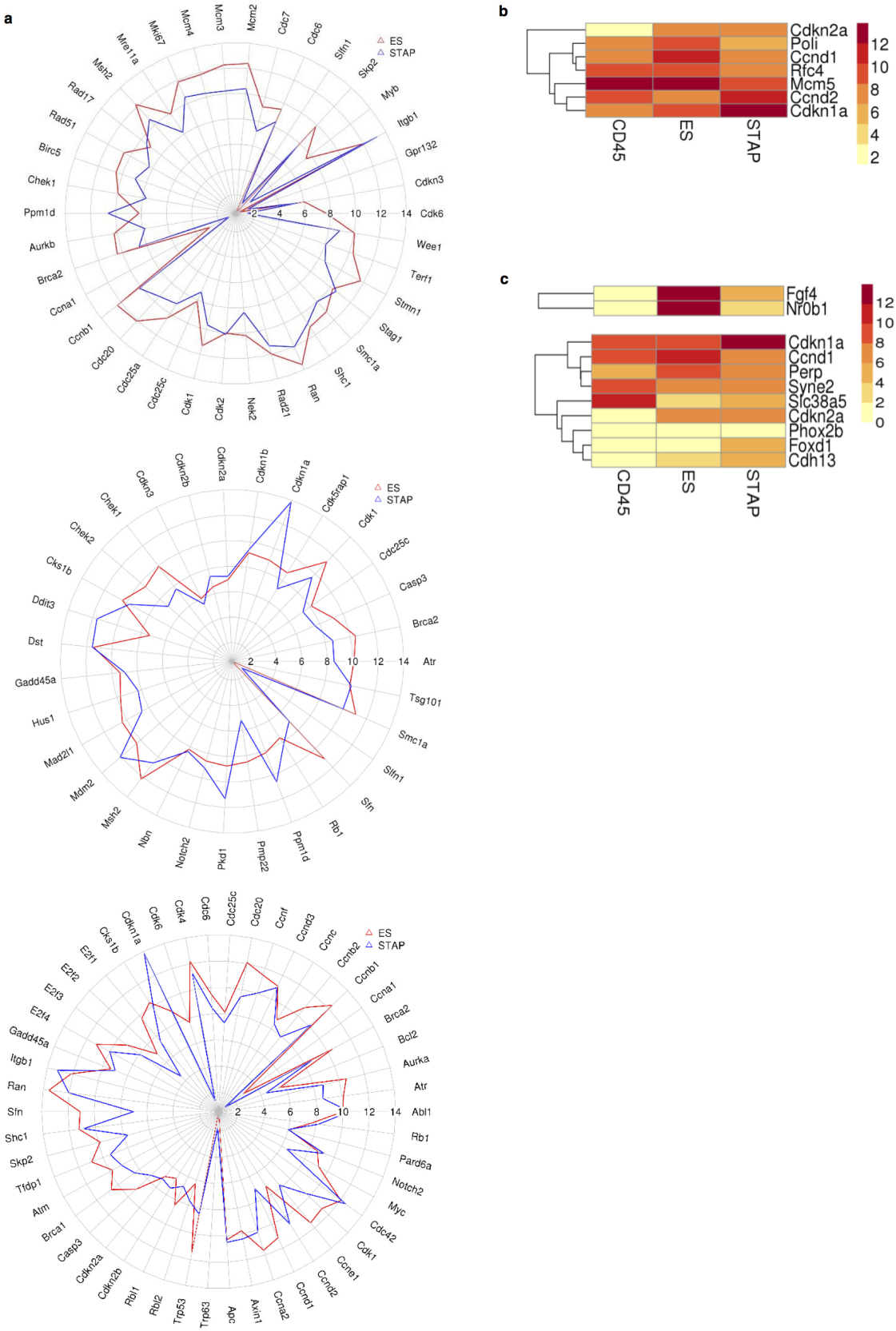

Extended Data Figure 4 | Transcriptome analyses for genes implicated in cell-cycle control and induced pluripotent stem-cell conversion. **a**, Comparison of expression values of genes involved in cell-cycle control in ES and STAP cells; the G to M cell cycle phases (upper), the cell cycle checkpoint and cell cycle arrest (middle), and the cell cycle regulation (bottom) are shown. Expression level was measured by $\log_2$ of mean normalized counts. **b**, Heat map for upregulated genes in cells undergoing reprogramming by 'Yamanaka factors'[14]. **c**, Heat maps for upregulated genes in pre-iPS cells[15] (top) and in partially reprogrammed cells by Yamanaka factors (bottom)[14]. Expression level was measured by $\log_2$ of mean normalized counts. Differentially expressed genes were identified by the DESeq package[21] and only genes with a false discovery rate of 1% were selected for comparison, unless mentioned otherwise.

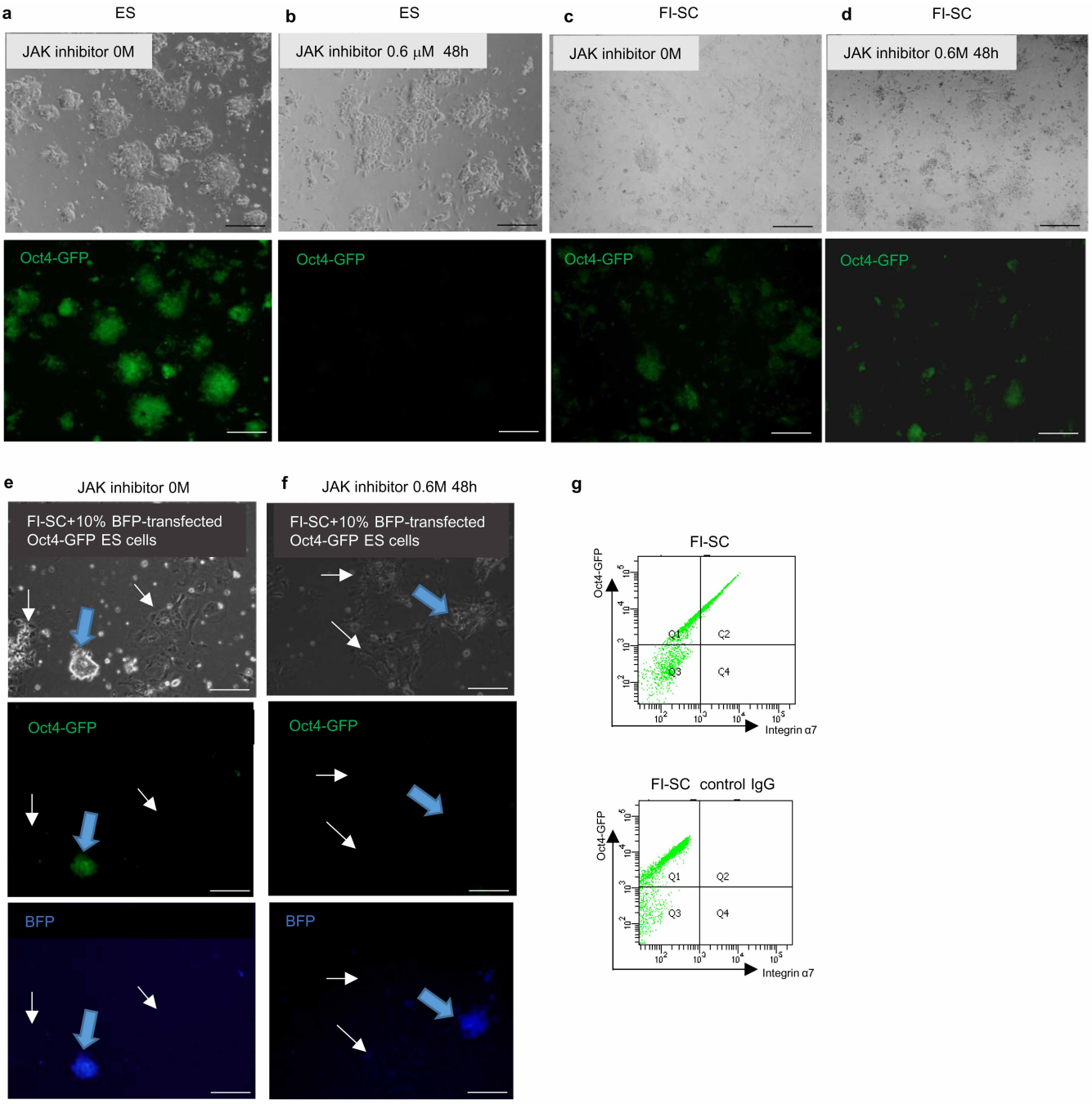

Extended Data Figure 5 | Responses of Fgf4-induced stem cells to signal modifications. a–f, JAK inhibitor treatment assay for Fgf4-induced stem cells. Fgf4-induced stem cells were cultured under feeder-free conditions and treated with 0.6 μM JAK inhibitor for 48 h. JAK inhibitor treatment assay eliminated ES cells (*Oct4*-GFP^{+}) from the culture (**a**, **b**). The level of *Oct4*-GFP expression in Fgf4-induced stem cells, which was moderate, was maintained even after JAK inhibitor treatment (**c**, **d**; three independent experiments). Scale bar, 100 μm. **e**, **f**, For an additional control, Fgf4-induced stem cells were plated in trophoblast stem-cell medium containing Fgf4 together with *Oct4*-GFP ES cells that constitutively expressed BFP (the number of plated cells was one-tenth of that of plated Fgf4-induced stem cells). Whereas BFP-expressing colonies (ES-cell-derived) still expressed *Oct4*-GFP in trophoblast stem-cell culture medium after 2 days (**e**), no *Oct4*-GFP^{+} colonies from BFP-expressing ES cells were observed in the JAK-inhibitor-treated culture (**f**). **g**, FACS analysis of integrin α7 expression in Fgf4-induced stem cells. Over 40% of Fgf4-induced stem cells strongly expressed both the pluripotency marker *Oct4*-GFP and the trophoblast marker integrin α7. The bottom panel shows an isotype control for integrin α7 antibody. In ES cells, integrin-α7-expressing cells were less than 0.1% (data not shown; three independent ES cell lines were examined).

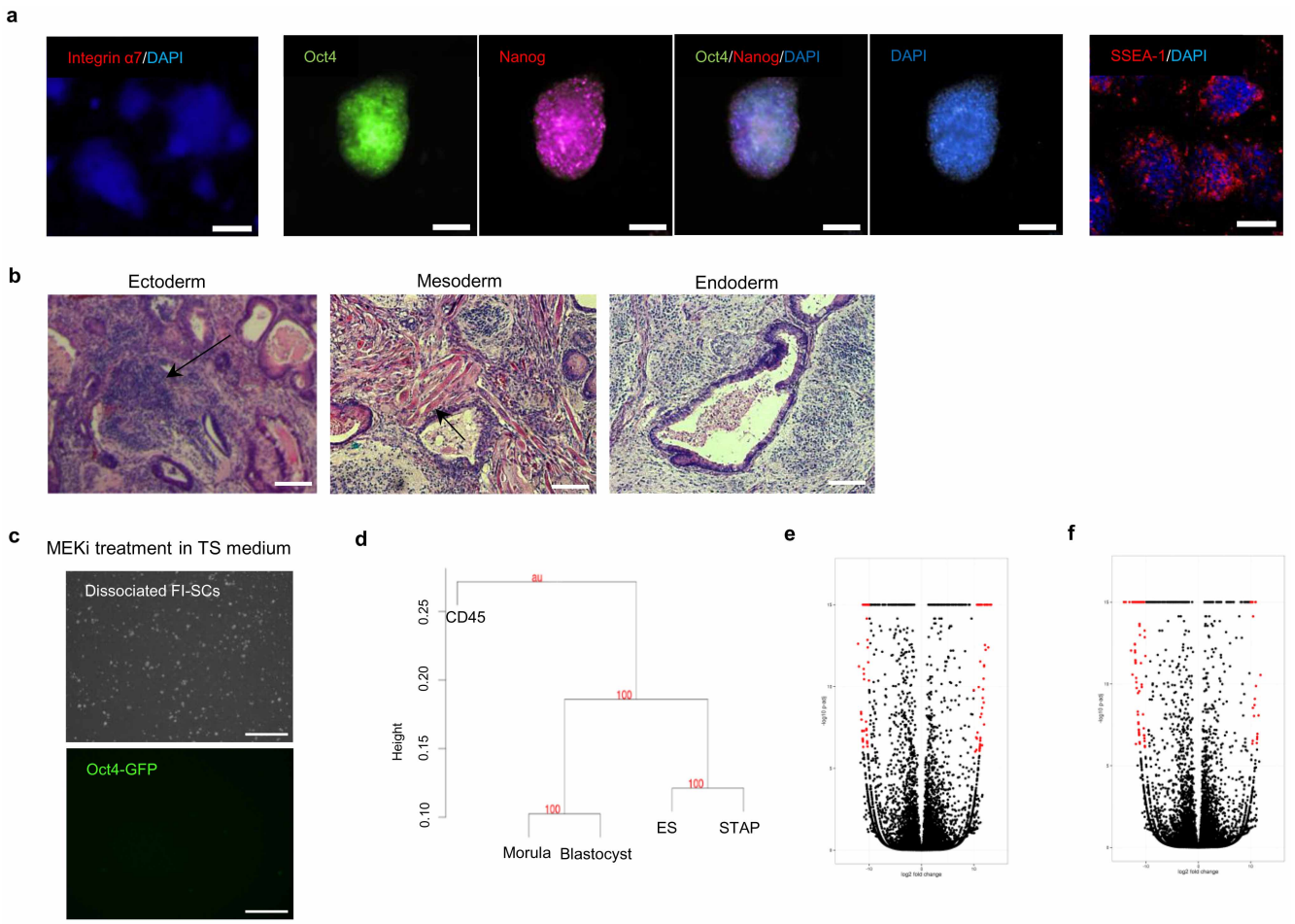

Extended Data Figure 6 | Characterization of ES-like cells converted from Fgf4-induced stem cells and comparison of STAP cells with early embryos. **a**, Immunohistochemistry of ES-like cells for trophoblast and pluripotency markers. ES-like cells converted from Fgf4-induced stem cells no longer expressed the trophoblast marker (integrin alpha 7), but they did express the pluripotency markers (Oct4, Nanog and SSEA-1). Scale bar, 100 μm. **b**, Pluripotency of ES-like cells converted from Fgf4-induced stem cells as shown by teratoma formation. Those cells successfully formed teratomas containing tissues from all three germ layers: neuroepithelium (left, arrow indicates), muscle tissue (middle, arrow indicates) and bronchial-like epithelium (right). Scale bar, 100 μm. **c**, MEK inhibitor treatment assay for *Oct4-gfp* Fgf4-induced stem cells in trophoblast stem-cell medium containing Fgf4. No substantial formation of *Oct4*-GFP^{+} colonies was observed from dissociated Fgf4-induced stem cells in MEK-inhibitor-containing medium. Scale bar, 100 μm. **d**, Cluster tree diagram from hierarchical clustering of global expression profiles. Red, AU *P* values. As this analysis included morula and blastocyst embryos from which only small amounts of RNA could be obtained, we used pre-amplification with the SMARTer Ultra Low RNA kit for Illumina Sequencing (Clontech Laboratories). **e**, **f**, Volcano plot of the expression profile of STAP cells compared to the morula (**e**) and blastocyst (**f**). Genes showing greater than 10-fold change and *P* value 1.0×10^{-6} are highlighted in red and are considered up- (or down-) regulated in the STAP cells.

RETRACTION

doi:10.1038/nature13599

Retraction: Bidirectional developmental potential in reprogrammed cells with acquired pluripotency

Haruko Obokata, Yoshiki Sasai, Hitoshi Niwa, Mitsutaka Kadota, Munazah Andrabi, Nozomu Takata, Mikiko Tokoro, Yukari Terashita, Shigenobu Yonemura, Charles A. Vacanti & Teruhiko Wakayama

Nature **505,** 676–680 (2014); doi:10.1038/nature12969

Several critical errors have been found in our Article (http://dx.doi.org/10.1038/nature12968) and Letter, which led to an in-depth investigation by the RIKEN Institute. The RIKEN investigation committee has categorized some of the errors as misconduct (see Supplementary Data 1 and Supplementary Data 2). Additional errors identified by the authors that are not discussed in RIKEN's report are listed below.

(1) Figure 1a and b in the Letter both show embryos generated from STAP cells, not a comparison of ES- and STAP-derived chimaeric embryos, as indicated in the legend.

(2) Extended Data Fig. 7d in the Article and Extended Data Fig. 1a in the Letter are different images of the same embryo and not, as indicated in the legends, a diploid chimaera embryo and tetraploid chimaera embryo.

(3) There is an erroneous description in Fig. 1a in the Letter. The right panel of Fig. 1a is not a 'long exposure' image at the camera level but a digitally enhanced one.

(4) In Fig. 4b of the Letter, STAP cell and ES cell are wrongly labelled in a reverse manner.

(5) In the Article, one group of STAP stem cells (STAP-SCs) was reported as being derived from STAP cells induced from spleens of F_1 hybrids from the cross of mouse lines carrying identical *cag-gfp* insertions in chromosome 18 in the background of 129/Sv and B6, respectively, and that they were maintained in the Wakayama laboratory. However, further analysis of the eight STAP-SC lines indicates that, while sharing the same 129×B6 F_1 genetic background, they have a different GFP insertion site. Furthermore, while the mice used for STAP cell induction are homozygous for the GFP transgene, the STAP-SCs are heterozygous. The GFP transgene insertion site matches that of the mice and ES cells kept in the Wakayama laboratory. Thus, there are inexplicable discrepancies in genetic background and transgene insertion sites between the donor mice and the reported STAP-SCs.

We apologize for the mistakes included in the Article and Letter. These multiple errors impair the credibility of the study as a whole and we are unable to say without doubt whether the STAP-SC phenomenon is real. Ongoing studies are investigating this phenomenon afresh, but given the extensive nature of the errors currently found, we consider it appropriate to retract both papers.

Supplementary Information is available in the online version of this Retraction.